ERASMUS UNIVERSITY ROTTERDAM

Erasmus School of Economics

The structure of overnight versus intraday prices

Master Thesis Quantitative Finance

Daan Fortuin (503339)

Supervisor Transtrend: M. Oort   Supervisor Transtrend: L. Hendrikx

Supervisor University: dr. R.J. Lange   Second Assessor : dr. O. Kleen

December 24, 2022

Abstract

After-hours trading has given investors the opportunity to trade after markets have closed. Returns can therefore be split into intraday and overnight returns. Overnight returns outperform intraday returns when sorting on upside close-to-close volatility, which is a proxy for retail investor attention. A possible explanation would be that retail investors buy around the open, drive up opening prices, which causes higher overnight returns and lower intraday returns. This effect is robust to the exact time of open and close. To corroborate these findings I model intraday and overnight volatility using Dynamic Conditional Score - EGARCH (DCS-EGARCH) models. The coupled-component DCS-EGARCH uses a sequential estimation procedure of kernel technology and maximum likelihood. The two-component DCS-EGARCH uses a simultaneous estimation procedure depending on only a filter and a quadratic spline. Although the methodology of these models differ, they both lead to the conclusion that intraday and overnight volatility differ significantly, in addition to a relative importance increase of overnight volatility. All things considered, intraday and overnight returns have different dynamics and should be modelled accordingly.

Contents

1 Introduction

The structure of overnight versus intraday prices of stocks and their return generating process has been an extensively researched topic in finance, since the opportunity to trade during market-closure (Berkman et al. (2012), Cooper et al. (2008), Kelly and Clark (2011)). Many papers find outperformance of overnight returns, from close-to-open, in comparison to intraday returns, from open-to-close, during the period around the dot-com bubble, where overnight trading, also called after-hours trading, can be split in post-market and pre-market trading. The predominant explanations for this phenomenon are retail investor attention (Berkman et al., 2012) and the liquidity premium (Cooper et al., 2008). Greater effects were found when sorting on higher close-to-close volatility, lower institutional ownership, difficulty to value and positive investor sentiment.

If the effect observed in the literature is persistent, it should be robust to the exact start and end of intraday trading. Otherwise the observed discrepancy could be wholly based on the particular dynamics around the open and close. Estimation assumptions are of great importance to the observed results, as the open and close are volatile moments. The exact endpoints used for comparison between overnight and intraday returns influences this estimation, especially considering the larger bid-ask spreads during market open and close.

This research field is currently relevant with respect to the shift in balance between retail investors and institutional investors. In the wake of the COVID-19 pandemic, 'meme stocks' such as GameStop and AMC Entertainment proved to be a battleground between retail investors and several large institutional investors. The literature suggests a possible strange effect of this competition between retail and institutional investors. Aggregate stock returns appear to be higher during overnight trading hours than intraday trading hours. This could be due to retail investors pushing up prices during the open because they can, in general, not trade overnight. Investors could make use of these characteristics, if these results would appear significantly in the data, and consequently adjust their trading strategies. A strategy including going long in the night and short in the day could be profitable in such a situation.

Most papers pertaining to this effect date back from the period before the global financial crisis. I therefore review this problem using a more recent data set and investigate if overnight returns still outperform intraday returns and if this phenomenon is robust

to the exact starting or ending time of the trading day. Furthermore, I look into the effects of sorting stocks in certain portfolios based on close-to-close upside volatility and institutional ownership. The sorting process needs an estimate of this upside volatility and I therefore forecast this using a relatively simple heterogeneous autoregressive (HAR) model incorporating structural changes, proposed by Gong and Lin (2021).

I show that the difference between overnight and intraday returns is significantly different from zero for the period 2016 to 2022 when using upside volatility sorting updated on a daily basis. The pandemic plays an important role in this phenomenon. There seems to be a change in retail investor behaviour in the last four to five years, which has accelerated since the COVID-19 pandemic. Retail investors appear to follow momentum strategies, assessed by sorting on close-to-close upside volatility. Retail investors, mostly only able to trade during market hours, concentrate their purchases during the open, resulting in high opening prices and higher overnight returns. This 'overnight anomaly' is most clearly observed in S&P 500 stocks, but also holds for Nasdaq 100 stocks and Dow 30 stocks. This phenomenon is robust to the exact start and end of the trading day and the anomaly is therefore not caused by the dynamics and more volatile movements around open and close. This robustness test uses the median of value weighted average minute prices for an 30 minute interval. Furthermore, institutional ownership has a negative effect on this occurred effect, which is motivated in the literature by Berkman et al. (2012).

This phenomenon in the data supports the notion of modeling overnight and intraday returns and their volatilities separately. Linton and Wu (2020) propose a semiparametric coupled component Dynamic Conditional Score - Exponential GARCH model (coupled component DCS-EGARCH model). This model enables the overnight and intraday volatilities to have different dynamic properties, which are clearly observed in the data including between these volatilities. I retrieve short and long run volatility series, for both overnight and intraday, to make conclusions about their behaviour, especially before, during and after the COVID-crash in March 2020. Linton and Wu (2020) use a dependence structure based on overnight versus intraday dynamics until 2017. As dynamics have changed, based on the data analysis, Iintroduce an adjusted base specification of the coupled component DCS-EGARCH model using a different dependence structure. Although this specification improves the model, it does not have an influence on the short and long run components. Although no increase of efficiency is found after changing the

base specification, it proves the robustness of the model to the used base specification.

Moreover, I use the methodology of Harvey and Lange (2018) to come up with a different estimation technique for the long run volatilities. Instead of the coupled component model, where I optimize the short and long run components sequentially, I only use a filter in the so-called two-component DSC-EGARCH to estimate the short and long run component simultaneously. I focus on 22 stocks in the Dow 30, because graphically presenting 456 plots for each model is not feasible. This data set is similar to Linton and Wu (2020). I extend the sample period from (1993-2017) to (1993-2022). The overnight anomaly is also expressively present in this sample of stocks and therefore sufficient and convenient for my analysis.

The DCS-EGARCH model proves to be robust to the used methodology. The results from the coupled component and two-component model correspond to a great extent. The long run component, total volatility and ratio (overnight to intraday) of total volatility behave similar across models and the same conclusions can be drawn from them. These conclusions include the relative importance increase from overnight volatilities to intraday volatilities, which is caused by a decrease of intraday volatility, rather than an increase of relative overnight volatility (on average). This effect is found for both the short run and long run processes. Furthermore, intraday and overnight volatility peaks were the same during the dot-com bubble and the financial crisis, but overnight volatility was significantly higher than intraday volatility during the COVID-19 crash. Nevertheless, overnight volatility remains smaller in absolute sense than intraday volatility over the entire sample period, a phenomenon already shown in the literature. In addition to these results, I find some short run dynamics. Overnight volatility is more leptokurtic. This increased during the the last two years, namely due to overnight crashes. On the other hand, intraday returns have even become more Gaussian during the last two years, which is also supported by the data analysis of the difference in return during the pandemic. The models also imply higher volatility after negative returns in general. Moreover, intraday returns are negatively affected by previous night and day returns, and overnight returns have a negative effect on subsequent negative returns.

All in all, I find a significant difference in return between overnight and intraday returns when sorting on upside volatility for the period 2016 to 2022. This effect is most striking since the COVID-19 pandemic. This upside volatility can already be forecast with

simple methods, such as a HAR model with structural changes. The difference in dynamics between intraday and overnight prices is, next to the return generating process, found in the volatility process. I extend the semi-parametric coupled component DCS-EGARCH model of Linton and Wu (2020) by using additional data and changing the base specification. Furthermore, I develop a new model called the two-component DCS-EGARCH, which uses a simultaneous optimization, instead of a sequential optimization, which is more time-efficient. The two-component model uses the methodology from Harvey and Lange (2018), is a parametric model and uses quadratic splines instead of kernel technology. Modelling intraday and overnight volatility is proven to be model-robust, as both models indicate the same results, namely a significant difference between intraday and overnight volatility, including a relative importance increase of overnight volatility. All results lead to the conclusion that intraday and overnight returns have different dynamics and should be modelled accordingly.

The remainder of this paper is structured as follows. Section 2 relates this paper to the existing literature. Section 3 informs about the data used and already gives some insights into the structure of overnight versus intraday returns. Section 4 describes the models from the literature, the new adjusted models and the evaluation measures. Next, we report the results of the described methodology in Section 5. Lastly, Section 6 summarizes the main results and provides ideas for further research.

2 Literature Review

After-hours trading and overnight returns are an interesting topic in the literature since the introduction of electronic communication networks (ECN) in 1969. ECNs accommodate investors to trade when financial markets are closed and to participate in so-called after-hours trading. After-hours trading became even more widespread in 1999, when ECNs became more widely available to retail investors. Hong and Wang (2000) gives a complete overview of the difference between overnight and intraday returns before after-hours trading was more widely available. They find higher activity around the open and close in combination with higher volatility during these periods of market closure and opening. Additionally, they show empirically that intraday returns are higher and more volatile than overnight returns.

6

The return-generating process has according to some papers changed since after-hours trading became more accessible to retail investors. Three papers, namely Berkman et al. (2012), Cooper et al. (2008) and Kelly and Clark (2011), find a significant difference between overnight and intraday returns for the period 1993 to 2008 using different methods. They claim that intraday returns are negative or zero, while overnight returns are significantly positive. All three papers list different reasons for this phenomenon, use different data and differ in focus.

Berkman et al. (2012) use a sample of the 3000 largest US stocks for the period 1996-2008 and an abridged sample of NASDAQ stocks for the period 1997-2001 including detailed information on the identity of market participants for each trade. They calculate log returns using quote midpoints and construct various variables to explain the difference in night versus day returns. These variables include two proxies for retail attention, three measures of retail buying at the open, two proxies for short sale constraints and three measures of transaction costs. Furthermore, they look at hard-to-value stocks and sentiment. Berkman et al. (2012) conclude that the difference between the overnight and intraday returns is caused by high opening prices. These high prices are caused by retail investor attention. Moreover, the effect is more prominently present for hard-to-value stocks, stocks with less institutional ownership and stocks with more sentiment.

Cooper et al. (2008) look at S&P 500 stocks, 14 exchange-traded funds (ETFs), 44 firms in the Amex Interactive Week Internet Index and S&P 500 E-mini futures. They conclude that the US equity premium is solely due to overnight returns for the period 1993-2006. They split the intraday returns in three periods and conclude that day reversals after positive overnight returns are due to high opening prices which decline in the first hour of trading. They perform robustness tests for calendar effects, growth of ECNs and decimalization and try to explain the high difference in night versus day returns by earnings announcements, liquidity effects and price pressure effects. Cooper et al. (2008) refer to further research for a full explanation of the night versus day return, as they can only explain a small portion of this effect by the illiquidity premium as suggested by Longstaff (1995), and to a smaller amount to risk, earnings surprises, return autocorrelation, decimalization and the growth of ECNs.

Thirdly, Kelly and Clark (2011) consider ETFs and differ from the previous two papers by using risk-adjusted excess returns instead of raw returns. They also compute volume

weighted average prices in comparison with the two other papers who use first/last traded prices. Their focus is on long-short trading strategies by making use of the difference in the night versus day returns for the period 1995-2006. One of five ETFs is profitable by exploiting this difference using the long-short strategy. Significance of this difference is determined by the Sharpe ratio test of Opdyke (2007), which has since been improved by Ledoit and Wolf (2008).

A fourth paper, Lachance (2015), finds the same results for on average almost six thousand stocks for the period 1995-2014. She claims that one out of five stocks has a significantly positive difference between night and day returns, which pays two times the market return for a volatility which is three times as small. These stocks also have an average negative intraday return.

Where the previous four papers look specifically to the difference in return in the US, other papers have looked at overnight volatility, different countries, other relations, trading strategies, earnings announcements, intraday patterns and options. French and Roll (1986) were among the first to look at overnight volatility and conclude that it was lower than intraday volatility because of less public information, fewer informed investors and fewer pricing errors. More recently, Linton and Wu (2020) show that the ratio of overnight to intraday volatility has increased in the last two decades for Dow Jones stocks and large stocks in the CRSP database. Linton and Wu (2020) use a coupled component model, which enables differentiation of dynamics of overnight and intraday volatility. This model is a dynamic conditional score model, for which Harvey (2013) laid the foundation. They use a two step estimation procedure to optimize both long and short run components. In addition to using this model, I adapt it with a part of the methodology from Harvey and Lange (2018), which allows me to do a one step estimation. They modify the GARCH filter to a two-component GARCH filter using a parameter restriction to create a long and short run component. Where Linton and Wu (2020) focus on proposing their model and applying it to past data, Harvey and Lange (2018) do not differentiate between overnight and intraday returns and concentrates on forecasting ability.

Cai and Qiu (2009) find significantly higher overnight returns compared to daily returns in 23 countries. They test the assertion of Miller (1977), which states that stocks are overpriced due to divergence of opinions by the absence of short selling. Divergence of opinions happens overnight, causes high opening prices and returns therefore are sig-

nificantly higher overnight. Aretz and Bartram (2015) finds quite the opposite, when conducting an analysis on 48,413 stock from 35 countries for the period 1993-2012. They find higher day returns than night returns, both having a similar volatility. Hendershott et al. (2020) studies the relation between stock prices and beta for both night and intraday returns. They find that overnight returns are positively related to beta and vice versa for intraday returns. This holds for beta-sorted portfolios, industry portfolios, book-to-market portfolios, individual US stocks and international stocks. Branch and Ma (2006) discover a negative correlation between overnight returns and intraday returns the following day. Branch and Ma (2012) expands this paper and gives a more detailed elaboration on the negative correlation. Lou et al. (2019) looks at multiple trading strategies for which they claim that returns are earned entirely overnight or earned entirely intraday. They link this behaviour to investor heterogeneity and claim that short-term investors could profit from their discovery due to the large economic magnitudes of their results, but that also long-term investors could profit by timing their orders either near the open or during the close. Basdekidou et al. (2017) also look at different strategies and anomalies, such as the overnight return temporal market anomaly. They also conclude that returns are earned entirely overnight or entirely intraday. Jiang et al. (2012) look at earnings announcements for S&P500 stocks from 2004-2008 released during after-hours and finds that trading, price change and price discovery are heightened during and just after the releases. The timing of earnings announcements is concentrated during market closure, as firms prefer to use informed traders to start the price discovery, where informed traders refer to traders with superior knowledge due to either access to private information or skillful processing of public information. Wood et al. (1985) split their analysis in four parts namely night, day, open and close. They find unusually high returns and volatitlities during open and close, while day returns, with exclusion from open and close, are discovered to behave normally. Muravyev and Ni (2020) investigate S&P500 index options and find positive day returns and negative night returns. This is robust across all maturities and moneyness classes, and also across equity options.

All in all, there is a lot of research on this topic. Many papers find the same dynamics, but give different causes. This also depends on the markets and data samples used. However, most papers are outdated and do not cover the period since the COVID-crash. I will therefore use methods from several studies using more recent data and assess the

several causes.

3 Data

This section evaluates the data, gives some descriptive statistics and already analyzes the data with some more advanced methods. Firstly, it covers the used variables, then describes all sample periods of the securities and their respective markets and finally gives evidence of larger overnight returns in comparison with day returns when sorting on particular variables.

3.1 Variable Assembly

The data consists of daily returns and price patterns around open and close. I decompose the daily returns into intraday and overnight returns. Log returns are used for convenience and do not alter the results. The intraday return is defined as the return from open to close and the overnight return as the return form close to open. The exact definition of open and close will be discussed hereafter. Log returns are defined as:

$$
\begin{aligned}
\text{Close-to-Open return} = \text{CTO}_t &= \log(\text{Open}_t/\text{Close}_{t-1}) \\
\text{Open-to-Close return} = \text{OTC}_t &= \log(\text{Close}_t/\text{Open}_t) \\
\text{Close-to-Close return} = \text{CTC}_t &= \log(\text{Close}_t/\text{Close}_{t-1}) \\
\text{Open-to-Open return} = \text{OTO}_t &= \log(\text{Open}_t/\text{Open}_{t-1}).
\end{aligned}
\tag{1}
$$

One thing is important to mention with regard to calculation. The night return (CTO_t) is followed by the intraday return (OTC_t), when calculating the difference between both series. This pattern is needed for calculation but has for a considerable time horizon, no implications on the results. Figure 1 shows a clarifying timeline. I analyse the difference as it would have direct implications on the (weak) efficient market hypothesis. The difference is defined as:

$$
\text{Difference in return} = \text{Overnight return} - \text{day return} = \text{DIFF}_t = \text{CTO}_t - \text{OTC}_t. \tag{2}
$$

Descriptive statistics are evaluated by taking standard t-tests on the time series average of the difference (DIFF_t). This is straightforward when evaluating an index, ETF (exchange traded fund) or single stock. However, my analysis is mainly on multiple stocks.

10

Therefore, I take the cross-sectional mean of all assets in the sample and thus calculating the cross-sectional mean for each point in time. This method is used in Berkman et al. (2012) to adjust for cross-sectional correlation as proposed in Bernard (1987). The mean and variance of the computed time-series is subsequently used for the corresponding t-tests. Newey-West standard errors (Newey and West, 1987) correct for serial correlation in the created time-series of cross-sectional means.

Cooper et al. (2008), Kelly and Clark (2011) and Berkman et al. (2012) report significance tests using tables. This forces them to look at only one period of time, as they can only report those estimates. I differ in visualisation of the results by using a rolling window and displaying the entire time series of DIFF_t. This increases interpretability and shows time variation. Next to that, it informs readers more extensively, as it gives far more details, as for a time-series of four years, the reader gets one thousands times more observations.

Inspired by Berkman et al. (2012), I use portfolio sorts based on volatility and institutional ownership. Berkman et al. (2012) link higher overnight returns to attention of retail investors. A proxy for the presence of retail investors is the squared close-to-close return of the previous day. The squared return is a rough measure for the volatility. We refer to this proxy as VOL_{t-1}:

$$\text{VOL}_{t-1} = \text{Close-to-close volatility yesterday} = \text{CTC}_{t-1}^2, \tag{3}$$

Berkman et al. (2012) use CTC_{t-1}^2. However, from the analysis I discover that total close-to-close volatility does not work as a good proxy in recent times, as sorting on this metric does not give a significant difference in overnight minus intraday return. However, upside close-to-close volatility is a good proxy and gives the same results for this era, as Berkman et al. (2012) report for the dot-com bubble period. Therefore, I introduce VOL_{t-1}^+:

$$\text{VOL}_{t-1}^+ = \text{Upside close-to-close volatility yesterday} = (\max\{\text{CTC}_{t-1}, 0\})^2, \tag{4}$$

where it is important to mention that sorting on this variable gives the same results as sorting on close-to-close return directly. However, I choose to define it as upside volatility for the purpose of the used forecasting procedure and the resemblance with the available literature.

Figure 1 gives a clear timeline of the used variables. It is important to realize that the VOL^+_{t-1} is only known at CLOSE_{t-1}. When sorting on this variable with the purpose of following a related trading strategy at time point CLOSE_{t-1}, the need to forecast VOL^+_{t-1} arises. The model used for the forecast will be discussed in the next section.

Another sorting variable used by Berkman et al. (2012) is Institutional Ownership (IO_t):

$$\text{IO}_t = \text{Institutional Ownership} = \frac{\text{shares outstanding hold by institutions}}{\text{divided by total shares}} \tag{5}$$

Data on institutional ownership comes from the the WRDS (Wharton Research Data Services) Thomson Reuters Institutional Holdings (13F) Database. Data is available on 450 S&P500 stocks, as we lose six stocks due to different use of tickers, absence of differentiation between series of the same stock, mergers and acquisitions during the research or unavailability. I lose another 130 stocks due to incoherent data in the WRDS database. Institutional Ownership exceeds 100% for these stocks, which is by definition impossible. Details on the stocks used can be found in Appendix A. Institutional Ownership is a quarterly reported variable.

Figure 1: Timeline returns and volatility
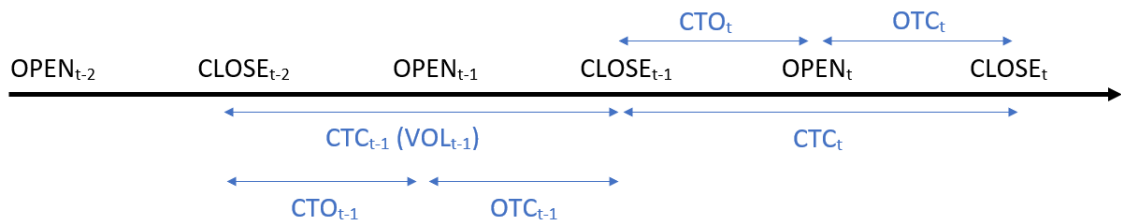
3.2 Markets and sample periods

This subsection covers the details of the markets and sample periods. The main sample I use consists of constituents of the S&P500 index, but some preliminary research consists of data from ETFs, the 30 stocks of the Dow Jones Industrial Average index and stocks tracking the NASDAQ 100 index.

3.2.1 ETFs

Kelly and Clark (2011) is one of few papers, which laid the foundation for the 'overnight anomaly'. They provide evidence of this anomaly using data on five ETFs, namely DIA, IWM, MDY, QQQ and SPY, tracking respectively the Dow 30, the Russell 2000, the S&P 400 Midcap, the Nasdaq 100 and the S&P 500. DIA, QQQ and SPY cover stocks with big market capitalization, MDY with medium market capitalization and IWM with small market capitalization. Figure 19 and Figure 20 in Appendix B show the time series of the $DIFF_t$ for each ETF. Table 5 reports the sample periods for each ETF. A rolling window of eight years is used to be able to compare directly to the results of Kelly and Clark (2011). Confidence intervals are based on Newey-West (Newey and West, 1987) standard errors for a 5% level. The difference in return ($DIFF_t$) is indeed significant for four out of five ETFs for the period considered by Kelly and Clark (2011). The fifth is almost significant, but the difference in result could be due to different estimation methods. This period is actually approximately the first data point of each time series in the figures, as it corresponds to the mean of that date and the eight years before. The anomaly disappears for all ETFs quite rapidly after this period. Although a (small) increase in $DIFF_t$ is found for all ETFs in the last eight to ten years, only IWM has a significant difference between overnight and intraday returns recently.

3.2.2 Dow Jones Industrial Average

After finding no expressive anomaly in the ETFs, I first consider a small sample of stocks, namely the Dow Jones Industrial Average, or Dow 30 for short. I find no direct evidence in the descriptive statistics of this sample, thus I sort stocks on overnight return to examine heterogeneity of overnight versus intraday prices. The overnight return for each stock during the last five years determined the corresponding tercile, low, medium or high, where a tercile contains one third of the stocks of a portfolio. The sample consists of 26 stocks (as four stocks had a horizon of less than 30 years), meaning six or seven stocks per tercile. A rolling window of twelve years is used and significance is determined as before. Figure 21 shows that stocks are heterogeneous in $DIFF_t$ for the Dow 30. It is important to note that these results come by definition of the sorting and are purely used to show for heterogeneity amongst stocks.

Figure 22 shows the overnight returns minus the intraday returns when sorted on

close-to-close upside volatility using a rolling window of five years. A clear pattern arises since April 2021, which accounts for the period 2017 to 2022, where a high VOL^+_{t-1} gives a higher return on day t, on average. This difference is significantly different from zero, rejecting the null hypothesis of equal return. Sorting on upside close-to-close volatility and proceeding in a long night short day strategy is thus profitable, without considering transaction costs. For this strategy, positions need to be balanced twice a day, which includes a lot of transaction costs. I will elaborate on this in the next section.

3.2.3 Nasdaq 100

The third sample includes the 123 largest stocks from the Nasdaq Exchange where large refers to market capitalization. I exclude 21 firms who have less than 2461 data points, which is almost 10 years of data as one year refers to 252 trading days. The initial sample of 123 stocks ends up to have 102 stocks after data cleaning, which is close to 100 and divisible by three. The last condition is important for the sorting process. More details about the used stocks can be found in Appendix A. The 102 stocks are divided in terciles of 34 stocks based on yesterdays upside close-to-close volatility (VOL^+_{t-1}). This approach is inspired by Berkman et al. (2012). By creating this variable I lose 2 observations per stock. Figure 23 in Appendix B shows the difference in return (overnight - intraday return) per tercile (high, medium and low VOL^+_{t-1} respectively) for a rolling window of five years. Confidence bounds are calculated by computing standard errors by taking cross-sectional means and using Newey-West standard errors of the time-series of means. The high tercile has a significant difference in return, or in other words, the overnight return is significantly larger than the intraday return. The medium and low tercile are both insignificant. Berkman et al. (2012) claims that this is the result of retail investors who buy at the open and thus raise opening prices. VOL^+_{t-1} is used as a proxy for retail attention. This phenomenon, outperformance of overnight returns, observed by several papers during the period around the dot-com bubble, has since the COVID-19 crisis risen to significant values, at least for large cap Nasdaq and Dow 30 stocks, when sorting on a proxy for retail attention. This could be due to a change in retail investor behaviour since the pandemic, as during the dot-com bubble, which is contrary to the (weak) Efficient Market Hypothesis. Another interesting feature is the steep decline in DIFF_{t-1}. This means that, in comparison to the period before and after, during the first

14

weeks of the COVID-19 pandemic night returns where smaller. Better said, crashes were more concentrated in the overnight periods than in the intraday periods. Considering this, the effect, as I use a rolling window of five years, is even larger when not considering the first few weeks or months of the pandemic. The difference in return yields approximately 0.07% per day, when using a trading strategy of going long in the night and short in the day without transaction costs, which means approximately 19% per year.

Figure 24 and Figure 25 show what happens when sorting in sextiles, meaning six equal groups of 17 stocks, instead of terciles. In the highest sixtile (high), the phenoma is far more significant and larger than before. The difference in return yields approximately 0.1% per day, when using a trading strategy of going long in the night and short in the day without transaction costs, which means approximately 29% per year (for the last five years). To compare, the annual return of the S&P500 was 8.9% the last five years and 12.5% the last ten years. All other sextiles are insignicant from zero and decrease per sextile, where high2 comes between high and medium. The lowest sextile however is increasing with respect to the sextile above (low). Again, a rolling window of five years is used and the begin of the pandemic is visible in each figure.

Trading costs should be taken into account when considering trading strategies. Trading costs are often divided in transaction costs and the bid-ask spread. The average transaction cost per stock is approximately 0.01% per trade. As this strategy involves selling at the open and buying at the close, 0.02% of the profit goes to the transaction cost. The bid-ask spread is an issue when dealing with quote data. However, since I use trade data, the bid-ask spread is already part of the price. I am thus left with a (large) 0.08% (0.10%-0.02%) profit per day. The question remains in which magnitude this strategy can be implemented. The 0.08% profit is realistic when trading one stock of each firm a day. Institutional investors are not interested in such quantities. The traded prices include the bid-ask spread at that moment for that particular stocks. When institutional investors want to trade in large volumes, the bid-ask spread could become larger as of the current supply and demand. This will diminish the profit rapidly. The trading strategy is thus profitable when trading small volumes, but will soon become unprofitable when increasing the volumes.

Finally, Figure 26 and Figure 27 show respectively the OTC_{t-1} and CTO_{t-1}. The day returns, OTC_{t-1}, are smallest for the high VOL_{t-1}^{+} and highest for the low VOL_{t-1}^{+}, but

all insignificant from zero. The night returns, CTO_{t-1}, are (for the last five years, so May 2017 to May 2022) significantly different from zero for the high and low tercile, and almost significant for the medium tercile. The small day returns for the high tercile thus cause the DIFF_{t-1} to be largest for the high tercile. Another interesting feature is the influence of the COVID-19 crisis on returns. Day returns are not affected at all by this crisis, while night returns are affected negatively. To conclude, the negative returns during the first few weeks of the corona pandemic and the dropping stock prices are located in the overnight returns.

3.2.4 S&P500

The next sample consists of constituents of the S&P500 as of April 4 2022. This sample includes 505 stocks from a wide variety of industries and sectors. I lose 49 stocks, which have an initial public offering (IPO) in the last ten years, to ensure a minimum of ten years data for each stock. The results are derived from the remaining 456 stocks. The used stocks are clearly described in Appendix A. The analysis is the same as before. Using a rolling window of five years, I compute the time series of cross-sectional means and use Newey-West standard errors for significance tests. Figure 2 shows the descriptive statistics of the S&P500 stocks.

Figure 2: Difference in return descriptive statistics for a five year rolling window
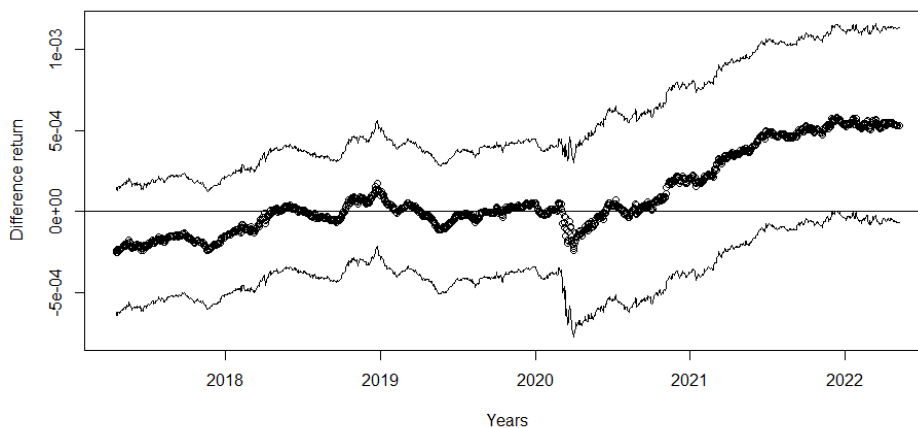
Whereas the difference in overnight versus intraday returns are not significantly different for the period 2013 to 2020, the steep increase in difference since the COVID-19 pandemic almost reaches significance for approximately the last five years, after a steep increase since March 2020. This increase is remarkable in comparison to the full sam-

16

ple period and indicates a change in overnight versus intraday price dynamics. For the Nasdaq sample, portfolio sorting is necessary to find a significant difference. For S&P500 stocks, the overnight anomaly is present far more pronounced for the last five to six years. There is again a large drop at March 2020, indicating that crashes found place mainly during market closure when the COVID-19 crisis started.

Figure 3 displays three terciles, namely sorted per day on VOL_{t-1}^+ (respectively high, medium and low). There is a clear pattern. High upside close-to-close volatility yesterday means a relatively high overnight and lower intraday return today due to higher opening prices forced by higher retail investor attention. High VOL_{t-1}^+ means a significant out-performance of overnight returns. The medium tercile is almost significant and lower in absolute value. The low tercile is even lower and more insignificant.

Once more, I use portfolio sorts on upside volatility to proxy for attention of retail investors. As mentioned before, I use upside close-to-close volatility, whereas Berkman et al. (2012) uses total close-to-close volatility. Using different proxies, we find the same results. This could be explained as a shift in behaviour of retail investors. Reacting to total volatility of a certain stock, during the dot-com period, could be explained by a dichotomy of retail investors. One part of retail investors reacts to upside volatility, due to for example the momentum argument, and the other part reacts to downside volatility, due to for example the argument which states a cheaper entry point. The previous five to six years, there is only a reaction to upside volatility. This could be explained by a shift in behaviour of retail investors to momentum strategies.

Sorting on VOL_{t-1}^+ is done daily. IO data is only available quarterly and it would also not change the sorting drastically if available daily. Therefore it is expected that these sorts do not influence the $DIFF_{t-1}$ that much. However, it is still an interesting sort, as IO is by definition negatively correlated with retail investing. Figure 4 gives the three sorts of IO and plots the difference in return time-series. The green line is the low IO sort and is thus expected to have a high amount of retail investors, which, by our hypothesis, should have a bigger $DIFF_{t-1}$. This behaviour is seen after the COVID-19 pandemic. The direct opposite happened before the pandemic. This hints to a shift in behaviour of retail investors after the pandemic. This is the same conclusion as from the three sorted portfolio on upside volatility. The low IO sort is always beneath the green time-series after March 2020 and always above before March 2020. This is in line with our

17

Figure 3: Difference in return for 3 sorts on different values of upside close-to-close volatility yesterday for a five year rolling window

Difference returns high close-to-close volatility

Difference returns medium close-to-close volatility

Difference returns low close-to-close volatility
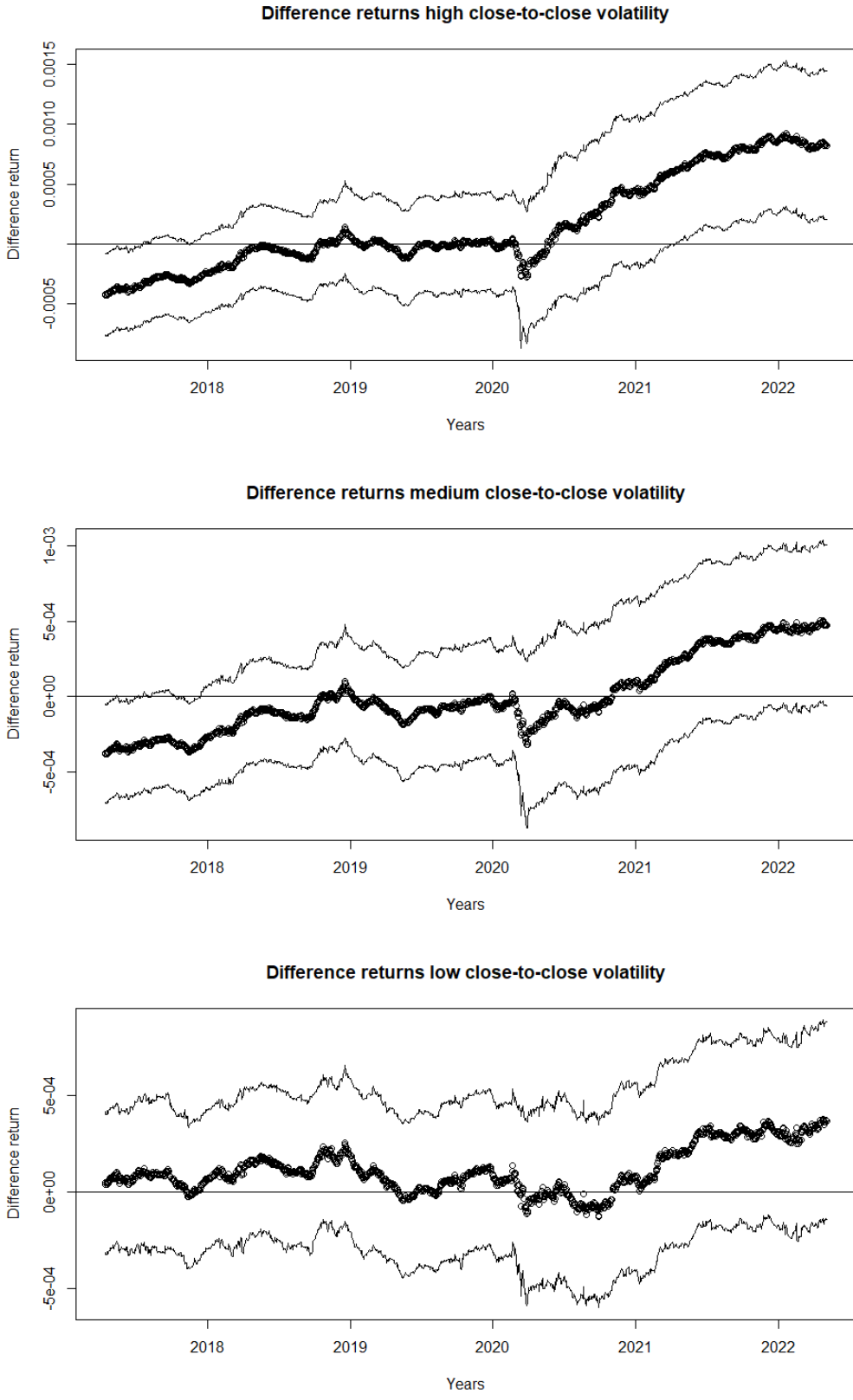
hypothesis. Appendix B includes the same plot with confidence bounds, namely Figure 28. The low and medium sort are significantly different from zero for the last five years, as I use a rolling window of five years. Nevertheless, the sorts do not differ substantially and are close to the descriptive statistics. Sorting on upside volatility will thus be more profitable. It should be noted that I use a slightly different set of stocks.

Figure 4: Difference in return sorted on institutional ownership for a five year rolling window
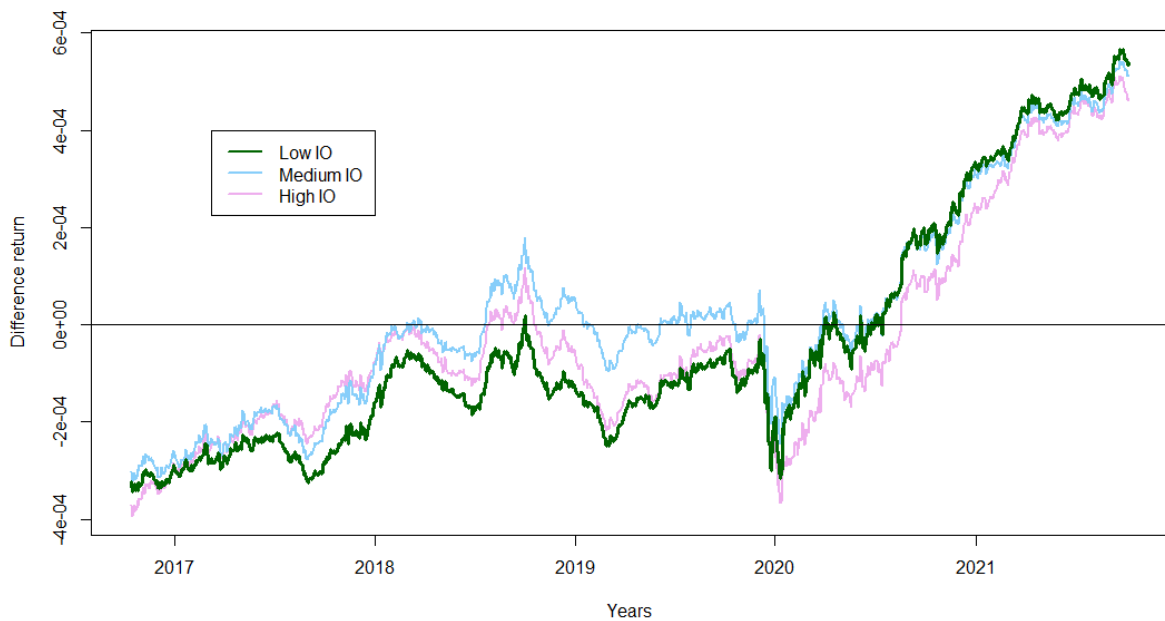
3.3 Robustness tests

Previous analysis uses first and last trade data for respectively the open and close. Open and close are volatile moments and trading at exactly the open or close is near impossible. Therefore I perform a robustness test to ensure that the difference in returns is not totally based on the dynamics around open and close. Transtrend provides minute data on approximately 120 stocks of the S&P500. Instead of one open price (first trade) and one close price (last trade), I use the minute data to create four prices, namely a pre-open price, post-open price, pre-close price and post-close price. I compute the Volume Weighted Average Price (VWAP) of each minute. Kelly and Clark (2011) take the VWAP of the first five minutes to compute the open and close prices. This method is not robust to the often much higher volumes at exactly the open or close. The VWAP of the first

five minutes will therefore be very close to the first traded price. To tackle this problem, I calculate the VWAP per minute for the 30 minutes before and after the open and close. This way I get four vectors of 30 values each. To compute the four new prices I take the median of each vector. Extreme observations are filtered out in this way and I get a fair price that is possible to trade for. I do exactly the same analysis again calculating the overnight return between the post-close and pre-open price. The intraday return is calculated between the post-open and pre-close price. US exchanges open at 09.30 AM and close at 04.00 PM. So exact definitions are:

$$\text{PRE-OPEN}_t = \text{Median of the VWAMP}_m \text{ of minutes 09.00 AM - 9.30 AM on day } t$$

$$\text{POST-OPEN}_t = \text{Median of the VWAMP}_m \text{ of minutes 09.30 AM - 10.00 AM on day } t$$

$$\text{PRE-CLOSE}_t = \text{Median of the VWAMP}_m \text{ of minutes 03.30 PM - 04.00 PM on day } t$$

$$\text{POST-CLOSE}_t = \text{Median of the VWAMP}_m \text{ of minutes 04.00 PM - 04.30 PM on day } t$$

where VWAMP_m is the Volume Weighted Average Minute Price in minute m.

Every stock is traded with enough volume during the day. However, before opening and after closure, data is scarce. After sorting the 120 stocks on available minute data, I use two samples of respectively ten and twenty stocks. For the ten-stock sample, 60% of the data is available if I only use days for which all ten stock have data. This improves to 79% when using all days for which at least eight of ten stocks have data. Having data means having at least one minute of data in all four intervals. For the twenty-stock portfolio, only 35% of the trading days is available when using all stocks. This improves to a decent percentage of 76 when using all days for which at least 16/20 stocks have data. I perform the analysis for the 10 out of 10 (64%), 8 out of 10 (79%) and 16 out of 20 (76%) stock samples.

Figure 5, Figure 6 and Figure 7 give the three samples for the time period January 2013 to May 2022 for a rolling window of four years and give the DIFF_t when using the VWAP method and the first/last traded price method. The rolling window is smaller for the simple reason that less data is available.

Figure 5: Difference in return using VWAP and first/last traded price for a four year rolling window. Using data on ten stocks. Only days with data on all ten stocks

Figure 6: Difference in return using VWAP and first/last traded price for a four year rolling window. Using data on ten stocks. Only days with data on at least eight stocks
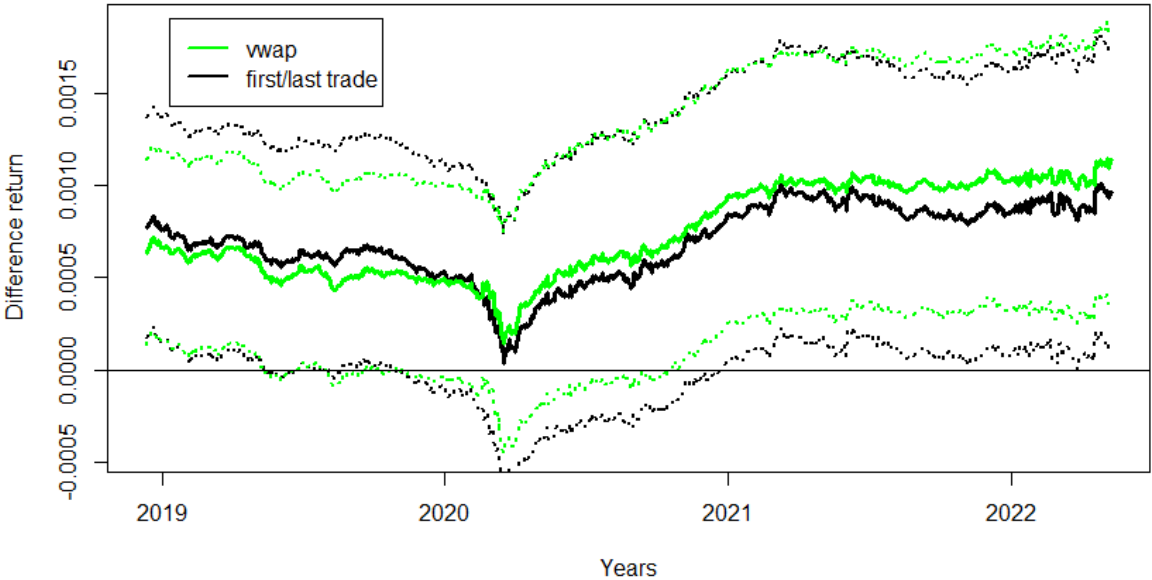
Figure 7: Difference in return using VWAP and first/last traded price for a four year rolling window. Using data on twenty stocks. Only days with data on at least sixteen stocks
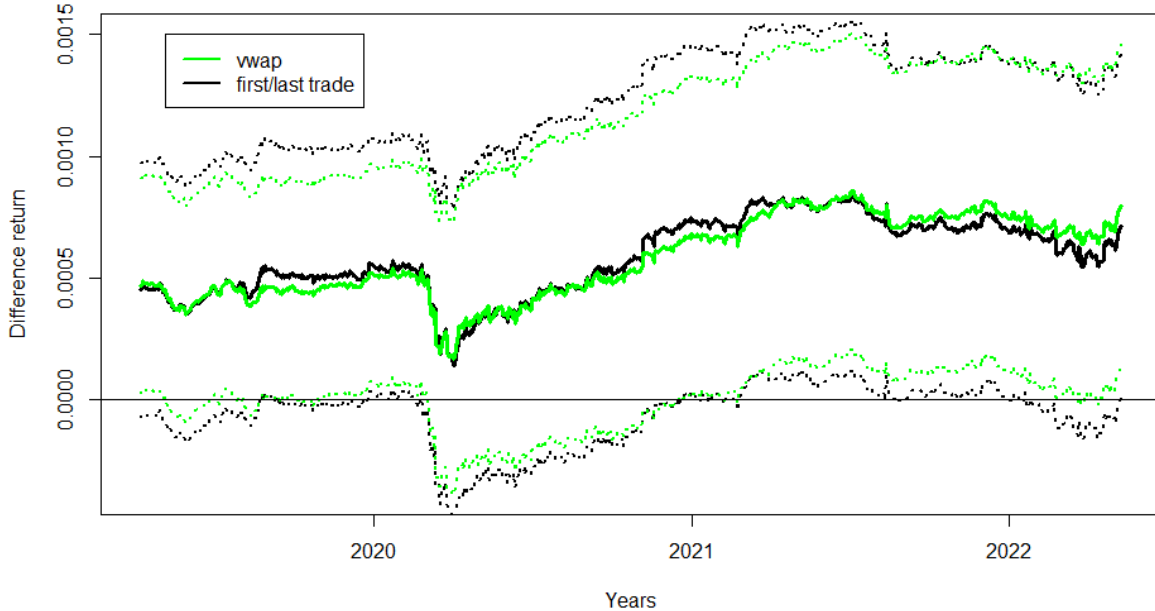
For all three figures it is important to note that significance of the results does not change, at the minimum for the 5% level. Using VWAP instead of first/last trade does thus not change the results. Dynamics around opening and closure do thus not account for the overnight anomaly. It could be argued that these sample are too small, but the reality teaches us that data during market closure is scarce. The VWAP uses only trade data and is thus based on realized trades. Of course, quote data could be used to determine pre-open or post-close prices, but the question arises how useful quotes are when not traded upon.

4 Methodology

4.1 HAR-UV-SC

In the previous section, data results implied that sorting on upside close-to-close volatility could be a profitable strategy. This upside close-to-close volatility needs to be forecasted to use this long-short strategy in respectively the night and day. There is a wide variety of volatility models in the literature. Nevertheless, upside/downside volatility is a less

researched measure. One of few recent papers which do look into downside volatility is Gong and Lin (2021). They propose a heterogeneous autoregressive model of downside volatility (HAR-DV) and advise to use structural changes (HAR-DV-SC) when estimating downside volatility. I use this model to convert it to an upside volatility model to estimate the upside close-to-close volatility of S&P500 stocks.

The model uses upside realized semivariance to proxy for upside volatility. This idea originates from Barndorff-Nielsen et al. (2008). Our model uses daily realized upside volatility. Daily upside volatility is defined as follows:

$$\text{UV}_t^D = I[r_t > 0] \; r_t^2, \tag{6}$$

with

$$r_t = \frac{\text{Close}_t}{\text{Close}_{t-1}} - 1, \tag{7}$$

where $I[]$ is an indicator function and Close_{t-1} is the close price at (*t-1*). The weekly and monthly upside realized volatility are defined as follows:

$$\text{UV}_t^W = \frac{\text{UV}_t^D + \text{UV}_{t-1}^D + \cdots + \text{UV}_{t-4}^D}{5}, \tag{8}$$

and

$$\text{UV}_t^M = \frac{\text{UV}_t^D + \text{UV}_{t-1}^D + \cdots + \text{UV}_{t-21}^D}{22}. \tag{9}$$

A week consists of five trading days, while a month, on average, consists of 22 trading days. Gong and Lin (2021) follow Corsi (2009) by stating that short-, mid-, and long-term downside volatilities affect short-term investors, mid- and long-term downside volatilities affect mid-term investors and that long-term downside volatilities affect long-term investors. They finally come up with the HAR-DV model, in my case the HAR-UV model, which is defined as:

$$\overline{\text{UV}}_{t+h} = c + \alpha_1 \text{UV}_t^D + \alpha_2 \text{UV}_t^W + \alpha_3 \text{UV}_t^M + \epsilon_{t+h}, \tag{10}$$

where $\overline{\text{UV}}_{t+h}$ is the average upside volatility between days t and $t + h$ and ϵ_{t+h} the error term.

The model gets extended by adding structural changes parameters. This extension makes the model more efficient, as shown in Gong and Lin (2021). This is done using dummy variables for certain time periods corresponding to the structural changes. Dummy $D_{i,t}$ is 1 for structural changes i. The HAR-UP-SC is defined as follows:

23

$$\overline{\mathrm{UV}}_{t+h} = c + \alpha_1 \mathrm{UV}_t^D + \alpha_2 \mathrm{UV}_t^W + \alpha_3 \mathrm{UV}_t^M + \sum_{i=1}^{S}(\delta_i \mathrm{D}_{i,t}) + \epsilon_{t+h}. \tag{11}$$

Structural changes are determined using the Inclán-Tiao cumulative sum of squares algorithm (ICSS algorithm), proposed in Inclan and Tiao (1994). This procedure works as follows. They first compute the cumulative sum of squares of the first to n observations of the return series:

$$C_n = \sum_{t=1}^{n} r_t^2. \tag{12}$$

They test for constant volatility by the following D_n statistic:

$$D_n = \frac{C_n}{C_T} - \frac{n}{T}, \tag{13}$$

with T being the total observations in the given time-series. They prove that this depends on some F-statistics:

$$D_n = \frac{(T-n)n}{T^2}\left(\frac{1 - F_{T-n,n}}{\frac{n}{T} + \frac{T-n}{T}F_{T-n,n}}\right), \tag{14}$$

with

$$F_{T-n,n} = \frac{(C_T - C_n)/(T-n)}{C_n/n}. \tag{15}$$

If the max $|D_n|$ is larger than the critical value, the corresponding n is taken as structural change, as the null hypothesis of equal variance is rejected. This algorithm is done repeatedly until the max $|D_n|$ is not larger than the critical value anymore. According to Inclan and Tiao (1994), under variance homogeneity, $\sqrt{T/2}D_k$ behaves like a Brownian bridge asymptotically. The 5% critical value is therefore equal to 1.358. This procedure is done on any stock to find structural changes in the in-sample time series.

4.2   Coupled component DCS-EGARCH

To model the ratio of overnight to intraday volatility, I use the coupled component dynamic conditional score exponential generalized autoregressive conditional heteroskedastic model, proposed by Linton and Wu (2020). In the following, I refer to this model as the coupled component.

Log returns are used in this model, defined as in equation (1). To increase interpretability, $CTO_t = r_t^N$ and $OTC_t = r_t^D$. Initially, I use the exact same model as Linton and Wu (2020), which states:

$$\begin{pmatrix} 1 & \delta \\ 0 & 1 \end{pmatrix} \begin{pmatrix} r_t^D \\ r_t^N \end{pmatrix} = \begin{pmatrix} \mu^D \\ \mu^N \end{pmatrix} + \begin{pmatrix} \pi_{11} & \pi_{12} \\ \pi_{21} & \pi_{22} \end{pmatrix} \begin{pmatrix} r_{t-1}^D \\ r_{t-1}^N \end{pmatrix} + \begin{pmatrix} u_t^D \\ u_t^N \end{pmatrix}, \tag{16}$$

with the conditional shocks u_t^D and u_t^N with mean zero. The error process u_t has an exponential form and depends on the short run effects λ and the long run effects σ. Therefore the process has conditional heteroskedasticity:

$$u_t = \begin{pmatrix} u_t^D \\ u_t^N \end{pmatrix} = \begin{pmatrix} \exp(\lambda_t^D) \exp(\sigma^D(t/T)) \, \epsilon_t^D \\ \exp(\lambda_t^N) \exp(\sigma^N(t/T)) \, \epsilon_t^N \end{pmatrix}. \tag{17}$$

The short run component λ evolves over time as follows:

$$\begin{aligned} \lambda_t^D = {}& \omega_D(1 - \beta_D) + \beta_D \lambda_{t-1}^D + \gamma_D m_{t-1}^D + \rho_D m_t^N \\ & + \gamma_D^*(m_{t-1}^D + 1)\mathrm{sign}(e_{t-1}^D) + \rho_D^*(m_t^N + 1)\mathrm{sign}(e_t^N), \end{aligned} \tag{18}$$

$$\begin{aligned} \lambda_t^N = {}& \omega_N(1 - \beta_N) + \beta_N \lambda_{t-1}^N + \gamma_N m_{t-1}^N + \rho_N m_t^D \\ & + \gamma_N^*(m_{t-1}^N + 1)\mathrm{sign}(e_{t-1}^N) + \rho_N^*(m_{t-1}^D + 1)\mathrm{sign}(e_{t-1}^D), \end{aligned} \tag{19}$$

where m_t^k, for $k \in \{D, N\}$:

$$m_t^k = \frac{(1 + \nu_k)(e_t^k)^2}{\nu_k \exp(2\lambda_t^k) + (e_t^k)^2}.$$

I use $e_t^k = \exp\left[-\tilde{\sigma}_t^k\left(\frac{t}{T}\right)\right] u_t^k$. This provides the dynamic relation between the short run process λ and the long run process σ. The exact definition of the innovation process m_t^k is based on a dynamic conditional score approach. For more details, I refer to Linton and Wu (2020). The parameters in the λ process have the following interpretation. ω_k is the unconditional mean of the short run volatility and β_k gives the perseverance of λ. Where $\gamma_D^{(*)}$ captures the influence of intraday innovation yesterday on λ_t^D, $\rho_D^{(*)}$ captures the effect of overnight innovations yesterday on λ_t^D. It is important to mention that yesterday is defined as the previous period and the notation of t and $t-1$ is solely based on the assumption of having the overnight return (r_t^N) being followed by the intraday return (r_t^D). The same interpretation holds for $\gamma_N^{(*)}$ and $\rho_N^{(*)}$, which measures the effect of lagged overnight shocks and previous period intraday shocks on the short run overnight volatility today respectively. The parameters γ_D^*, γ_N^*, ρ_D^* and ρ_N^* allow for so-called leverage effects, meaning that they use the sign of a direct (smoothed) innovation e_t^k and are not reliable on the sign of m_t^k, as m_t^k can not be smaller than minus one.

Let ϕ denote the parameter set as:

$$\phi = (\omega_D, \beta_D, \gamma_D, \gamma_D^*, \rho_D, \rho_D^*, \nu_D, \omega_N, \beta_N, \gamma_N, \gamma_N^*, \rho_N, \rho_N^*, \nu_N)^T \in \Phi \subset \mathbb{R}^{14} \tag{20}$$

The long run component σ_t^k, $k \in \{D, N\}$, is defined as follows, for $s \in (0,1)$:

$$\tilde{\sigma}^k(s) = \frac{1}{\alpha}\log\left(\frac{1}{T}\sum_{t=1}^{T} K(s - t/T)\left|u_t^k\right|^{\alpha}\right). \tag{21}$$

$K(\cdot)$ is a kernel with support $[-1, 1]$. I use the Epanechnikov kernel as it has the lowest mean square error of known kernels, and is therefore an often used kernel.

For identification purposes, I re-center $\sigma(s)^k$:

$$\tilde{\sigma}^k\left(\frac{t}{T}\right) = \tilde{\sigma}^k\left(\frac{t}{T}\right) - \frac{1}{T}\sum_{t=1}^{T}\tilde{\sigma}^k\left(\frac{t}{T}\right), \tag{22}$$

where $\frac{t}{T} \in (0,1)$ by definition , having the same domain as s.

After estimating the coefficients of the model in equation (16) using least squares, I can retrieve u_t. Using u_t, I initialize $\tilde{\sigma}^k(s)$ and determine e_t^k, for $k \in \{D, N\}$:

$$e_t^k = \exp\left[-\tilde{\sigma}_t^k\left(\frac{t}{T}\right)\right]u_t^k. \tag{23}$$

The log-likelihood function for ϕ, where θ denotes the function $\tilde{\sigma}^k(s)$ for $s \in (0, 1)$, can then be written as:

$$l_T(\phi; \tilde{\theta}) = \frac{1}{T}\sum_{t=1}^{T}\left(l_t^D(\phi; \tilde{\theta}) + l_t^N(\phi; \tilde{\theta})\right), \tag{24}$$

$$l_t^k = -\lambda_t^k(\phi; \tilde{\theta}) - \frac{\nu_k + 1}{2}\ln\left(1 + \frac{(\tilde{e}_t^k)^2}{\nu_k \exp(2\lambda_t^k(\phi; \tilde{\theta}))}\right) + \ln\Gamma\left(\frac{\nu_k + 1}{2}\right) - \frac{1}{2}\ln\nu_k - \ln\Gamma\left(\frac{\nu_k}{2}\right).$$

Γ is the gamma function and I initialize $\lambda_1^k = \omega_k$. ϕ is estimated by maximizing $\lambda_T(\phi; \tilde{\theta})$ with respect to $\phi \in \Phi$ and I get $\tilde{\phi}$ and $\tilde{\lambda}_t^k$. This is done using a so-called GARCH filter. The likelihood is optimized using this filter and a non-linear optimizer. I will refer to this optimization as the filter optimization. I then calculate $\tilde{\eta}_t^k$ as:

$$\tilde{\eta}_t^k = \exp(-\tilde{\lambda}_t^k(\tilde{\phi}; \tilde{\theta}))\, u_t^k.$$

In the next step, I maximize the following log-likelihood with respect to $\hat{\sigma}^k(s)$, where $\hat{\sigma}^k(s)$ is the optimized value of $\tilde{\sigma}^k(s)$ for each value of s separately:

$$L_T^k(\hat{\sigma}^k(s); \tilde{\phi}, s) = -\frac{1}{T}\sum_{t=1}^{T} K(s - t/T)\left[\hat{\sigma}^k(s) + \frac{\tilde{\nu}_k + 1}{2}\ln\left(1 + \frac{(\tilde{\eta}_t^k \exp(-\hat{\sigma}^k(s))^2}{\tilde{\nu}_k}\right)\right]. \tag{25}$$

This optimization is performed with the same non-linear optimizer and I will refer to this optimization as the sigma optimization.

I conduct both these optimizations, the filter and the sigma, repeatedly until convergence. Convergence is defined as the difference in parameter values upon the previous optimization and is, just as in Linton and Wu (2020), mathematically defined as:

$$\Delta_r = \sum_{j=D,N} \int \left[\hat{\sigma}^{j,[r]}(u) - \hat{\sigma}^{j,[r-1]}(u)\right]^2 du + \left(\hat{\phi}^{[r]} - \hat{\phi}^{[r-1]}\right)^T \left(\hat{\phi}^{[r]} - \hat{\phi}^{[r-1]}\right). \tag{26}$$

The optimization procedure stops when $\Delta_r \leq \tau$ for some small value τ.

4.3   Two-component DCS-EGARCH

Another way to specify both the short and long run is proposed by Harvey and Lange (2018). They propose to split the short run component, see equations (18) and (19), in two parts, where now one serves as the short run component and one as the long run component. This means that equation (18) switches, for $i \in \{1,2\}$, to:

$$\lambda_t^D = \omega_D + \lambda_{1,t}^D + \lambda_{2,t}^D, \tag{27}$$

and

$$
\begin{aligned}
\lambda_{i,t}^D = &\ \beta_{i,D}\lambda_{i,t-1}^D + \gamma_{i,D}m_{t-1}^D + \rho_{i,D}m_t^N\gamma_{i,D}^*(m_{t-1}^D + 1)\mathrm{sign}(e_{t-1}^D) \\
&+ \rho_{i,D}^*(m_t^N + 1)\mathrm{sign}(e_t^N).
\end{aligned}
\tag{28}
$$

Equation (19) changes, for $i \in \{1,2\}$, to:

$$\lambda_t^N = \omega_N + \lambda_{1,t}^N + \lambda_{2,t}^N, \tag{29}$$

and

$$
\begin{aligned}
\lambda_{i,t}^N = &\ \beta_{i,N}\lambda_{t-1}^N + \gamma_{i,N}m_{t-1}^N + \rho_{i,N}m_t^D + \gamma_{i,N}^*(m_{t-1}^N + 1)\mathrm{sign}(e_{t-1}^N) \\
&+ \rho_{i,N}^*(m_{t-1}^D + 1)\mathrm{sign}(e_{t-1}^D).
\end{aligned}
\tag{30}
$$

This model is only defined for $\beta_{1,k} \neq \beta_{2,k}$, for $k \in \{D,N\}$, where we define $\beta_{1,k} > \beta_{2,k}$ and thus $\lambda_{1,t}^k$ being the long run component.

The estimation procedure changes as σ^k is replaced by $\lambda_{1,t}^k$. For that reason, equation (23) changes to:

$$e_t^k = u_t^k. \tag{31}$$

Equation (24) remains unchanged and is optimized using the same non-linear optimizer as before. The short and long run components are optimized using the filter and at the same time. This makes this procedure more time-efficient than the coupled component model, as I do not need equation (25).

4.3.1 Quadratic Spline

[Harvey and Lange (2018)](#) suggests to model the long run $\lambda_{1,t}^k$ using exogenous variables by way of a quadratic spline. This quadratic spline, introduced by [Engle and Rangel (2008)](#), is defined, for $t = 1, \ldots, T$, as:

$$\lambda_{1,t}^k = \pi_0^k + \sum_{i=1}^K \pi_i^k \max\{t - t_{i-1}, 0\}^2. \tag{32}$$

T is split into K equally ranged intervals, where $t_0 = 0$, $t_1 = T/K$, $t_2 = 2T/K, \ldots$, $t_K = T$. The optimal K is determined by a information criterion. Although [Harvey and Lange (2018)](#) claim that the spline is less preferable from multiple points of view, it gives a better visual representation of the long run component, which is more interpretable. In addition, the long run components of both models are comparable in this way.

4.4 Adjusted model

The coupled component and the two-component model both use the same base specification as given in equation (16). This specification allows overnight returns to depend on lagged (overnight and intraday) returns. Intraday returns depend on lagged intraday returns and and overnight returns with the same t. However, recent data indicates that overnight and intraday returns can be explained by lagged upside close-to-close volatility. For this reason, I include this variable in the base specification. As I use the squared return for a proxy for (upside) volatility, it is in essence the same to use the max function over zero and the lagged close-to-close return. Therefore the included variable $r_t^{\text{CTC},+}$ is defined as:

$$r_t^{\text{CTC},+} = \max\left\{0, r_t^{\text{CTC}}\right\}, \tag{33}$$

where $r_t^{\text{CTC}} = (r_t^D + r_t^N)$.

I let the overnight and intraday return depend on the new variable in equation (33) and the remaining part of the model in equation (16) stays the same. The new base specification therefore is:

$$\begin{pmatrix} 1 & \delta \\ 0 & 1 \end{pmatrix} \begin{pmatrix} r_t^D \\ r_t^N \end{pmatrix} = \begin{pmatrix} \mu^D \\ \mu^N \end{pmatrix} + \begin{pmatrix} \pi_{11} & \pi_{12} \\ \pi_{21} & \pi_{22} \end{pmatrix} \begin{pmatrix} r_{t-1}^D \\ r_{t-1}^N \end{pmatrix} + \begin{pmatrix} \xi^D \\ \xi^N \end{pmatrix} r_{t-1}^{\text{CTC},+} + \begin{pmatrix} u_t^D \\ u_t^N \end{pmatrix}. \tag{34}$$

4.5 Constancy of ratio test

To statistically test the constancy of the ratio of long run overnight volatility to long run intraday volatility, I use the constancy of ratio test considered by Linton and Wu (2020). I test the following null hypothesis:

$$H_0 : \exp(\sigma_0^N(s)) = \rho \exp(\sigma_0^D(s)).$$

The alternative hypothesis states a time varying ratio. The considered t-ratio $\hat{t}(s)$ follows a standard normal distribution under the null hypothesis and is defined as:

$$\hat{t}(s) = \frac{\sqrt{Th}(\hat{\rho}(s) - \hat{\rho})}{\sqrt{\hat{\omega}(s)}},$$

with:

$$\hat{\rho}(s) = \frac{\exp(\hat{\sigma}^N(s))}{\exp(\hat{\sigma}^D(s))},$$

$$\hat{\rho} = \int_0^1 \frac{\exp(\hat{\sigma}^N(s))}{\exp(\hat{\sigma}^D(s))} ds,$$

$$\hat{\omega}(s) = \hat{\rho}^2 \|K\|_2^2 \left(\frac{\hat{\nu}_N + 3}{2\hat{\nu}_N} + \frac{\hat{\nu}_D + 3}{2\hat{\nu}_D} \right).$$

I plot the test statistic $\hat{t}(s)$ for $s \in (0,1)$ and determine the significance using confidence intervals. $\|K\|_2^2$ is defined as:

$$\|K\|_2^2 = \int K(s)^2 ds,$$

where I use the Epanechnikov kernel. This kernel $K(s)$ is defined as:

$$K(s) = \frac{3}{4} \left(1 - s^2 \right),$$

with $s \in (0,1)$. Therefore:

$$\int K(s)^2 ds = \frac{9}{16} \left(s - \frac{2}{3} s^3 + \frac{1}{5} s^5 \right).$$

The proof of the equation above can be found in Appendix D.

4.6 Evaluation measures

I evaluate the dynamics of the overnight and intraday volatilities considering the short and long run components. The long run component of the coupled component is $\sigma^k(s)$.

This measure is demeaned for identification purposes in each step of the algorithm. The long run component of the two-component, $\lambda_{1,t}^k$, does not have demeaning necessities. However, to compare both components, I consider

$$\lambda_{1,t}^{k,demeaned} = \lambda_{1,t}^k - \frac{1}{T}\sum_{t=1}^{T}\lambda_{1,t}^k \tag{35}$$

throughout the whole next section, if not mentioned otherwise. Hence, I will use the demeaned function above of $\lambda_{1,t}^k$.

Although both short and long run can be considered individually, the development of the total volatility for both day and night is interesting as well. Therefore I take the following equation as a measure for total volatility in the coupled component model, which is a combination of the short and long run components:

$$\sqrt{\frac{\nu_k}{\nu_k - 2}\exp\left[2\lambda_t^k + 2\sigma_t^k\left(\frac{t}{T}\right)\right]}. \tag{36}$$

Notice that this measure depends on ν_k. When ν_k goes to infinity, the scalar upfront goes to one. However, when ν_k is close to two, this scalar becomes larger than one and penalizes the total volatility for the leptokurtic behaviour of the error distribution.

For the two-component model this equation changes. Harvey and Lange (2018) considers $\exp(\lambda_{2,t}^k)$ for the short run and $\exp(\omega_k + \lambda_{1,t}^k)$ for the long run. I change the short run to $\exp(\omega_k + \lambda_{2,t}^k)$ for comparison reasons with the other model due to demeaning. As the estimation procedure of both models differs significantly, I take these measures to compare the models. Notice that I did not use this in equation (35), for the simple reason that demeaning will immediately get rid of this adjustment. Equation (36), for the total volatility, changes for the two-component to:

$$\sqrt{\frac{\nu_k}{\nu_k - 2}\exp\left[2\omega_k + 2\lambda_{1,t}^k + 2\lambda_{2,t}^k\right]}. \tag{37}$$

Furthermore I consider the ratio of total volatility overnight to total volatility intraday (for the coupled component):

$$\frac{\sqrt{\frac{\nu_N}{\nu_N-2}\exp\left[2\lambda_t^N + 2\sigma_t^N\left(\frac{t}{T}\right)\right]}}{\sqrt{\frac{\nu_D}{\nu_D-2}\exp\left[2\lambda_t^D + 2\sigma_t^D\left(\frac{t}{T}\right)\right]}}, \tag{38}$$

and for the two-component:

$$\frac{\sqrt{\frac{\nu_N}{\nu_N-2}\exp\left[2\omega_N + 2\lambda_{1,t}^N + 2\lambda_{2,t}^N\right]}}{\sqrt{\frac{\nu_D}{\nu_D-2}\exp\left[2\omega_D + 2\lambda_{1,t}^D + 2\lambda_{2,t}^D\right]}}. \tag{39}$$

5 Results

In this section I discuss the results, which can be divided into two parts, namely the in-sample estimates, out-of-sample estimates and results of the HAR-UV-SC model, and the outcomes of the coupled component and the two-component model. Although the latter two models are of higher importance, I will begin with the HAR-UV-SC model for the simple reason of keeping a logically ordered narrative.

5.1 HAR-UV-SC

The HAR-UV-SC model consists of the estimation of the structural change parameters and the autoregressive parameters. The structural change estimates are determined by the ICSS algorithm. The sets of parameters are reported and visually shown for the in-sample analysis. As the out-of-sample analysis estimates the parameter using a rolling window, I only discuss the outcome of the use of these estimated upside volatilities in the sorted portfolio analysis, as before.

5.1.1 ICSS algorithm

The ICSS algorithm is performed on every stock of the S&P500. Figure 8 shows the results for the stocks Apple (AAPL), American Tower Corporation (AMT) and Akamai Technologies (AKAM). AMT has the least structural changes, AKAM the most and AAPL has an average amount of structural changes. The green and red lines give three times the standard deviation of the returns series. For normally distributed variables this should include 99% of the observations. Return series are not normally distributed, so a smaller percentage should be expected between those bounds, because of the heavier tail distributions.

Figure 8 shows that the ICSS algorithm depends heavily on the distribution of returns. When this distribution has a higher kurtosis, meaning more large absolute returns, the algorithm finds more structural changes. This is by definition, but can also be clearly seen in the figure, as the shakier the time-series, the more structural changes are found. Furthermore, the biggest outliers are found during the COVID-19 pandemic which is by far the biggest crisis in this sample period.

Figure 8: Structural changes found by the ICSS algorithm for respectively AAPL, AMT and AKAM for a five year rolling window
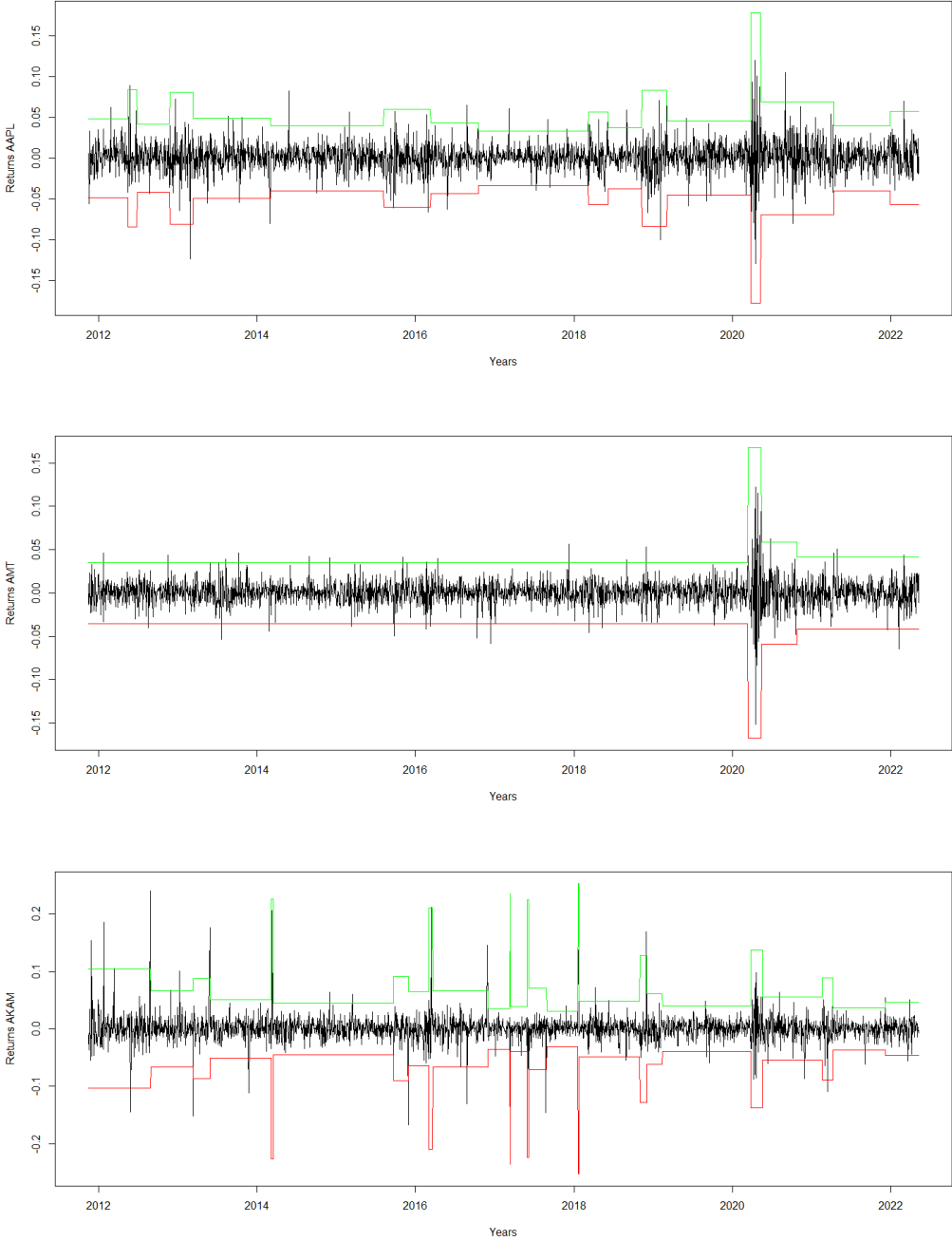
5.1.2 In-sample analysis

In-sample estimates of the three stocks, AAPL, AMT and AKAM, are given in Table 1. Significance levels for 0.1% are (***), 1% are (**), 5% are (*), and 10% are (·).

Table 1: In-sample estimates for the HAR-UV-SC model for AAPL, AMT and AKAM

	AAPL	AMT	AKAM		AAPL	AMT	AKAM
c	0.00027***	0.00012***	0.00024***	δ_{12}	0.00001		-0.00009
α_1	0.07672	0.01135	-0.03199	δ_{13}	-0.00013*		-0.00018**
α_2	-0.15291*	0.13315	-0.06130	δ_{14}	0.00095**		-0.00009
α_3	-0.03769	-0.38181	-0.49393**	δ_{15}	0.00004		-0.00010·
δ_1	-0.00008	-0.00003*	0.00084*	δ_{16}	-0.00016**		0.00007
δ_2	0.00036	0.00154*	0.00014	δ_{17}			0.01165***
δ_3	-0.00016**	0.00012*	0.00093	δ_{18}			0.00004
δ_4	-0.00001		0.00006	δ_{19}			0.00115
δ_5	-0.00012*		0.00466	δ_{20}			-0.00001
δ_6	-0.00013*		-0.00001	δ_{21}			-0.00004
δ_7	0.00001		0.00001	δ_{22}			0.00215*
δ_8	-0.00013·		0.00013	δ_{23}			-0.00001
δ_9	-0.00019**		0.00417	δ_{24}			0.00015
δ_{10}	-0.00004		0.00008	δ_{25}			-0.00013*
δ_{11}	-0.00017*		-0.00012·				

The constant is significant for all three stocks. α_2 is significant and negative for AAPL. This means that the lagged weekly upside volatility has a negative effect on the volatility today. The same conclusion holds for AKAM for α_3 and thus the lagged monthly upside volatility. Furthermore, structural change dummies are regularly significant for all three stocks.

5.1.3 Out-of-sample analysis

I use the rolling fixed-window prediction method for the out-of-sample estimation. This method is also used in Gong and Lin (2021). This method uses a rolling window of 1000 observations for each estimation and prediction. This means that for every single forecast, the ICSS algorithm is performed, as well as the estimation of the HAR-UV-SC parameters. Having 2658 observations, I have 1658 upside volatility forecasts. These volatility forecasts are used to sort the stocks into terciles every day. The same procedure

is performed as before, where I use a rolling window of four years. This leaves us with approximately two and a half years of output. Figure 9 shows the difference in return, overnight vs intraday, for the three different terciles, which are sorted on high, medium and low VOL_{t-1}^{+}.

Figure 9 shows the difference in returns when sorting on the estimated upside volatilities by the HAR-UV-SC model. Sorting on these estimates is profitable as the difference is significantly different from zero for the high tercile. This means a non-zero profit, when using this strategy for the last four years using the HAR-UV-SC estimates. The medium tercile is not significantly different from zero for a 5% level and the low tercile is even lower. Although the estimates enable a profit, the results is by far not as pronounced as when using realized upside volatilities. This could be due to the simplicity of the HAR-UV-SC model, which in fact only uses autoregressive terms and structural changes. This model could easily be extended, although this is not the aim of the paper.

5.2 DCS-EGARCH

After finding thorough evidence of an overnight anomaly and the relatively easy forecasting of upside volatility with the cause of exploiting this anomaly, I use the anomaly and the interaction of overnight and intraday returns to model the overnight and intraday volatility separately. For this purpose, I first estimate the base specification as given in Linton and Wu (2020). Then I try to improve this model by adding information found in the data section. I analyse the impact of the incorporation of the new variables. Then I estimate the coupled component DCS-EGARCH model of Linton and Wu (2020). I extend the coupled component from Linton and Wu (2020) in two dimensions. I first add the data from 2017-2022 to the model. Secondly, I change this model with insights from Harvey and Lange (2018) to model the long run (volatility) in a different way. This model will be called the two-component DCS-EGARCH.

For this analysis I use stocks from the Dow 30, which have data available since 1993. Eight stocks are removed from the sample due to few data (CRM, DOW, GS and V) and incorrect/incomplete data before 2001 (BA, CAT, DIS and KO), which leads to biased parameter estimates. The 22 stocks I use for the analysis are: AAPL, AMGN, AXP, CSCO, CVX, HD, HON, IBM, INTC, JNJ, JPM, MCD, MMM, MRK, MSFT, NKE, PG, TRV, UNH, VZ, WBA and WMT.

Figure 9: Difference in return for 3 sorts on different values of upside close-to-close volatility yesterday using the HAR-UV-SC for a four year rolling window
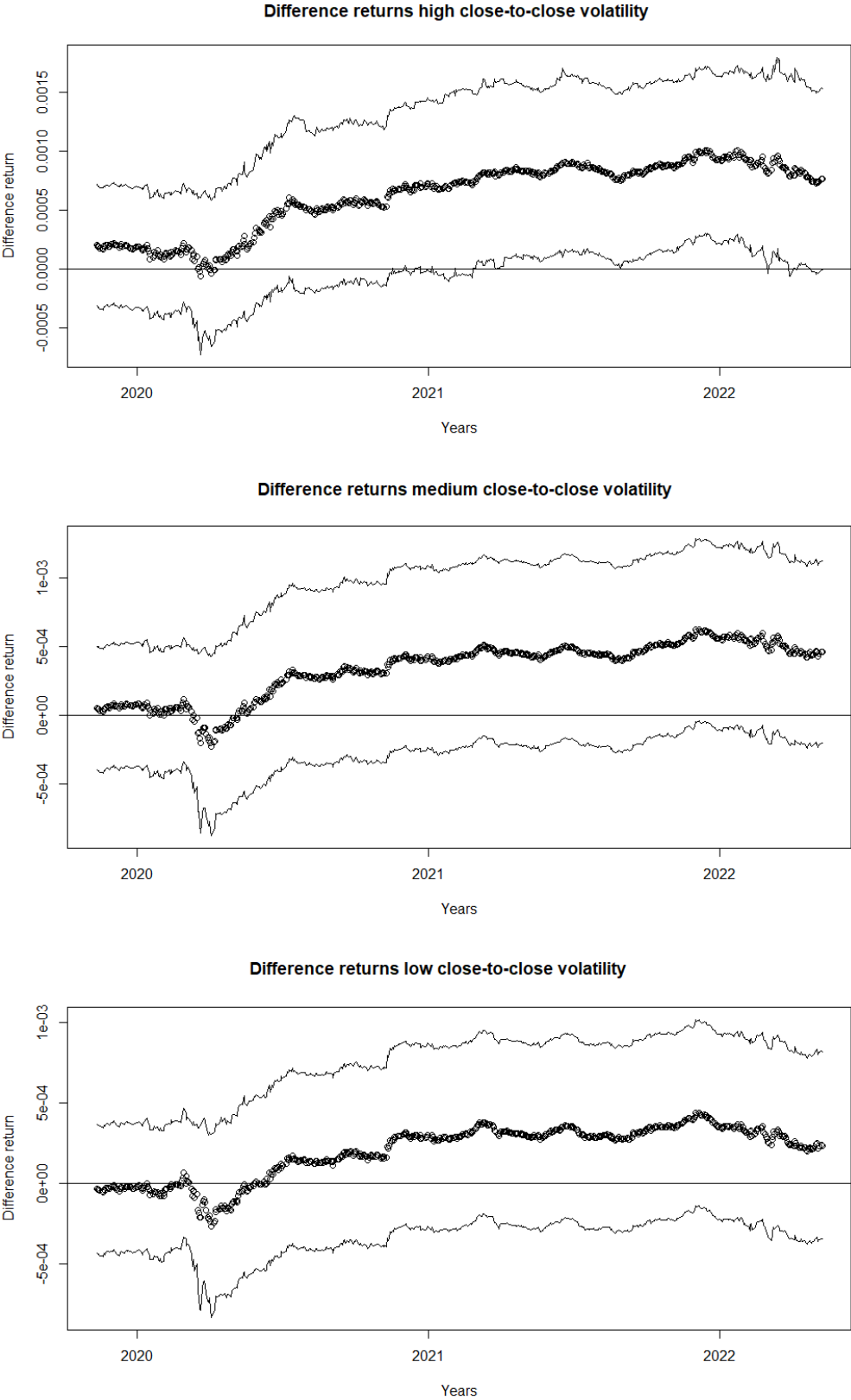
5.2.1 Standard base specification

I first estimate the standard base specification used by Linton and Wu (2020), as shown in equation (16). Table 6 shows the parameters estimates for the standard base specification for the period 4 Janaury 1993 until 3 August 2022. The values are close, but not identical, to the estimates in Linton and Wu (2020), which is to be expected as five years of data has been added. I generally draw the same conclusion, namely a positive δ for ten out of twelve significant values. In combination with a negative π_{11} for all significant values, which means that both overnight and intraday returns have a negative effect on subsequent intraday returns. π_{12} and π_{21} have, considering only significant estimates, seven negative and five positive, and eight negative and three positive values respectively. No unambiguous conclusion can be derived from those estimates. However, in contradiction with Linton and Wu (2020), I find twelve negative out of twelve significant values for π_{22}, which means a negative effect of the overnight return on the subsequent overnight return. This could be explained by the big crashes during the COVID-19 pandemic, which mostly occurred overnight and were of relatively large magnitude, as seen in the data section. Finally, the parameters estimates for μ_D and μ_N are positive for most stocks, 18 and 17 times respectively.

5.2.2 Adjusted base specification

The adjusted coupled component model has an adjustment on the base specification, which can be found in equation (34). I incorporate insights from the data with this specification, namely the overnight anomaly. As the overnight anomaly is only present in abundance after the start of the COVID-19 pandemic, I first consider the parameter estimates of this model with data from May 2020 to May 2022. Table 7 shows the parameter estimates for the adjusted base specification for the period May 2020 until May 2022. I see different dynamics for this specific period. Although δ is positive (seven times out of seven significant estimates) and π_{11} is negative again (five times out of seven significant estimates), I find a more pronounced pattern for π_{12}, π_{21} and π_{22}. π_{12} is positive (six out seven) and π_{21} is negative (five out five). This means, for those particular stocks, day returns have the same sign as night returns the day before and that day returns have a negative effect on subsequent night returns. π_{22} is negative again (eight out of nine), meaning a negative effect of the overnight return on the subsequent overnight return. The

new parameters, ξ_D and ξ_N, follow my expectations. ξ_D is most of the time negative or zero, and ξ_N is positive or zero. This explains the positive difference found in earlier (the positive difference in the return due to close-to-close volatility), and the addition of these parameters is in that sense valuable, as some parameters are significantly different from zero.

Table 8 in Appendix C gives the parameter estimates of the adjusted model. I find ten positive values out of 13 significant values. π_{11} is also negative again among most stocks. This is all in line with earlier results. π_{12} and π_{21} have no clear pattern, just as in the standard model for this time period. Also π_{22} is negative for ten out of ten significant stocks and zero otherwise. The interesting thing is the number of significant values among ξ_D and ξ_N. Although not consistent in sign, more than eight and thirteen significant estimates are found respectively. The added variables are expected to have a particular sign in the subsample beginning in 2020, but these variables thus also have predictable power in the entire sample. This could potentially make the upcoming volatility models more efficient.

To directly see the result of the potential efficiency increase, the used innovations, namely u_t^k, should be analysed from both base specifications. Figure 29 and Figure 30 show respectively the innovations u_t^D and u_t^N from both models plotted against each other to see if the changed base specification gives rise to a different set of innovations. This is interesting as the innovations are the only input to the DCS-EGARCH models, as can be seen in equation (17).

The figures show that the innovations from both models are almost identical. This could be seen as a trivial case, as both models look alike and only differ in two variables. However, if I plot the innovations from the adjusted model against a model with only a constant, the same pattern, innovations on the 45 degree line, evolves. I can thus conclude that the base specification is not of big influence to the outcome of the eventual models. Therefore I use the standard base specification in the upcoming models. On the other hand, the absence of such a influence is beneficial in the way that the model is robust to the chosen base specification.

5.2.3 Coupled component

I estimate the coupled component model by optimizing the likelihood functions in equation (24) and equation (25). After repeatedly optimizing these functions sequentially, I end up with an optimized set of parameters ϕ, as in equation (20), and the long run function $\sigma^k(s)$. The parameters ϕ can be found in Table 9 and in Table 10. ω_D is mostly positive and always larger than ω_N, which is always negative. It should be noted that I consider an exponential model, and that ω^k, the unconditional mean of the short run volatility, can not be negative in exponential form. The intraday short run volatility is thus larger than the overnight short run volatility. β_D and β_N are large, but significantly smaller than one, indicating a stable, yet autoregressive, process. However, these terms are smaller than in Linton and Wu (2020) suggesting less correlation in short term volatility in the period 2017 to 2022. γ_D and ρ_D are always positive and significant. The same holds for γ_N and ρ_N. This implies, in combination with the significant and negative terms γ_D^*, ρ_D^*, γ_N^* and ρ_N^*, that negative returns are followed by higher volatility. The values are roughly the same as in Linton and Wu (2020). This does not apply to ν_D and ν_N. These parameters refer to the degree of freedom from the distribution of volatilities. ν_D is lower on average (value of 2.92) and ν_N is larger on average (value of 8.45). This means more leptokurtic overnight volatilities and the other way around for intraday returns. The earlier seen data already indicates that COVID-19 crashes mostly occurred during the night, giving rise to a more leptokurtic distribution. In combination with smaller ω_k for overnight returns, I conclude that overnight returns are less volatile but their distribution has more kurtosis.

A more formal way of showing the difference in dynamics between overnight and intraday volatility is conducting a Wald test on the parameter estimates. The p-values of these tests can be found in Table 11 just as the null hypothesis. The null hypothesis states equality between the overnight and intraday parameters. The equality of the unconditional mean ω_k and the degree-of-freedom parameter ν_k are rejected for all stocks. The parameters γ_k, γ_k^*, ρ_k and ρ_k^* are seldom rejected. However, in contrast to Linton and Wu (2020), I reject the equality of β_k very often. This means that the autoregressive dynamics have changed during the last five years, probably caused by the reversals and crashes during March 2020. This results is also reflected in the p-values of the joint null hypothesis, which is also more often rejected. Short term dynamics have therefore diverged in the last couple of years for intraday versus overnight volatility.

Figure 31 presents the long run component $\sigma^k(s)$. This function is optimized repeatedly to convergence. It is important to remember that both functions, intraday and overnight, are standardized multiple times. The intraday long run volatility is actually higher than the overnight long run volatility. However, using this approach the long run relative dynamics can be observed. For most stocks, the overnight component is smaller than before the financial crisis (second vertical grey dotted line) and is higher than the intraday component after. Another communal characteristic, for both intraday and overnight, are the maxima around the crisis periods, indicated by the grey dotted lines. The dynamics during the pandemic differ from the dynamics during the other two crises periods. Relative overnight volatilities rise higher during this crisis, while rising to the same relative level as intraday volatilities during the other two crises.

The ratio of total overnight to total intraday volatility, as given in equation (38), is shown in Figure 32. The ratio is increasing for almost all stocks during the sample period. Most stocks have the largest peak during the corona crisis, but another often appearing peak is found around 2011/2012. This is the period when the long run (standardized) overnight volatility became relatively larger than its intraday opposite. The interpretation of the absolute value of the ratio, sometimes greater than one, is not that simple. The ratio uses the total volatility, which is a combination of the long and short run component. Although the short run component is reliable, the long run component is standardized repeatedly and the ratio can therefore not be interpreted as a fair ratio. However, the increase of this ratio does have a nice interpretation as a relative increase in overnight to intraday volatility.

I consider the total volatility for each stock in Figure 33. The definition for the total volatility is of great influence on the given results. The total volatility consists of both the long and short run component. Both are in practice greater in magnitude for intraday returns. The long run is however standardized. Although the short run is larger, the total volatility does not differ that much in size. This is due to the scalar $\frac{\nu_k}{\nu_k-2}$. This scalar goes to one for ν going to infinity. Intraday returns have less kurtosis with a average ν_D of 8.45. ν_N is 2.92 on average. As a result, the total overnight volatility is scaled by 3.2, while the total intraday volatility is scaled by 1.3. In the figure, this comes down to a relative scaling of 1.6 $\left(\frac{\sqrt{8.45/6.45}}{\sqrt{2.92/0.92}}\right)$ in favour of the overnight volatility. Although the scaling is reasonable, as it includes the heavy tails of the overnight returns, it remains

the question if it should be included in a total volatility equation. Nevertheless, the most important feature of the Figure is whether or not both time series converge, diverge or remain at the same relative height. Basically every two time series converge over the sample period. This is due to the decrease of total intraday volatility after the dot-com bubble. The ratio of overnight to intraday total volatility increases as a result and is in accordance with Figure 32. Overnight returns are also found to top intraday returns in absolute magnitude during crises periods as indicated by the greater total volatility in these time intervals.

Finally, I consider the t-statistics from the constancy of ratio test in Figure 34. The pattern of these t-statistics is in line with the ratios of overnight to intraday volatility, namely increasing over time. As the test is considered with respect to the mean, all t-statistics cross the 95% confidence bounds in approximately one half on the time series. Stocks, such as WBA and WMT, which have a rather constant ratio, fall between these bounds for most periods and thus have a constant volatility ratio. However, most stocks have an increasing volatility ratio and the null hypothesis of a constant ratio is rejected for most periods.

5.2.4 two-component

The estimation procedure of the two-component differs from the coupled component. Instead of optimizing the short and long run component sequentially, the short and long run component are estimated simultaneously. This make it more time-efficient. Both components are estimated using a filter. The long run from the coupled component uses kernel technology giving it a relatively smooth function, although it is not perfectly smooth as the wider the kernel, the smoother the function. A filter has by default a more shaky pattern. To enable a fair comparison between both specifications (coupled and two-component), I use a quadratic spline to transform the long run component $\lambda_{1,t}^k$ into a smooth function. The results of these transformations can be found in Figure 35. $\lambda_{1,t}^k$ is smoother than $\sigma^k(s)$ due to previous mentioned reasons. $\lambda_{1,t}^k$ follows $\sigma^k(s)$ really well. The overnight and intraday functions intersect at the same time and the dominant function matches as well. A difference is the curvature of the overnight function. Where both intraday and overnight have the same curvature in Figure 31, in Figure 35 the intraday function has relatively more curvature. This is explained by the standardization. This

happens multiple times in the coupled component estimation, but only once in the two-component estimation. The overnight functions are flatter for that reason. The same conclusions as for the coupled component hold. At approximately one half of the sample period, the overnight long run component becomes larger than the intraday long run component. Notice again that this is relative, as both functions have been standardized. Intraday volatility is actually larger.

Figure 36 displays the ratios of overnight to intraday total volatility. The patterns are roughly the same as for the coupled component model. Two things stand out. Firstly, the ratios are smoother and denser, as direct consequence of the smoother long run components. Secondly, the local minima and maxima do match up for both models. The ratios are increasing over the total interval and again I find maxima for all stocks around 2011/2012, mainly due to the relative larger long run component since that time.

After all, Figure 37 gives the total volatility for the intraday and overnight returns. The two-component model captures the total volatility well when using the coupled component as benchmark. The functions look again denser and smoother due to the quadratic spline. The value of K (see equation 32) equals 15, which captures the curvature nicely. Total intraday volatility converges to total overnight volatility generally. The volatility values on the y-axis for both models are not comparable and do not have a clear interpretation. This is due to the estimation procedure. The total volatility depends on ν_k, the short run component and the long run component. ν_k differs between models as it is optimized simultaneously or sequentially. The long run component is standardized ones or several times and the short run parameters also have a different dependece structure due to the estimation procedures. Therefore, we should concentrate on the relative behaviour of the overnight and intraday volatilities and the shape of the corresponding functions. These are definitely comparable. Although both methodologies differ substantially, the results are roughly the same in terms of pattern and relative dynamics. The results are thus robust to the methodology, which provides a stronger conclusion.

5.2.5 Case study: Amgen and Microsoft

Although the long run, ratio and total volatility of both models have been compared and discussed individually, it is interesting to zoom in on two particular stocks. In this way I can directly compare the two models more efficiently and cover some other characteristics

as well. The choice of these two stocks is random and could be replaced with any of the stocks. Amgen (AMGN) and Microsoft (MSFT) are the considered stocks.

Figure 10 compares the long run components of AMGN, with $\sigma^k(s)$ in the left subfigure and $\lambda_{1,t}^k$ on the right. The three vertical lines represent the following crises: dot-com bubble (10 March 2000), financial crisis (16 September 2008) and the corona crisis (9 March 2020). These vertical lines are the same for all upcoming figures. The intersections are almost parallel and the surpassion of the overnight long run volatility happens for both models around 2006. The relative importance of overnight volatility has thus been increasing over the sample period. The local maxima during the COVID-19 pandemic shows that it is and still is important to differiate between intraday and overnight returns. Extreme local values are visible in both subfigures and maxima are most of the time reached during the crises moments. The spline smoothness parameter K has a value of fifteen and manages to capture the same level of curvature.
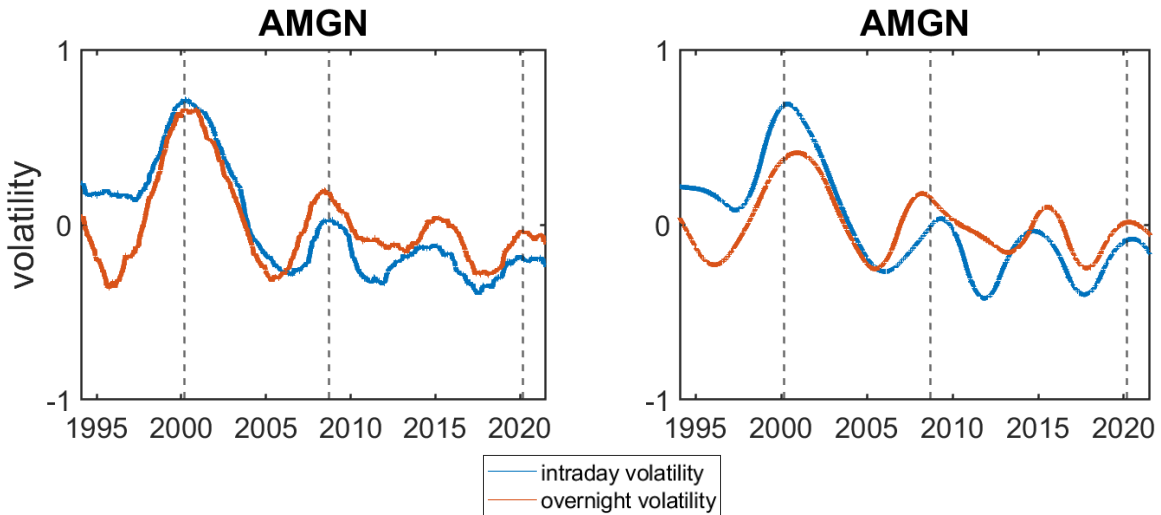
Figure 10: The long run component $\sigma^k(\cdot)$, for $k \in \{D, N\}$, of the coupled component (left) and the long run component $\lambda_{1,t}^k$, for $k \in \{D, N\}$, of the two-component (right).

The ratios of total volatilities can be found in Figure 11. The definition of these ratios are given in equation (38) and equation (39). The coupled component (left) and two-component (right) behave quite similar. The two-component is a bit smoother and denser due to the smoothness of the quadratic spline in the long run component. Both have maxima around 2009 and 2011. Both models capture an increasing trend and thus a relative increase of overnight volatility to intraday volatility.

Figure 11: The ratio of overnight to intraday volatility, where volatility is measured as $\sqrt{\frac{\nu_k}{\nu_k-2}\exp\left[2\lambda_t^k + 2\sigma_t^k\left(\frac{t}{T}\right)\right]}$ for the coupled component (left) and as $\sqrt{\frac{\nu_k}{\nu_k-2}\exp\left[2\omega_k + 2\lambda_{2,t}^k + 2\lambda_{1,t}^k\right]}$ for the two-component (right).

Although the (relative) ratio increase, it is interesting to plot both volatility separately as well. Figure 12 shows the total volatility for both models. The patterns by both EGARCH models are almost identical in terms of increase, decrease, local minima and local maxima. The scale differs by a multiple, but this is due to the difference in methodology. The scale is in any case not relevant, as the total volatility consists of standardized variables and parameters, which are optimized to a lesser extent. For this reason, the focus should lay on the dynamics. These are matches quite fairly. In both figures there is convergence of the time series, indicating an importance increase of the overnight volatility, already seen in Figure 11. Most maxima are during the crises periods as expected.

Now I consider the same analysis for the Microsoft stock. Figure 13 shows the long run components of both models, which have a lot of shared features. They have the same local maxima/minima, intersect at the same moments in time and have maxima at the indicated crises dates. The main difference is the level of smoothness. The long run volatility of the stock is thus model robust.

The total volatility ratio of MSFT is shown in Figure 14. The ratios behave differently at first sight. However, the maxima at 1998, 2005, 2012 and 2016 do match. One as well as the other have a drop during the dot-com bubble and the financial crisis, which is quite inconsistent with the other stocks, but consistent across models. In addition, the ratios are increasing over the entire sample period, but seem to stabilize to a certain degree.
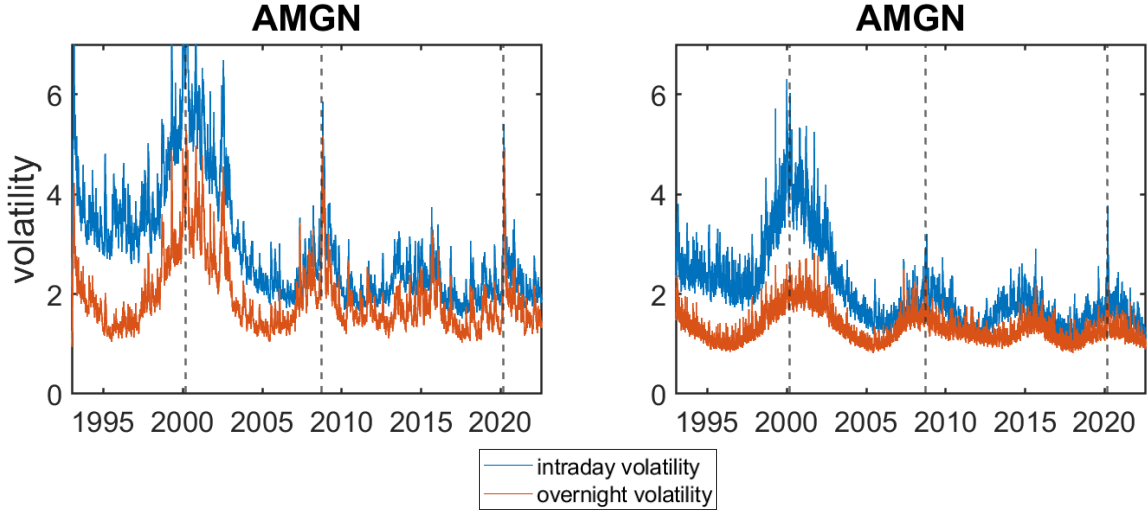
Figure 12: Total intraday and overnight volatility, measured as $\sqrt{\frac{\nu_k}{\nu_k-2}\exp\left[2\lambda_t^k + 2\sigma_t^k\left(\frac{t}{T}\right)\right]}$ for the coupled component (left) and as $\sqrt{\frac{\nu_k}{\nu_k-2}\exp\left[2\omega_k + 2\lambda_{2,t}^k + 2\lambda_{1,t}^k\right]}$ for the two-component (right).
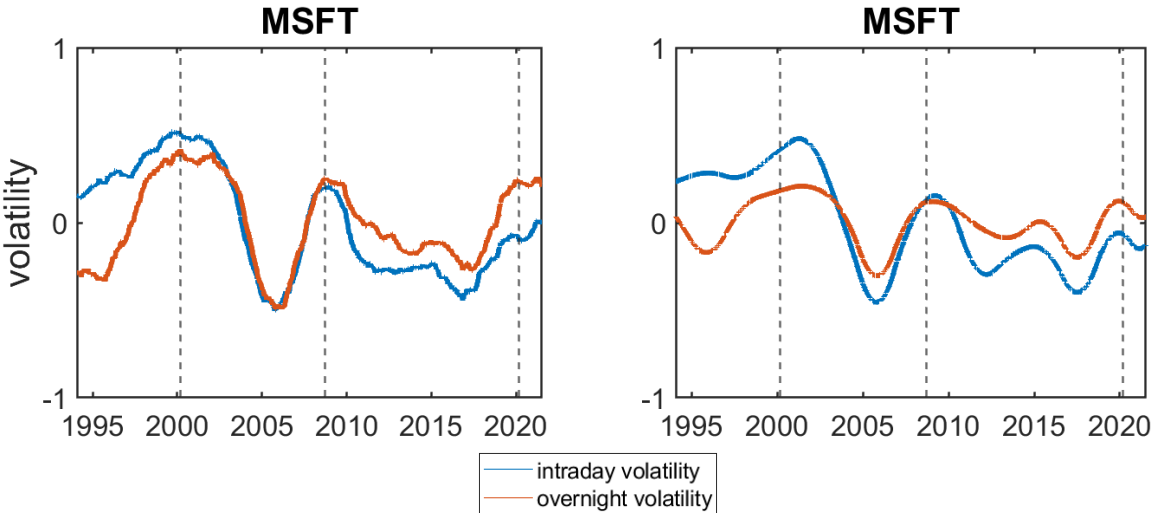
Figure 13: The long run component $\sigma^k(\cdot)$, for $k \in \{D, N\}$, of the coupled component (left) and the long run component $\lambda_{1,t}^k$, for $k \in \{D, N\}$, of the two-component (right).

The V-shape for the period 2020-2022 is not unusual, as seen in multiple stock ratios.

The total volatilities are depicted in Figure 15. Convergence of overnight and intraday returns, higher intraday volatility in absolute value, higher intraday volatility before the financial crisis in relative sense and the maxima during crises periods are all features of this Figure and the before discussed total volatility plots. These features are clearly matched in both models. The only difference is displayed in the scale, which is due the difference in methodology and caused by the (under-)optimizing of the short run parameters, as the

44
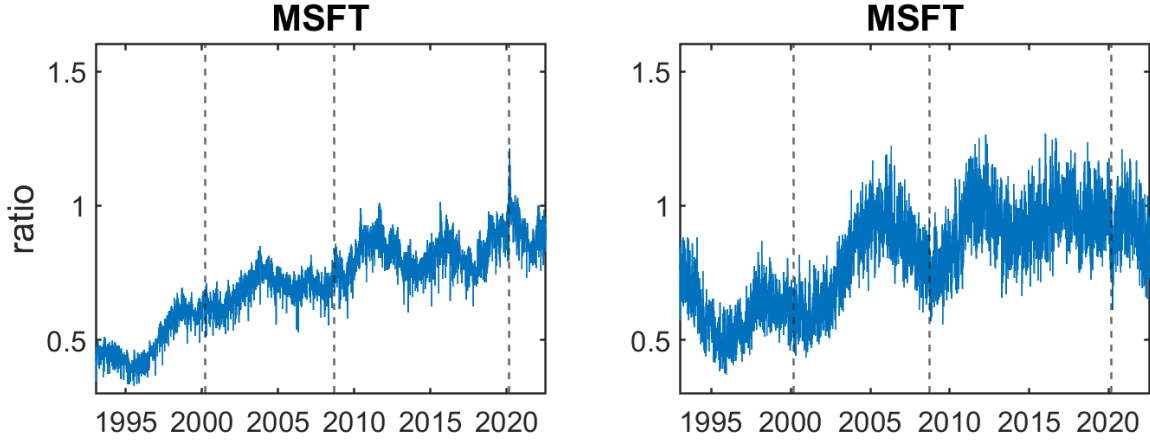
Figure 14: The ratio of overnight to intraday volatility, where volatility is measured as $\sqrt{\frac{\nu_k}{\nu_k-2}\exp\left[2\lambda_t^k + 2\sigma_t^k\left(\frac{t}{T}\right)\right]}$ 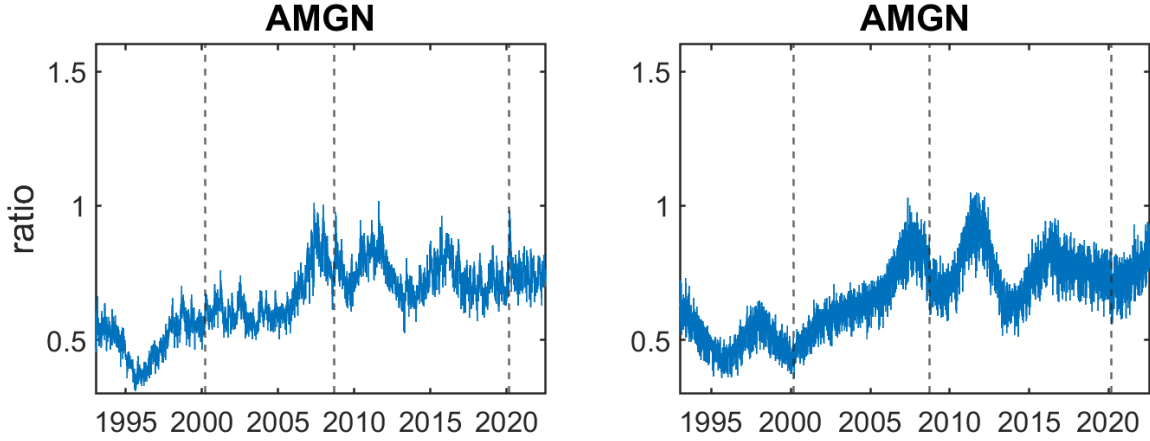for the coupled component (left) and as $\sqrt{\frac{\nu_k}{\nu_k-2}\exp\left[2\omega_k + 2\lambda_{2,t}^k + 2\lambda_{1,t}^k\right]}$ for the two-component (right).

long run components are actually matched in scale.
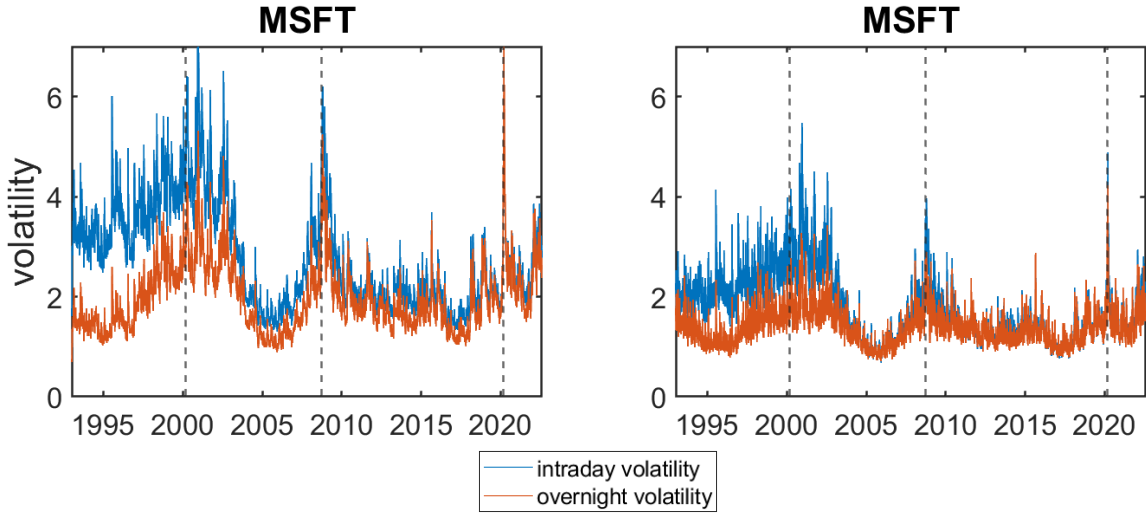
Figure 15: Total intraday and overnight volatility, measured as $\sqrt{\frac{\nu_k}{\nu_k-2}\exp\left[2\lambda_t^k + 2\sigma_t^k\left(\frac{t}{T}\right)\right]}$ for the coupled component (left) and as $\sqrt{\frac{\nu_k}{\nu_k-2}\exp\left[2\omega_k + 2\lambda_{2,t}^k + 2\lambda_{1,t}^k\right]}$ for the two-component (right).

I will now cover some characteristics which, due to the use of multiple functions, are hard to interpret when shown for all stocks at once as in Appendix C. These characteristics focus on the two-component model. Figure 16 shows the unstandardized long run filter $\lambda_{1,t}^k$ with their corresponding splines for AMGN and MSFT. The difference in long run volatility between intraday and overnight returns stands out. This provides the evidence

45

that the total volatility (ratios) should be evaluated with care. Splines are fitted to the filter with K equal to 5, 10 and 15. When K becomes larger, the spline is fitted to a greater extent to the filter, which will cause an increase in curvature. The choice of K is a typical bias-variance trade off when used for forecasting, but is solely based on linking the two models to the best extent. It turns out that K equal to 15 has the best fit, as this value is used among all long run components from the two-component model. The estimation procedure of the two-component uses a filter as explained in the methodology section. As a result, the long run filter $\lambda_{1,t}^k$ is not a smooth function as shown in the figure. In combination with the quadratic spline method, the long run component can be matched to $\sigma^k(s)$. The optimization procedure of the coupled component has this spline feature thus build-in in the sequential likelihood optimization. The 'smoothing' process in this likelihood optimization is caused by the kernel technology, which by definition uses a weighted average of observations (rolling window) resulting in a (relatively) smoothed function.
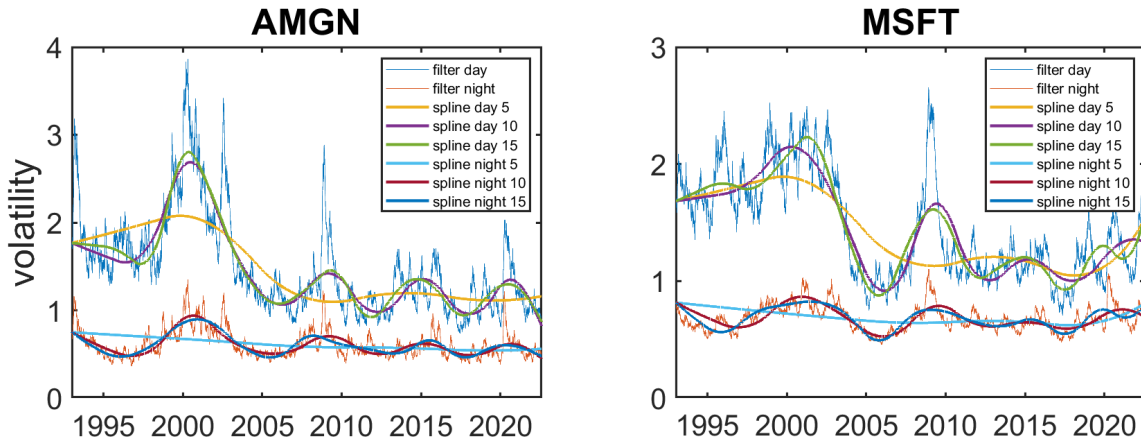
Figure 16: The long run filter $\lambda_{1,t}^k$ ($k \in \{D, N\}$) with splines for $K \in \{5, 10, 15\}$ of the two-component.

The unstandardized long run filters of intraday and overnight returns are depicted in Figure 17. This time in combination with the short run processes. The blue lines refer to the intraday volatility, where the red lines refer to the overnight volatility. The short run process $\lambda_{2,t}^k$ is shaky and moves around the unconditional mean ω_k of the short run process, which is larger for the intraday returns for all stocks (table 10). The long run filter $\lambda_{1,t}^k$ is less shaky. For both stocks, $\lambda_{1,t}^D$ converges to $\lambda_{1,t}^N$ over the sample period. The relative importance increase of overnight volatility is thus explained by a decrease of

intraday long run volatility, rather than by an increase of overnight long run volatility. This phenomenon is also visible for almost all stocks in Figure 33 and Figure 37. However, in those figures, the long run component is standardized and the result is mainly driven by the short run process and the relative change in long run volatility. Figure 17 displays that also the long run process complements this phenomenon.
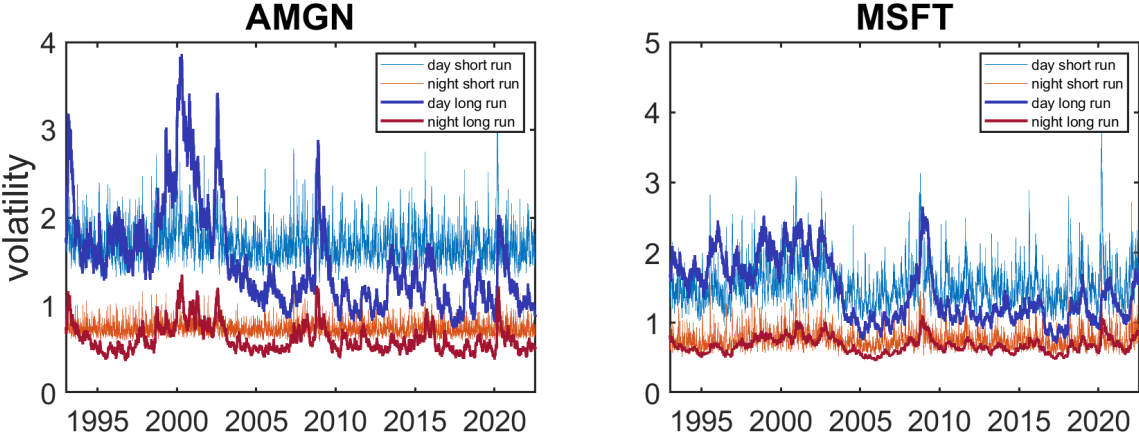
Figure 17: Short and long run component for intraday and overnight volatility of the two-component.
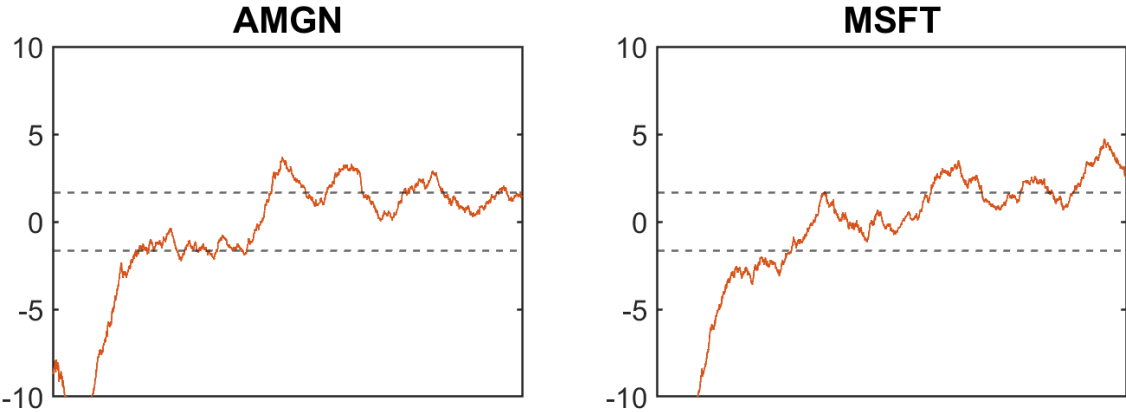
Figure 18: T-statistics of the constancy of ratio test for the ratio of intraday and overnight volatility of the coupled component.

Lastly, Figure 18 shows the t-statistics of the constancy of ratio test for the ratio of intraday and overnight volatility of the coupled component for both AMGN and MSFT. Both stocks have an increasing ratio and thus also an increasing t-statistic. Constancy is rejected for both stocks before the dot-com bubble and numerous times for shorts periods

after. Nevertheless, both stocks have a quite constant ratio since 2000. The constancy of the ratio of MSFT is effected mostly by the COVID-19 crisis.

6 Conclusion

This study examines the difference between intraday and overnight returns. The empirical results show that overnight minus intraday returns are significantly greater than zero for the period 2016-2022 when sorting on upside close-to-close volatility. This indicates a change of retail investor behaviour and activity. The difference in return is robust against the dynamics around market opening and closure, which are volatile moments.

Adding multiple components to dynamic conditional score EGARCH models can provide for separately modelling the returns allowing for different dynamical properties. I develop the two-component model, which nicely captures all features from the coupled component model and is more time-efficient.

Overnight volatility increases in relative importance, which is caused by a decrease of intraday volatility over the period 1993-2022. Overnight volatility however stays smaller than intraday volatility in absolute terms, although overnight returns are more leptokurtic.

In conclusion, intraday and overnight returns have quite different dynamics and should be modelled accordingly. This could be done using a DCS-EGARCH model, as these models are robust to the exact specification.

This analysis could be extended in several directions. One interesting direction would be to use retail investor data to test the direct relation between (upside) volatility and retail investor strategies. Next to that, the analysis could be performed on several different markets and products. Additionally, the assumptions of the kernel size, the curvature parameter of the spline and the non-linear optimization could be investigated.

Bibliography

K. Aretz and S. M. Bartram. Making money while you sleep? Anomalies in international day and night returns. <u>Anomalies in International Day and Night Returns (July 24, 2015)</u>, 2015.

O. E. Barndorff-Nielsen, S. Kinnebrock, and N. Shephard. Measuring downside risk-realised semivariance. <u>CREATES Research Paper</u>, (2008-42), 2008.

V. A. Basdekidou et al. The overnight return temporal market anomaly. <u>International Journal of Economics and Finance</u>, 9(3):1–10, 2017.

H. Berkman, P. D. Koch, L. Tuttle, and Y. J. Zhang. Paying attention: Overnight returns and the hidden cost of buying at the open. <u>Journal of Financial and Quantitative Analysis</u>, 47(4):715–741, 2012.

V. L. Bernard. Cross-sectional dependence and problems in inference in market-based accounting research. <u>Journal of Accounting Research</u>, pages 1–48, 1987.

B. S. Branch and A. J. Ma. The overnight return, one more anomaly. <u>One More Anomaly (September 6, 2006)</u>, 2006.

B. S. Branch and A. J. Ma. Overnight return, the invisible hand behind intraday returns? <u>Journal of Applied Finance (Formerly Financial Practice and Education)</u>, 22(2), 2012.

T. T. Cai and M. Qiu. International evidence on overnight return anomaly. <u>Unpublished working paper. Massey University</u>, 2009.

M. J. Cooper, M. T. Cliff, and H. Gulen. Return differences between trading and non-trading hours: Like night and day. <u>Unpublished working paper. Virginia Tech</u>, 2008.

F. Corsi. A simple approximate long-memory model of realized volatility. <u>Journal of Financial Econometrics</u>, 7(2):174–196, 2009.

R. F. Engle and J. G. Rangel. The spline-GARCH model for low-frequency volatility and its global macroeconomic causes. <u>The Review of Financial Studies</u>, 21(3):1187–1222, 2008.

K. R. French and R. Roll. Stock return variances: The arrival of information and the reaction of traders. Journal of Financial Economics, 17(1):5–26, 1986.

X. Gong and B. Lin. Effects of structural changes on the prediction of downside volatility in futures markets. Journal of Futures Markets, 41(7):1124–1153, 2021.

A. Harvey and R.-J. Lange. Modeling the interactions between volatility and returns using EGARCH-M. Journal of Time Series Analysis, 39(6):909–919, 2018.

A. C. Harvey. Dynamic models for volatility and heavy tails: with applications to financial and economic time series, volume 52. Cambridge University Press, 2013.

T. Hendershott, D. Livdan, and D. Rösch. Asset pricing: A tale of night and day. Journal of Financial Economics, 138(3):635–662, 2020.

H. Hong and J. Wang. Trading and returns under periodic market closures. The Journal of Finance, 55(1):297–354, 2000.

C. Inclan and G. C. Tiao. Use of cumulative sums of squares for retrospective detection of changes of variance. Journal of the American Statistical Association, 89(427):913–923, 1994.

C. X. Jiang, T. Likitapiwat, and T. H. McInish. Information content of earnings announcements: Evidence from after-hours trading. Journal of Financial and Quantitative Analysis, 47(6):1303–1330, 2012.

M. A. Kelly and S. P. Clark. Returns in trading versus non-trading hours: The difference is day and night. Journal of Asset Management, 12(2):132–145, 2011.

M.-E. Lachance. Night trading: Lower risk but higher returns? Unpublished working paper. San Diego State University, 2015.

O. Ledoit and M. Wolf. Robust performance hypothesis testing with the Sharpe ratio. Journal of Empirical Finance, 15(5):850–859, 2008.

O. Linton and J. Wu. A coupled component DCS-EGARCH model for intraday and overnight volatility. Journal of Econometrics, 217(1):176–201, 2020.

F. A. Longstaff. How much can marketability affect security values? The Journal of Finance, 50(5):1767–1774, 1995.

D. Lou, C. Polk, and S. Skouras. A tug of war: Overnight versus intraday expected returns. Journal of Financial Economics, 134(1):192–213, 2019.

E. M. Miller. Risk, uncertainty, and divergence of opinion. The Journal of Finance, 32 (4):1151–1168, 1977.

D. Muravyev and X. C. Ni. Why do option returns change sign from day to night? Journal of Financial Economics, 136(1):219–238, 2020.

W. K. Newey and K. D. West. A simple, positive semi-definite, heteroskedasticity and autocorrelationconsistent covariance matrix. Econometrica, 55(3):703–708, 1987.

J. D. J. Opdyke. Comparing Sharpe ratios: So where are the p-values? Journal of Asset Management, 8(5):308–336, 2007.

R. A. Wood, T. H. McInish, and J. K. Ord. An investigation of transactions data for NYSE stocks. The Journal of Finance, 40(3):723–739, 1985.

Appendix A   Data composition

A.1   S&P500

The main sample consists of the 504 S&P500 stocks as of April 4, 2022. This includes the changes on April 4, 2022, when Camden (CPT) was added and People's United Financial (PBCT) was removed. Although the name of the S&P500 would anticipate otherwise, the index contains 504 stocks, because five constituents have two share classes (Alphabet, Discovery, Fox Corporation, News Corp, Under Armour). Table 2 gives the exact composition of the sample.

Table 2: Main sample: S&P500 constituents

Ticker	Name	Ticker	Name
MMM	3M	AOS	A. O. Smith
ABT	Abbott Laboratories	ABBV	AbbVie
ABMD	Abiomed	ACN	Accenture
ATVI	Activision Blizzard	ADM	ADM
ADBE	Adobe	AAP	Advance Auto Parts
AMD	Advanced Micro Devices	AES	AES Corp
AFL	Aflac	A	Agilent Technologies
APD	Air Products & Chemicals	AKAM	Akamai Technologies
ALK	Alaska Air Group	ALB	Albemarle Corporation
ARE	Alexandria Real Estate Equities	ALGN	Align Technology
ALLE	Allegion	LNT	Alliant Energy
ALL	Allstate Corp	GOOGL	Alphabet (Class A)
GOOG	Alphabet (Class C)	MO	Altria Group
AMZN	Amazon	AMCR	Amcor
AEE	Ameren Corp	AAL	American Airlines Group
AEP	American Electric Power	AXP	American Express
AIG	American International Group	AMT	American Tower
AWK	American Water Works	AMP	Ameriprise Financial
ABC	AmerisourceBergen	AME	Ametek
AMGN	Amgen	APH	Amphenol
ADI	Analog Devices	ANSS	Ansys
ANTM	Anthem	AON	Aon
APA	APA Corporation	AAPL	Apple

Table 2: Main sample: S&P500 constituents

Ticker	Name	Ticker	Name
AMAT	Applied Materials	APTV	Aptiv
ANET	Arista Networks	AJG	Arthur J. Gallagher & Co.
AIZ	Assurant	T	AT&T
ATO	Atmos Energy	ADSK	Autodesk
ADP	Automatic Data Processing	AZO	AutoZone
AVB	AvalonBay Communities	AVY	Avery Dennison
BKR	Baker Hughes	BLL	Ball Corp
BAC	Bank of America	BBWI	Bath & Body Works Inc.
BAX	Baxter International	BDX	Becton Dickinson
BRKB.VI	Berkshire Hathaway	BBY	Best Buy
BIO	Bio-Rad Laboratories	TECH	Bio-Techne
BIIB	Biogen	BLK	BlackRock
BK	BNY Mellon	BA	Boeing
BKNG	Booking Holdings	BWA	BorgWarner
BXP	Boston Properties	BSX	Boston Scientific
BMY	Bristol Myers Squibb	AVGO	Broadcom
BR	Broadridge Financial Solutions	BRO	Brown & Brown
BF-B	Brown–Forman	CHRW	C. H. Robinson
CDNS	Cadence Design Systems	CZR	Caesars Entertainment
CPB	Campbell Soup	COF	Capital One Financial
CAH	Cardinal Health	KMX	CarMax
CCL	Carnival Corporation	CARR	Carrier Global
CTLT	Catalent	CAT	Caterpillar
CBOE	Cboe Global Markets	CBRE	CBRE
CDW	CDW	CE	Celanese
CNC	Centene Corporation	CNP	CenterPoint Energy
CDAY	Ceridian	CERN	Cerner
CF	CF Industries	CRL	Charles River Laboratories
SCHW	Charles Schwab Corporation	CHTR	Charter Communications
CVX	Chevron Corporation	CMG	Chipotle Mexican Grill
CB	Chubb	CHD	Church & Dwight
CI	Cigna	CINF	Cincinnati Financial
CTAS	Cintas Corporation	CSCO	Cisco Systems
C	Citigroup	CFG	Citizens Financial Group

Continued on Next Page

Table 2: Main sample: S&P500 constituents

Ticker	Name	Ticker	Name
CTXS	Citrix Systems	CLX	Clorox
CME	CME Group	CMS	CMS Energy
KO	Coca-Cola Company	CTSH	Cognizant Technology Solutions
CL	Colgate-Palmolive	CMCSA	Comcast
CMA	Comerica	CAG	Conagra Brands
COP	ConocoPhillips	ED	Consolidated Edison
STZ	Constellation Brands	CPRT	Copart
GLW	Corning	CTVA	Corteva
COST	Costco	CTRA	Coterra
CCI	Crown Castle	CSX	CSX
CMI	Cummins	CVS	CVS Health
DHI	D. R. Horton	DHR	Danaher Corporation
DRI	Darden Restaurants	DVA	DaVita
DE	Deere & Co.	DAL	Delta Air Lines
XRAY	Dentsply Sirona	DVN	Devon Energy
DXCM	DexCom	FANG	Diamondback Energy
DLR	Digital Realty Trust	DFS	Discover Financial Services
DISCA	Discovery (Series A)	DISCK	Discovery (Series C)
DISH	Dish Network	DG	Dollar General
DLTR	Dollar Tree	D	Dominion Energy
DPZ	Domino's Pizza	DOV	Dover Corporation
DOW	Dow	DTE	DTE Energy
DUK	Duke Energy	DRE	Duke Realty Corp
DD	DuPont	DXC	DXC Technology
EMN	Eastman Chemical	ETN	Eaton Corporation
EBAY	eBay	ECL	Ecolab
EIX	Edison International	EW	Edwards Lifesciences
EA	Electronic Arts	LLY	Eli Lilly & Co
EMR	Emerson Electric Company	ENPH	Enphase Energy
ETR	Entergy	EOG	EOG Resources
EFX	Equifax	EQIX	Equinix
EQR	Equity Residential	ESS	Essex Property Trust
EL	Estée Lauder Companies	ETSY	Etsy
RE	Everest Re	EVRG	Evergy

Continued on Next Page

Table 2: Main sample: S&P500 constituents

Ticker	Name	Ticker	Name
ES	Eversource Energy	EXC	Exelon
EXPE	Expedia Group	EXPD	Expeditors
EXR	Extra Space Storage	XOM	ExxonMobil
FFIV	F5 Networks	FB	Facebook
FAST	Fastenal	FRT	Federal Realty Investment Trust
FDX	FedEx	FIS	Fidelity National Information Services
FITB	Fifth Third Bancorp	FRC	First Republic Bank
FE	FirstEnergy	FISV	Fiserv
FLT	Fleetcor	FMC	FMC Corporation
F	Ford	FTNT	Fortinet
FTV	Fortive	FBHS	Fortune Brands Home & Security
FOXA	Fox Corporation (Class A)	FOX	Fox Corporation (Class B)
BEN	Franklin Resources	FCX	Freeport-McMoRan
CEG	Gap	GRMN	Garmin
IT	Gartner	GNRC	Generac Holdings
GD	General Dynamics	GE	General Electric
GIS	General Mills	GM	General Motors
GPC	Genuine Parts	GILD	Gilead Sciences
GPN	Global Payments	GL	Globe Life
GS	Goldman Sachs	HAL	Halliburton
SEDG	Hanesbrands	HAS	Hasbro
HCA	HCA Healthcare	PEAK	Healthpeak Properties
HSIC	Henry Schein	HES	Hess Corporation
HPE	Hewlett Packard Enterprise	HLT	Hilton Worldwide
HOLX	Hologic	HD	Home Depot
HON	Honeywell	HRL	Hormel
HST	Host Hotels & Resorts	HWM	Howmet Aerospace
HPQ	HP	HUM	Humana
HBAN	Huntington Bancshares	HII	Huntington Ingalls Industries
IBM	IBM	IEX	IDEX Corporation
IDXX	Idexx Laboratories	MOH	IHS Markit
ITW	Illinois Tool Works	ILMN	Illumina
INCY	Incyte	IR	Ingersoll Rand
INTC	Intel	ICE	Intercontinental Exchange

Continued on Next Page

Table 2: Main sample: S&P500 constituents

Ticker	Name	Ticker	Name
IFF	International Flavors & Fragrances	IP	International Paper
IPG	Interpublic Group	INTU	Intuit
ISRG	Intuitive Surgical	IVZ	Invesco
IPGP	IPG Photonics	IQV	IQVIA
IRM	Iron Mountain	JBHT	J. B. Hunt
JKHY	Jack Henry & Associates	J	Jacobs Engineering Group
SJM	JM Smucker	JNJ	Johnson & Johnson
JCI	Johnson Controls	JPM	JPMorgan Chase
JNPR	Juniper Networks	EPAM	Kansas City Southern
K	Kellogg's	KEY	KeyCorp
KEYS	Keysight Technologies	KMB	Kimberly-Clark
KIM	Kimco Realty	KMI	Kinder Morgan
KLAC	KLA Corporation	KHC	Kraft Heinz
KR	Kroger	LHX	L3Harris Technologies
LH	LabCorp	LRCX	Lam Research
LW	Lamb Weston	LVS	Las Vegas Sands
SBNY	Leggett & Platt	LDOS	Leidos
LEN	Lennar	LNC	Lincoln National
LIN	Linde	LYV	Live Nation Entertainment
LKQ	LKQ Corporation	LMT	Lockheed Martin
L	Loews Corporation	LOW	Lowe's
LUMN	Lumen Technologies	LYB	LyondellBasell
MTB	M&T Bank	MRO	Marathon Oil
MPC	Marathon Petroleum	MKTX	MarketAxess
MAR	Marriott International	MMC	Marsh & McLennan
MLM	Martin Marietta Materials	MAS	Masco
MA	Mastercard	MTCH	Match Group
MKC	McCormick & Company	MCD	McDonald's
MCK	McKesson Corporation	MDT	Medtronic
MRK	Merck & Co.	MET	MetLife
MTD	Mettler Toledo	MGM	MGM Resorts International
MCHP	Microchip Technology	MU	Micron Technology
MSFT	Microsoft	MAA	Mid-America Apartments
MRNA	Moderna	MHK	Mohawk Industries

Table 2: Main sample: S&P500 constituents

Ticker	Name	Ticker	Name
TAP	Molson Coors Beverage Company	MDLZ	Mondelez International
MPWR	Monolithic Power Systems	MNST	Monster Beverage
MCO	Moody's Corporation	MS	Morgan Stanley
MSI	Motorola Solutions	MSCI	MSCI
NDAQ	Nasdaq	NTAP	NetApp
NFLX	Netflix	NWL	Newell Brands
NEM	Newmont	NWSA	News Corp (Class A)
NWS	News Corp (Class B)	NEE	NextEra Energy
NLSN	Nielsen Holdings	NKE	Nike
NI	NiSource	NSC	Norfolk Southern
NTRS	Northern Trust	NOC	Northrop Grumman
NLOK	NortonLifeLock	NCLH	Norwegian Cruise Line Holdings
NRG	NRG Energy	NUE	Nucor
NVDA	Nvidia	NVR	NVR
NXPI	NXP	ORLY	O'Reilly Automotive
OXY	Occidental Petroleum	ODFL	Old Dominion Freight Line
OMC	Omnicom Group	OKE	Oneok
ORCL	Oracle	OGN	Organon & Co.
OTIS	Otis Worldwide	PCAR	Paccar
PKG	Packaging Corporation of America	PH	Parker-Hannifin
PAYX	Paychex	PAYC	Paycom
PYPL	PayPal	PENN	Penn National Gaming
PNR	Pentair	CPT	People's United Financial
PEP	PepsiCo	PKI	PerkinElmer
PFE	Pfizer	PM	Philip Morris International
PSX	Phillips 66	PNW	Pinnacle West Capital
PXD	Pioneer Natural Resources	PNC	PNC Financial Services
POOL	Pool Corporation	PPG	PPG Industries
PPL	PPL	PFG	Principal Financial Group
PG	Procter & Gamble	PGR	Progressive Corporation
PLD	Prologis	PRU	Prudential Financial
PTC	PTC	PEG	Public Service Enterprise Group
PSA	Public Storage	PHM	PulteGroup
PVH	PVH	QRVO	Qorvo

Continued on Next Page

Table 2: Main sample: S&P500 constituents

Ticker	Name	Ticker	Name
QCOM	Qualcomm	PWR	Quanta Services
DGX	Quest Diagnostics	RL	Ralph Lauren Corporation
RJF	Raymond James Financial	RTX	Raytheon Technologies
O	Realty Income Corporation	REG	Regency Centers
REGN	Regeneron Pharmaceuticals	RF	Regions Financial Corporation
RSG	Republic Services	RMD	ResMed
RHI	Robert Half International	ROK	Rockwell Automation
ROL	Rollins	ROP	Roper Technologies
ROST	Ross Stores	RCL	Royal Caribbean Group
SPGI	S&P Global	CRM	Salesforce
SBAC	SBA Communications	SLB	Schlumberger
STX	Seagate Technology	SEE	Sealed Air
SRE	Sempra Energy	NOW	ServiceNow
SHW	Sherwin-Williams	SPG	Simon Property Group
SWKS	Skyworks Solutions	SNA	Snap-on
SO	Southern Company	LUV	Southwest Airlines
SWK	Stanley Black & Decker	SBUX	Starbucks
STT	State Street Corporation	STE	Steris
SYK	Stryker Corporation	SIVB	SVB Financial
SYF	Synchrony Financial	SNPS	Synopsys
SYY	Sysco	TMUS	T-Mobile US
TROW	T. Rowe Price	TTWO	Take-Two Interactive
TPR	Tapestry	TGT	Target Corporation
TEL	TE Connectivity	TDY	Teledyne Technologies
TFX	Teleflex	TER	Teradyne
TSLA	Tesla	TXN	Texas Instruments
TXT	Textron	COO	The Cooper Companies
HIG	The Hartford	HSY	The Hershey Company
MOS	The Mosaic Company	TRV	The Travelers Companies
DIS	The Walt Disney Company	TMO	Thermo Fisher Scientific
TJX	TJX Companies	TSCO	Tractor Supply Company
TT	Trane Technologies	TDG	TransDigm Group
TRMB	Trimble	TFC	Truist Financial
TWTR	Twitter	TYL	Tyler Technologies

Table 2: Main sample: S&P500 constituents

Ticker	Name	Ticker	Name
TSN	Tyson Foods	USB	U.S. Bancorp
UDR	UDR	ULTA	Ulta Beauty
UAA	Under Armour (Class A)	UA	Under Armour (Class C)
UNP	Union Pacific	UAL	United Airlines
UPS	United Parcel Service	URI	United Rentals
UNH	UnitedHealth Group	UHS	Universal Health Services
VLO	Valero Energy	VTR	Ventas
VRSN	Verisign	VRSK	Verisk Analytics
VZ	Verizon Communications	VRTX	Vertex Pharmaceuticals
VFC	VF Corporation	VTRS	Viatris
V	Visa	VNO	Vornado Realty Trust
VMC	Vulcan Materials	WRB	W. R. Berkley Corporation
GWW	W. W. Grainger	WAB	Wabtec
WBA	Walgreens Boots Alliance	WMT	Walmart
WM	Waste Management	WAT	Waters Corporation
WEC	WEC Energy Group	WFC	Wells Fargo
WELL	Welltower	WST	West Pharmaceutical Services
WDC	Western Digital	FDS	Western Union
WRK	WestRock	WY	Weyerhaeuser
WHR	Whirlpool Corporation	WMB	Williams Companies
WTW	Willis Towers Watson	WYNN	Wynn Resorts
XEL	Xcel Energy	NDSN	Xilinx
XYL	Xylem	YUM	Yum! Brands
ZBRA	Zebra Technologies	ZBH	Zimmer Biomet
ZION	Zions Bancorp	ZTS	Zoetis

For the main analysis, stocks with less than ten years of data are removed. I end up with 456 stocks. The removed 48 stocks are: ABBV, ALLE, AMCR, ANET, APTV, BRKB.VI, CARR, CDAY, CDW, CEG, CFG, CTLT, CTVA, CZR, DOW, ENPH, EPAM, ETSY, FANG, FB, FOX, FOXA, FTV, HLT, HPE, HWM, IQV, IR, KEYS, KHC, LW, MRNA, NCLH, NOW, NWS, NWSA, OGN, OTIS, PAYC, PSX, PYPL, QRVO, SEDG, SYF, TWTR, UA, WRK, ZTS.

A.2   Institutional Ownership

When doing the analysis on institutional ownership, I lose, for mentioned reasons, six stocks. Stocks lost in institutional ownership: BF-B, CMCSA, DISCA, DISCK, GOOGL, MOS

A.3   Dow 30

The constituents of the Dow 30 can be found in Table 3. All stocks are present in the S&P500 and can thus be searched by name in Table 2.

Table 3: Dow 30 constituents

Tickers Dow 30					
MMM	CAT	GS	JNJ	NKE	VZ
AXP	CVX	HD	JPM	PG	V
AMGN	CSCO	HON	MCD	CRM	WBA
AAPL	KO	INTC	MRK	TRV	WMT
BA	DOW	IBM	MSFT	UNH	DIS

Selecting only constituents for the analysis with at least 30 years of data, I lose: DOW, GS, CRM and V.

A.4   Nasdaq 100

The 123 largest stock on the Nasdaq exchange can be found in Table 4. Most stocks are presented in the S&P500 and can thus be searched by name in Table 2.

Table 4: Nasdaq stocks

Tickers Nasdaq 123								
AAPL	ATVI	COIN	EQIX	GOOGL	LRCX	NTES	ROST	TXN
ABNB	AVGO	COST	ERIC	HON	LULU	NVDA	SBAC	VOD
ADBE	AZN	CPRT	EXC	HZNP	MAR	NXPI	SBUX	VRSK
ADI	BIDU	CRWD	EXPE	IDXX	MCHP	ODFL	SGEN	VRTX
ADP	BIIB	CSCO	FANG	ILMN	MDB	ORLY	SIRI	WBA
ADSK	BKNG	CSGP	FAST	INTC	MDLZ	PANW	SIVB	WBD
AEP	BKR	CSX	FB	INTU	MELI	PAYX	SNPS	WDAY
ALGN	BNTX	CTAS	FISV	ISRG	MNST	PCAR	SNY	WTW
AMAT	CCEP	CTSH	FITB	JD	MRNA	PDD	TEAM	XEL
AMD	CDNS	DDOG	FTNT	KDP	MRVL	PEP	TMUS	ZM
AMGN	CERN	DLTR	GFS	KHC	MSFT	PYPL	TROW	ZS
AMZN	CHTR	DXCM	GILD	KLAC	MU	QCOM	TSCO	
ANSS	CMCSA	EA	GMAB	LCID	NDAQ	REGN	TSLA	
ASML	CME	EBAY	GOOG	LI	NFLX	RIVN	TTD	

Selecting only constituents for the analysis which meet the criteria, I lose 21 stocks: PYPL, ABNB, JD, TEAM, MRNA, KHC, WDAY, CRWD, PDD, DDOG, BNTX, COIN, LCID, RIVN, ZM, ZS, TTD, GFS, MDB, FANG and LI.

A.5   Robustness test

For this analysis I (can) only use a small sample of stocks. Figure 5 and Figure 6 use the ten following stocks: AAPL, TSLA, AMZN, MSFT, PFE, NVDA, GOOGL, VZ, F and WFC. Figure 7 uses the following stocks in addition to the previous named stocks: CVX, DIS, CAT, CCL, WMT, IBM, JNJ, MS, PG and CSCO.

Appendix B   Preliminary Results

B.1   ETFs

Table 5: Sample periods ETFs

		Sample Period	
ETF	Tracking	From	To
DIA	Dow 30	20-01-1998	19-04-2022
IWM	Russell 2000	29-12-2000	19-04-2022
MDY	S&P400 Midcap	04-05-1995	19-04-2022
QQQ	Nasdaq 100	10-03-1999	19-04-2022
SPY	S&P500	02-01-1996	19-04-2022

Figure 19: Difference in return for ETFs (1)
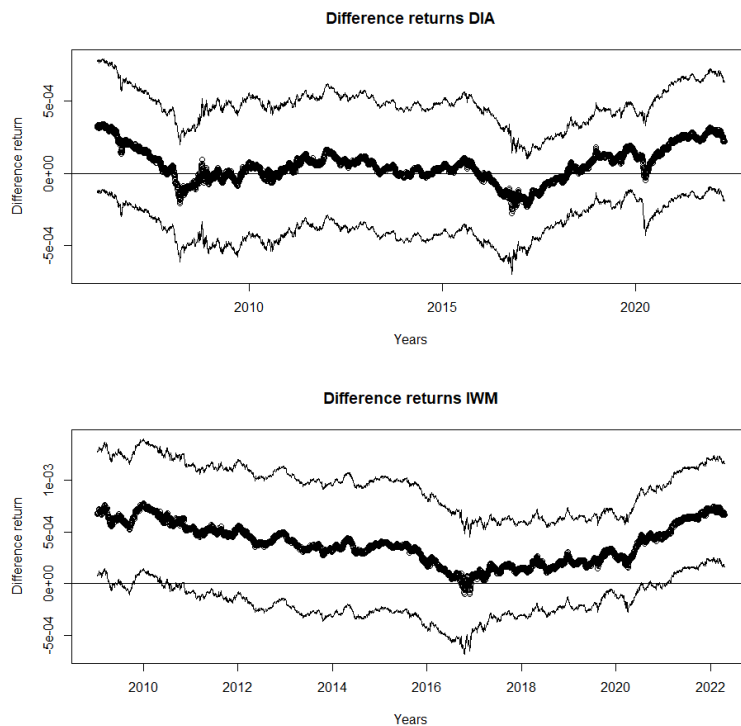
Notes. Eight year rolling window

Figure 20: Difference in return for ETFs (2)
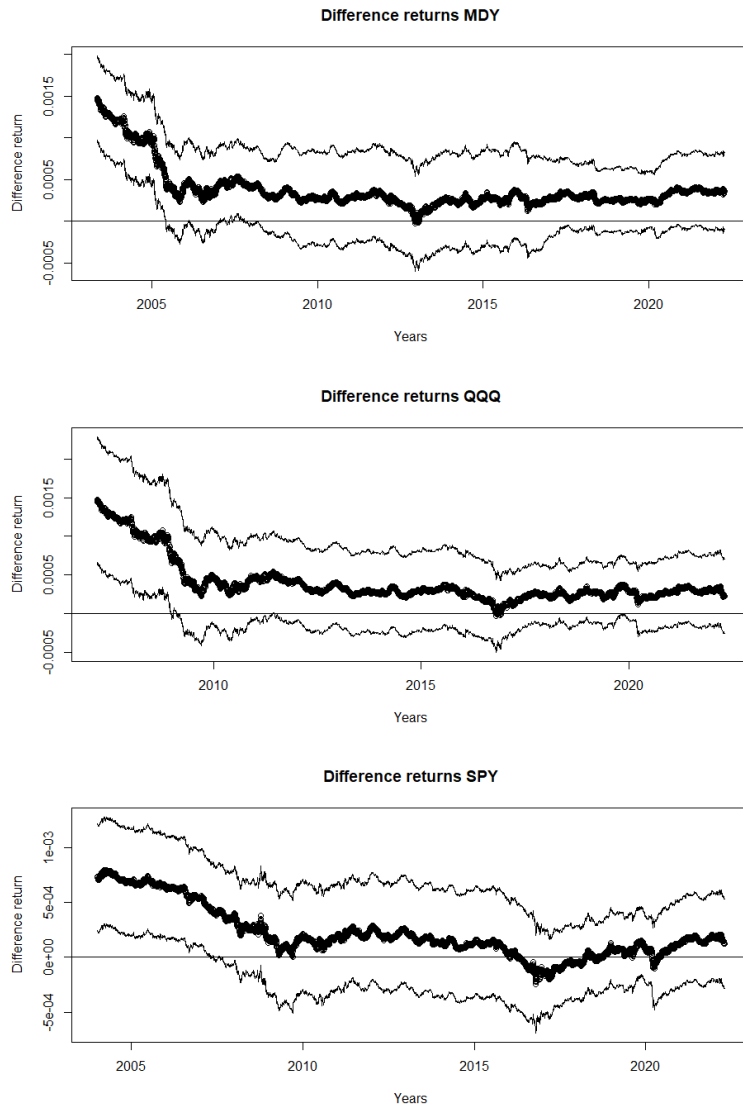
Notes. Eight year rolling window

B.2 Dow Jones Industrial Average

Figure 21: Difference in return by sorting on CTO_t
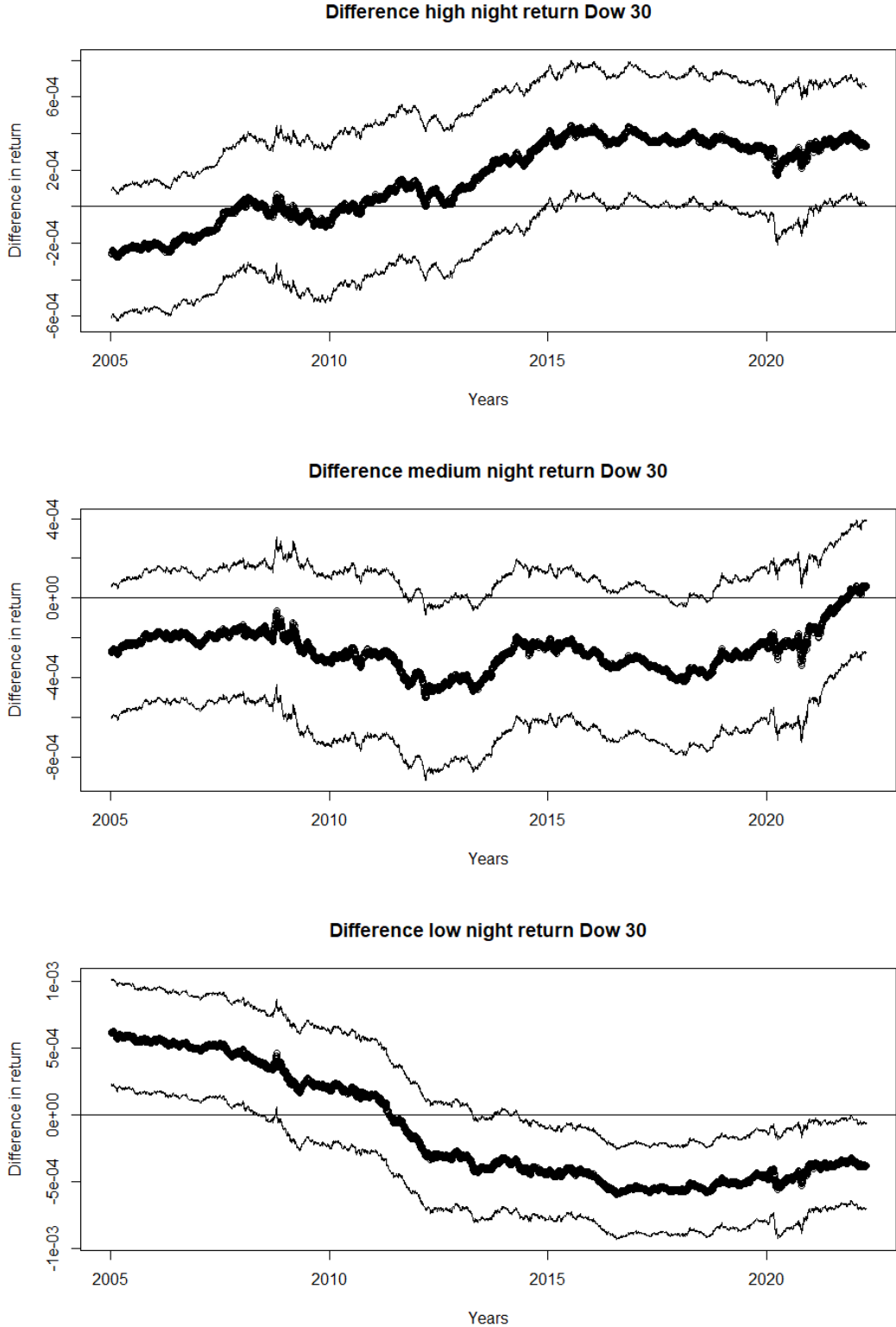
Notes. Twelve year rolling window, sorted on five years

Figure 22: Difference in return for 3 sorts on different values of upside close-to-close volatility yesterday

Difference returns high close-to-close upside volatility

Difference returns medium close-to-close upside volatility

Difference returns low close-to-close upside volatility

Notes. Five year rolling window

65
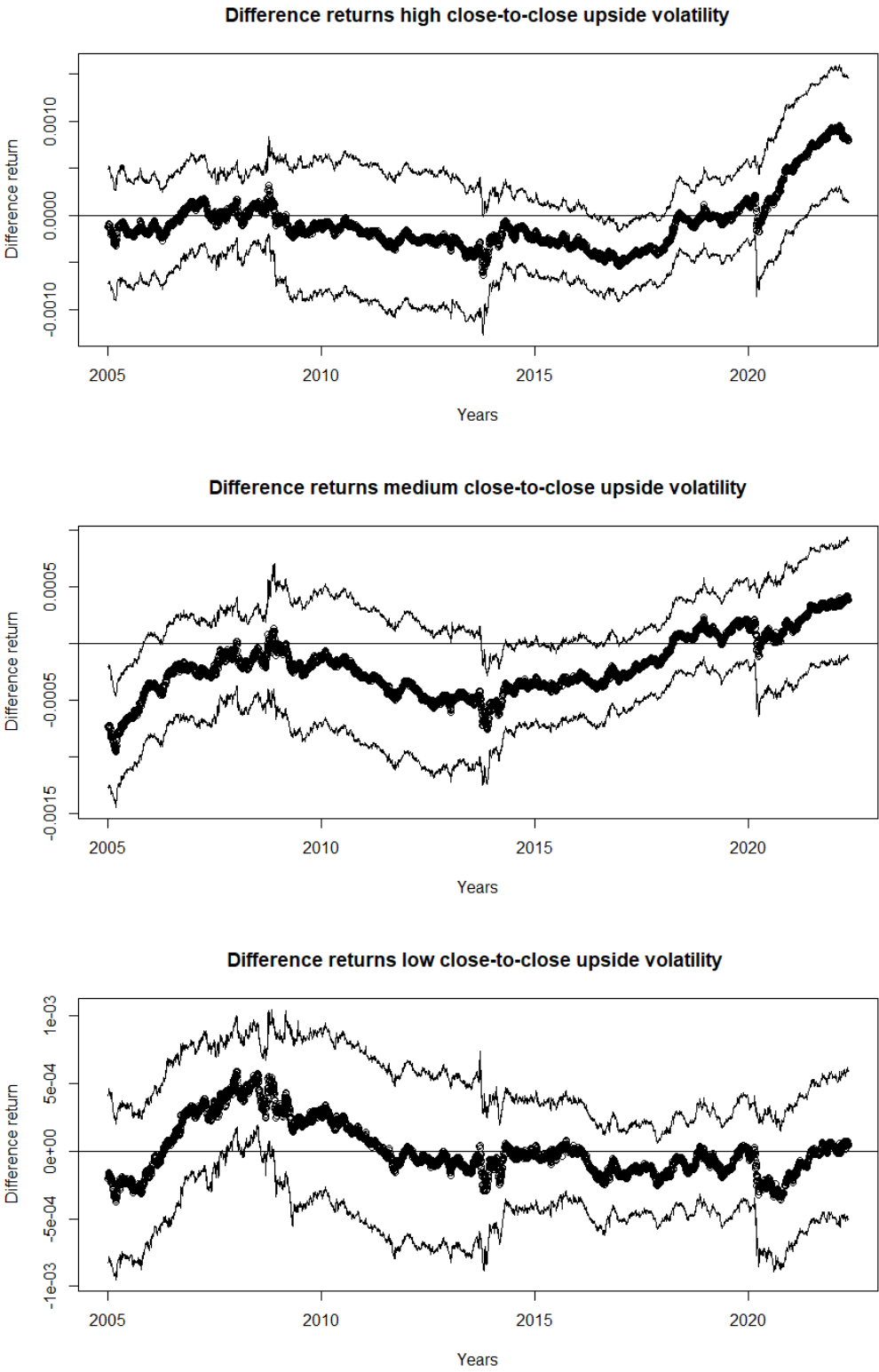
B.3 Nasdaq 102

Figure 23: Difference in return for 3 sorts on different values of upside close-to-close volatility yesterday

Difference returns high close-to-close volatility

Difference returns medium close-to-close volatility

Difference returns low close-to-close volatility
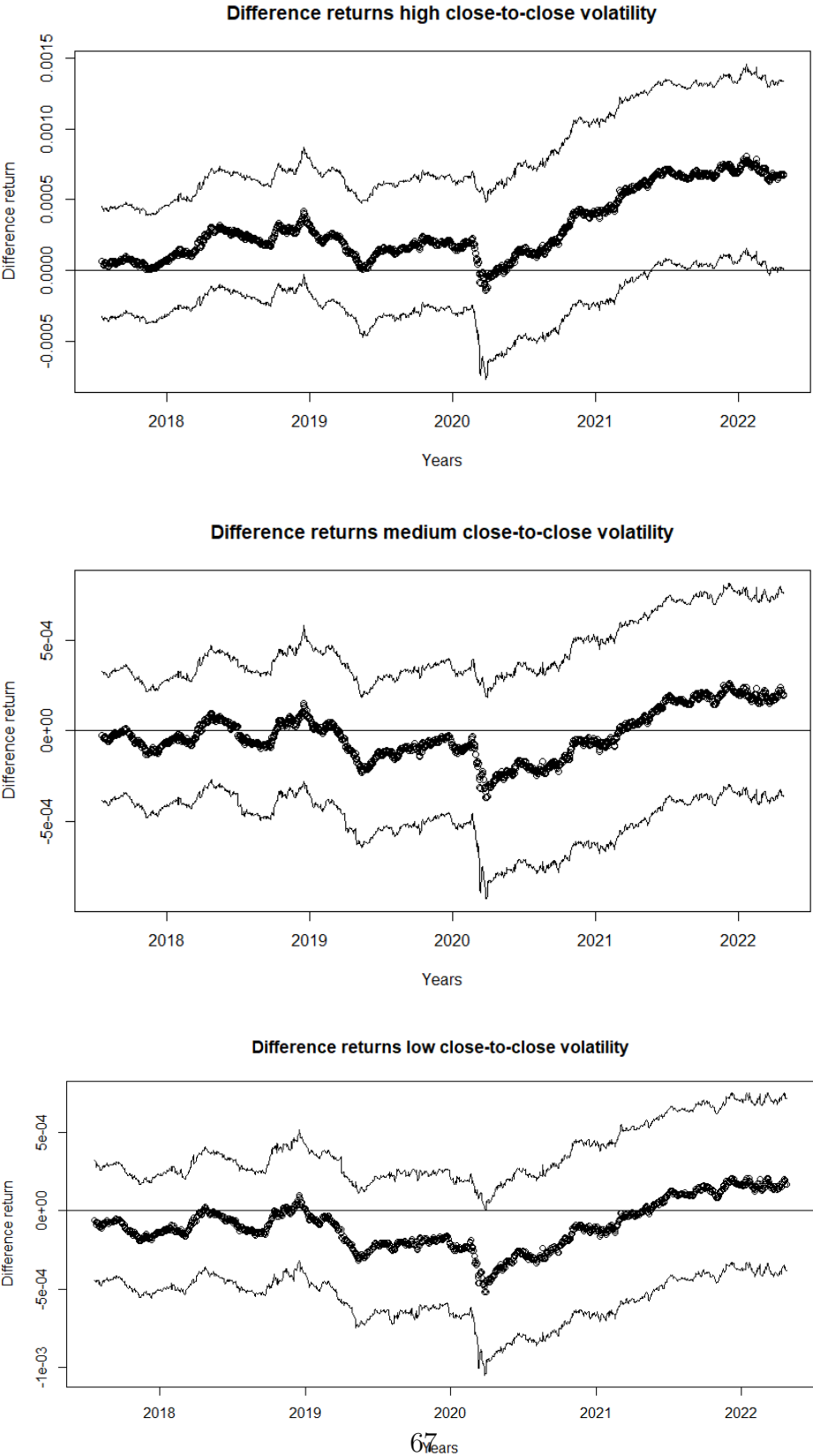
Notes. Five year rolling window

Figure 24: Difference in return for 6 sorts on different values of upside close-to-close volatility yesterday

Difference returns high close-to-close volatility

Difference returns high2 close-to-close volatility

Difference returns medium close-to-close volatility
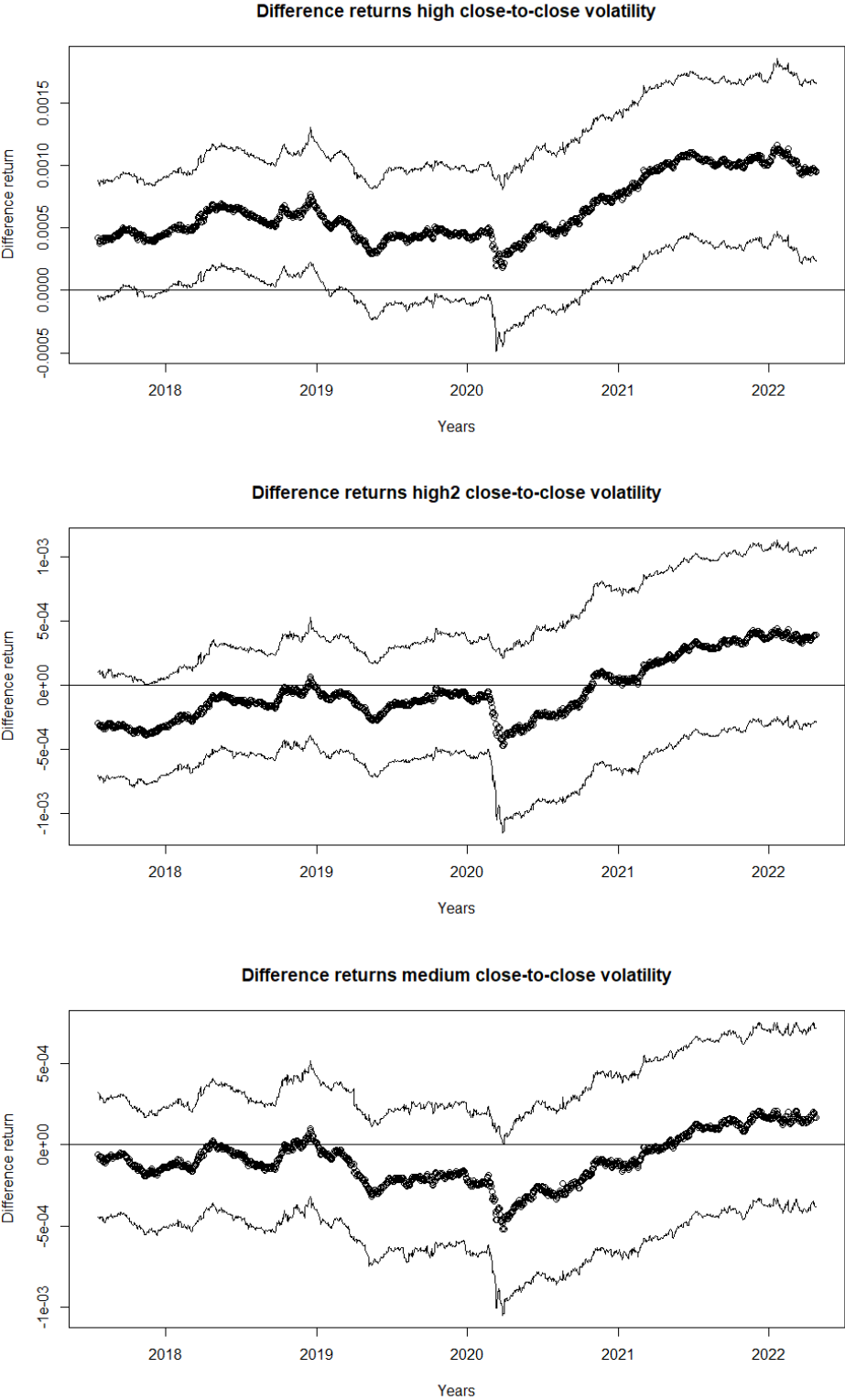
Notes. Five year rolling window

Figure 25: Difference in return for 6 sorts on different values of upside close-to-close volatility yesterday
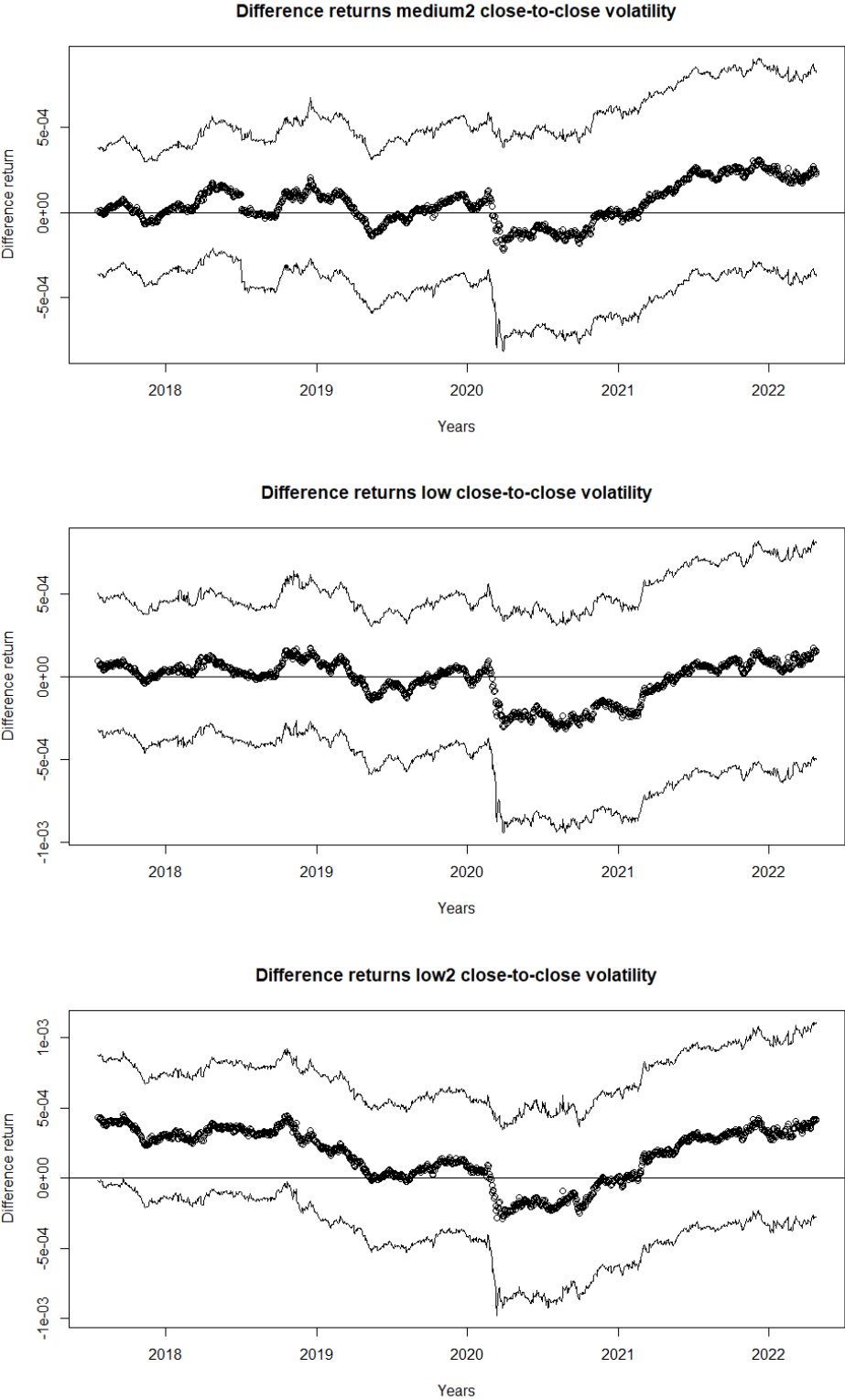
Notes. Five year rolling window

Figure 26: Day return for 3 sorts on different values of upside close-to-close volatility yesterday

day returns high close-to-close volatility

day returns medium close-to-close volatility

day returns low close-to-close volatility
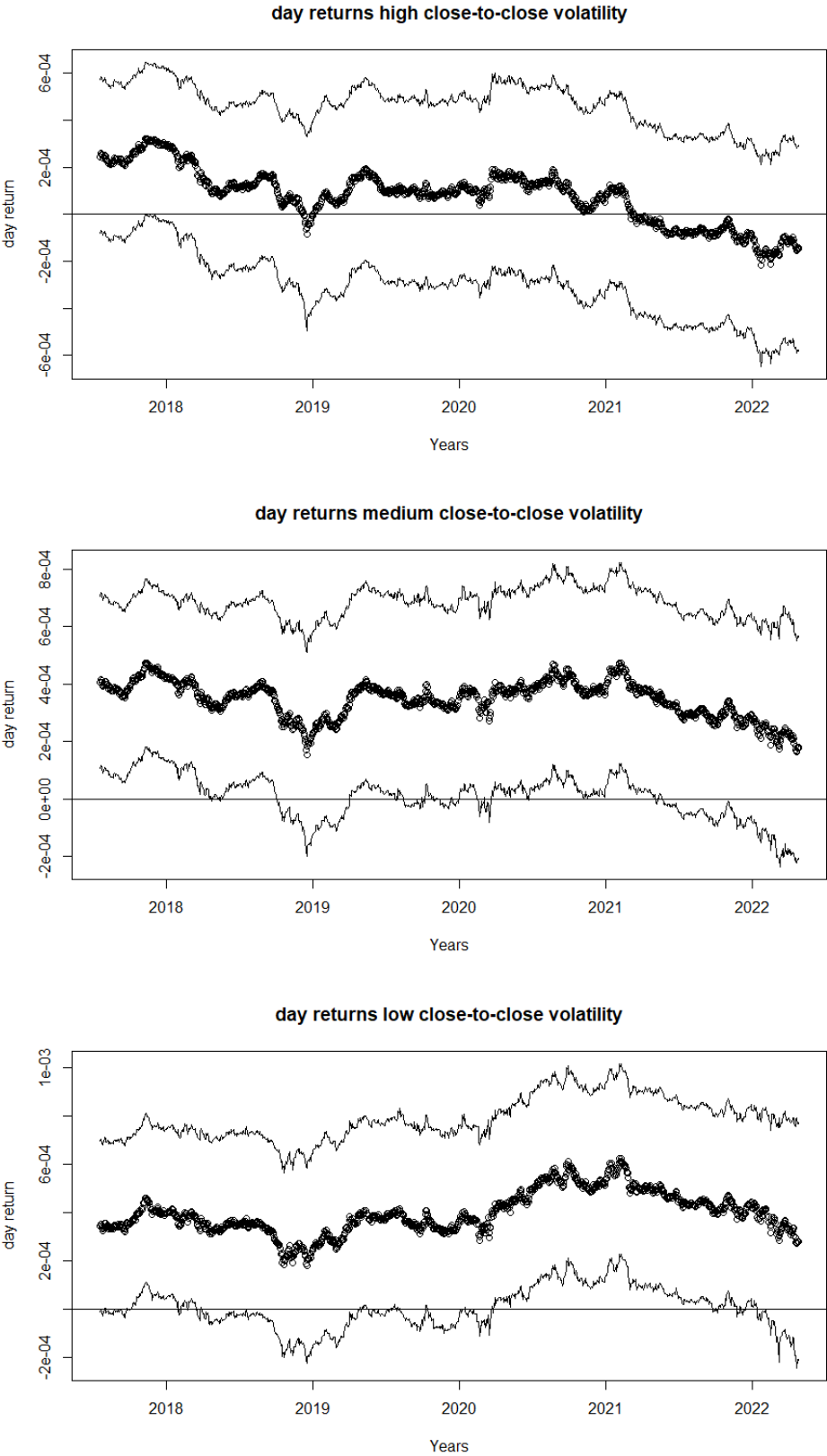
Notes. Five year rolling window

Figure 27: Night return for 3 sorts on different values of upside close-to-close volatility yesterday

night returns high close-to-close volatility

night returns medium close-to-close volatility

night returns low close-to-close volatility
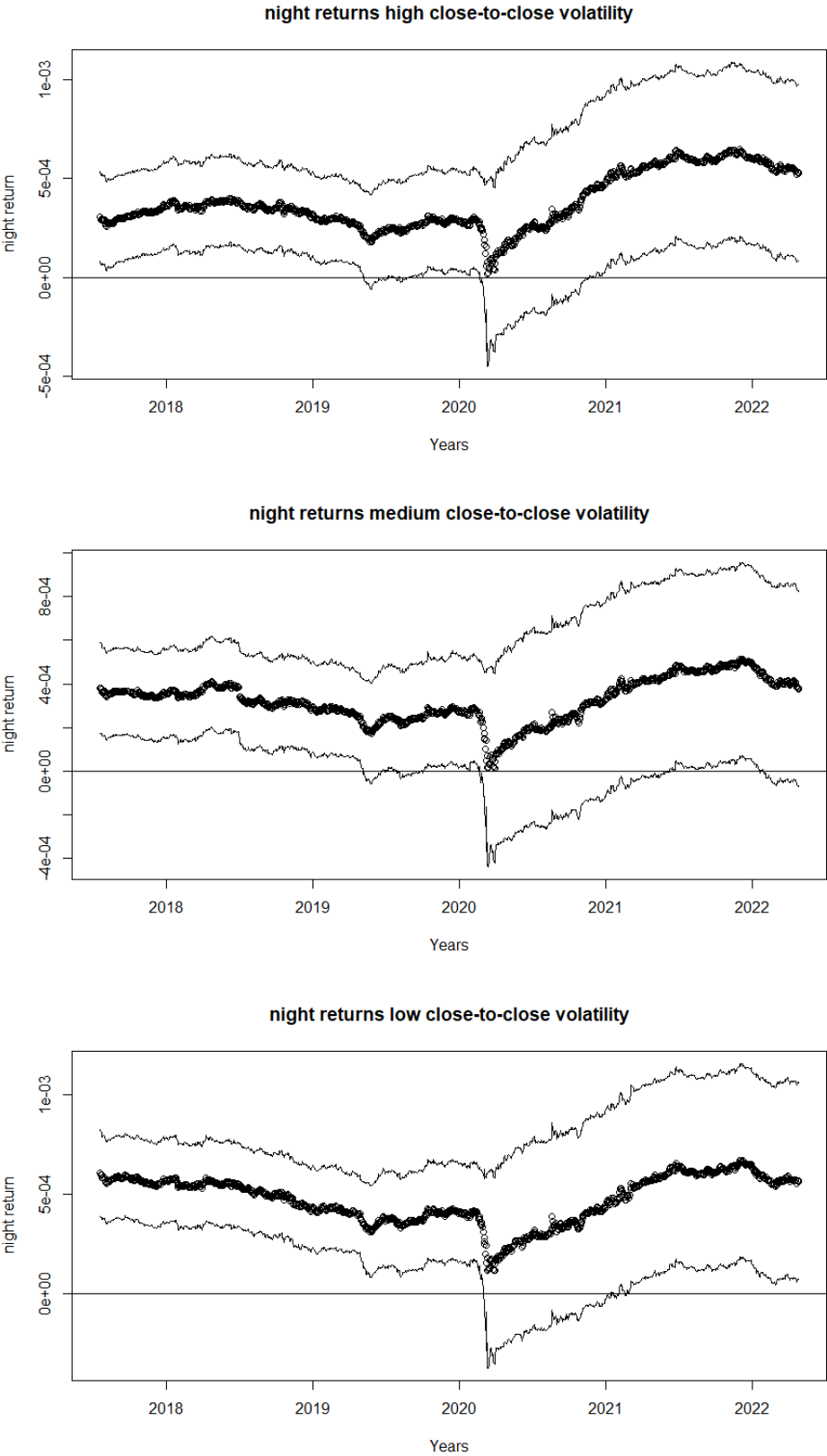
Notes. Five year rolling window

Figure 28: Difference in return sorted on institutional ownership with confidence bounds
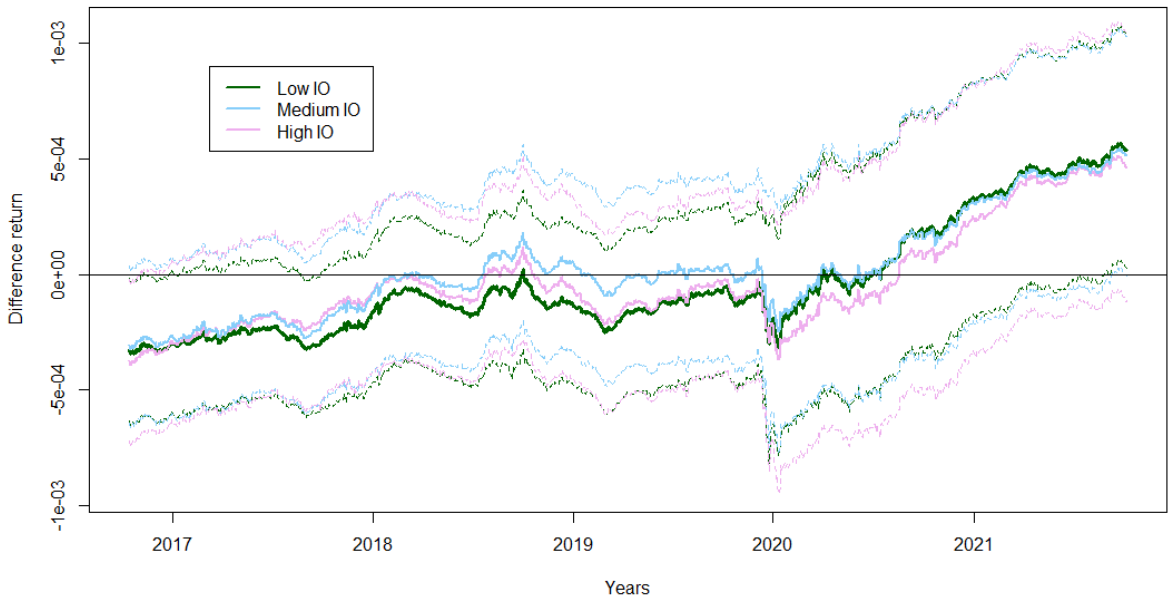
Notes. Five year rolling window

Appendix C   Additional tables and figures

Table 6: Estimates of the standard base specification for the period 4 January 1993 - 3 August 2022

	δ	μ_D	μ_N	π_{11}	π_{12}	π_{21}	π_{22}
AAPL	0.0375	-0.0159	0.0892	-0.0632	0.0591	-0.0113	0.0045
	(0.0151)	(0.0261)	(0.0201)	(0.0116)	(0.0151)	(0.0089)	(0.0116)
AMGN	0.1172	-0.0091	0.0598	-0.0228	0.0384	-0.0465	-0.0277
	(0.0182)	(0.0213)	(0.0136)	(0.0116)	(0.0182)	(0.0074)	(0.0116)
AXP	-0.0777	0.0179	0.0250	-0.0507	0.0096	-0.0118	-0.0497
	(0.0186)	(0.0213)	(0.0133)	(0.0116)	(0.0186)	(0.0072)	(0.0116)
CSCO	0.0242	-0.0110	0.0631	-0.0681	0.0040	0.0179	-0.0307
	(0.0175)	(0.0244)	(0.0161)	(0.0116)	(0.0175)	(0.0076)	(0.0116)
CVX	-0.1066	0.0061	0.0230	-0.0689	-0.0237	-0.0175	-0.0435
	(0.0182)	(0.0161)	(0.0102)	(0.0116)	(0.0183)	(0.0073)	(0.0116)
HD	0.0123	0.0206	0.0268	0.0108	-0.0764	0.0174	-0.0126
	(0.0178)	(0.0190)	(0.0124)	(0.0116)	(0.0178)	(0.0075)	(0.0116)
HON	0.0510	0.0015	0.0371	-0.0078	-0.0350	0.0161	-0.0140
	(0.0176)	(0.0188)	(0.0123)	(0.0116)	(0.0176)	(0.0076)	(0.0116)
IBM	-0.0251	0.0380	-0.0036	-0.0389	0.0537	-0.0039	-0.0652
	(0.0165)	(0.0166)	(0.0116)	(0.0116)	(0.0165)	(0.0081)	(0.0116)
INTC	-0.0051	0.0006	0.0330	-0.0687	0.0364	-0.0107	-0.050
	(0.0158)	(0.0222)	(0.0163)	(0.0116)	(0.0158)	(0.0085)	(0.0116)
JNJ	0.0637	0.0282	0.0092	-0.0177	-0.0221	0.0059	-0.0042
	(0.0187)	(0.0133)	(0.0082)	(0.0116)	(0.0187)	(0.0072)	(0.0116)
JPM	-0.0144	-0.0007	0.0317	-0.0740	-0.0033	0.0124	-0.0668
	(0.0179)	(0.0225)	(0.0145)	(0.0116)	(0.0179)	(0.0075)	(0.0116)
MCD	0.0982	0.0438	-0.0007	-0.0319	-0.0193	-0.0186	0.0080
	(0.0182)	(0.0151)	(0.0096)	(0.0116)	(0.0182)	(0.0074)	(0.0116)
MMM	-0.0142	0.0146	0.0097	-0.0124	-0.0030	-0.0333	-0.0277
	(0.0190)	(0.0147)	(0.0090)	(0.0116)	(0.0189)	(0.0071)	(0.0116)
MRK	0.0041	0.0282	-0.0086	-0.0048	-0.0346	-0.0001	-0.0038
	(0.0172)	(0.0165)	(0.0111)	(0.0116)	(0.0172)	(0.0078)	(0.0116)
MSFT	-0.0370	0.0263	0.0374	-0.0679	0.0137	-0.0092	-0.0397
	(0.0172)	(0.0188)	(0.0126)	(0.0116)	(0.0172)	(0.0078)	(0.0116)
NKE	0.0295	0.0483	0.0026	0.0134	-0.0320	-0.0040	-0.0234
	(0.0175)	(0.0196)	(0.0129)	(0.0116)	(0.0175)	(0.0077)	(0.0116)
PG	0.0869	0.0798	-0.0450	-0.0477	0.0329	-0.0351	-0.0330
	(0.0166)	(0.0139)	(0.0097)	(0.0116)	(0.0166)	(0.0081)	(0.0116)
TRV	0.0843	0.0228	0.0089	-0.0583	-0.0973	-0.0223	-0.0466
	(0.0203)	(0.0182)	(0.0104)	(0.0116)	(0.0203)	(0.0066)	(0.0116)
UNH	-0.0295	0.0270	0.0413	0.0172	-0.0421	-0.0040	-0.0190
	(0.0193)	(0.0220)	(0.0132)	(0.0116)	(0.0193)	(0.0070)	(0.0116)
VZ	0.0423	0.0078	0.0019	-0.0364	-0.0439	-0.0150	0.0012
	(0.0203)	(0.0157)	(0.0090)	(0.0116)	(0.0203)	(0.0066)	(0.0116)
WBA	0.0802	0.0409	-0.0140	-0.0262	-0.0097	-0.0188	-0.0203
	(0.0191)	(0.0185)	(0.0112)	(0.0116)	(0.0191)	(0.0070)	(0.0116)
WMT	0.0697	0.0043	0.0262	-0.0348	0.0069	-0.0099	0.0021
	(0.0189)	(0.0163)	(0.0100)	(0.0116)	(0.0189)	(0.0071)	(0.0116)
average	0.0012	0.0181	0.0200	-0.0319	-0.0039	-0.0069	-0.0243

Table 7: Estimates of the adjusted base specification for the period 18 May 2020 - 10 May 2022

	δ	μ_D	μ_N	π_{11}	π_{12}	π_{21}	π_{22}	ξ_D	ξ_N
AAPL	0.0126	0.1162	-0.0288	-0.0420	-0.0805	0.0140	-0.1513	-0.0928	0.1819
	(0.0640)	(0.1073)	(0.0755)	(0.0705)	(0.0893)	(0.0496)	(0.0625)	(0.1109)	(0.0776)
AMGN	0.1176	-0.0067	0.0032	-0.0068	-0.0391	-0.0645	0.0811	-0.0071	0.0366
	(0.0697)	(0.0816)	(0.0527)	(0.0741)	(0.0851)	(0.0477)	(0.0548)	(0.1118)	(0.0722)
AXP	-0.0905	0.0870	0.0424	0.0525	0.2230	-0.0096	-0.1489	-0.1861	0.1439
	(0.0513)	(0.1026)	(0.0901)	(0.0646)	(0.0813)	(0.0567)	(0.0711)	(0.0954)	(0.0836)
CSCO	0.1077	0.0454	-0.0442	-0.1035	0.0466	-0.0665	0.0129	0.0465	0.0005
	(0.0532)	(0.0769)	(0.0651)	(0.0658)	(0.0677)	(0.0556)	(0.0573)	(0.1021)	(0.0864)
CVX	0.0137	-0.0111	0.0778	-0.1357	0.0092	0.0677	-0.0197	0.0812	-0.0211
	(0.0518)	(0.1030)	(0.0895)	(0.0692)	(0.0759)	(0.0601)	(0.0660)	(0.1028)	(0.0894)
HD	0.0401	0.1476	0.0732	0.0601	0.2502	0.0507	0.0070	-0.2699	-0.0608
	(0.0761)	(0.0883)	(0.0522)	(0.0686)	(0.0880)	(0.0405)	(0.0521)	(0.1189)	(0.0704)
HON	0.1213	-0.0664	0.0188	-0.0968	0.0401	0.0171	-0.1088	0.0998	0.1222
	(0.0555)	(0.0838)	(0.0680)	(0.0661)	(0.0794)	(0.0536)	(0.0642)	(0.1087)	(0.0880)
IBM	-0.0843	-0.0121	0.0243	-0.0475	0.0954	-0.0040	-0.0892	-0.0074	0.0186
	(0.0562)	(0.0762)	(0.0611)	(0.0646)	(0.0669)	(0.0518)	(0.0534)	(0.0960)	(0.0769)
INTC	-0.0052	0.2093	-0.0082	0.0880	0.1334	-0.0591	0.0513	-0.3767	-0.0082
	(0.0487)	(0.1005)	(0.0931)	(0.0629)	(0.0545)	(0.0582)	(0.0504)	(0.0980)	(0.0907)
JNJ	0.1952	-0.0002	0.0021	-0.0393	-0.0344	-0.1242	-0.0887	0.0026	0.1139
	(0.0659)	(0.0618)	(0.0423)	(0.0741)	(0.0901)	(0.0504)	(0.0614)	(0.1192)	(0.0813)
JPM	0.0137	0.0027	0.0621	-0.0165	0.1114	0.0475	-0.0513	-0.1124	0.0905
	(0.0471)	(0.0894)	(0.0854)	(0.0682)	(0.0729)	(0.0651)	(0.0696)	(0.0978)	(0.0934)
MCD	0.2382	0.0592	0.1155	0.0137	0.2044	0.0275	-0.0457	-0.1568	-0.0922
	(0.0665)	(0.0667)	(0.0449)	(0.0766)	(0.0873)	(0.0518)	(0.0591)	(0.1191)	(0.0805)
MMM	0.0875	-0.1076	0.0578	-0.1260	0.0614	0.0133	-0.0664	0.1113	-0.0161
	(0.0668)	(0.0795)	(0.0535)	(0.0694)	(0.0807)	(0.0468)	(0.0543)	(0.1142)	(0.0770)
MRK	0.0572	-0.0866	0.0775	-0.0863	-0.1586	-0.0158	0.1250	0.1091	-0.0106
	(0.0534)	(0.0668)	(0.0562)	(0.0653)	(0.0698)	(0.055)	(0.0585)	(0.0956)	(0.0806)
MSFT	-0.0229	0.0770	-0.0245	-0.1117	0.0415	-0.0718	-0.0990	-0.0966	0.1369
	(0.0664)	(0.0954)	(0.0647)	(0.0689)	(0.0870)	(0.0466)	(0.0589)	(0.1121)	(0.0758)
NKE	0.0359	-0.0650	0.1284	-0.0127	0.0904	0.0170	-0.0791	-0.0678	0.0290
	(0.0479)	(0.0899)	(0.0843)	(0.0631)	(0.0766)	(0.0593)	(0.0720)	(0.0972)	(0.0914)
PG	0.2776	-0.0148	0.0502	-0.1644	-0.1319	-0.0456	-0.0044	0.1524	-0.0397
	(0.0863)	(0.066)	(0.0344)	(0.0761)	(0.1102)	(0.0397)	(0.0575)	(0.1281)	(0.0669)
TRV	0.1320	-0.1412	-0.0084	-0.1686	-0.0037	-0.1294	-0.2026	0.2584	0.2058
	(0.0636)	(0.0922)	(0.0653)	(0.0736)	(0.0884)	(0.0518)	(0.0620)	(0.1150)	(0.0810)
UNH	0.1955	0.1063	-0.0279	0.0544	0.1672	-0.1045	-0.1811	-0.1162	0.1910
	(0.0661)	(0.0845)	(0.0575)	(0.0781)	(0.0936)	(0.0530)	(0.0632)	(0.1175)	(0.0795)
VZ	0.0290	-0.0105	0.0130	0.0322	0.2361	-0.0085	-0.0085	-0.0729	-0.0082
	(0.0795)	(0.0559)	(0.0317)	(0.0679)	(0.0929)	(0.0385)	(0.0526)	(0.1090)	(0.0618)
WBA	-0.0930	-0.0043	-0.0131	0.0336	0.1845	-0.0072	-0.1641	-0.0316	0.0716
	(0.0798)	(0.1115)	(0.0629)	(0.0748)	(0.0932)	(0.0422)	(0.0521)	(0.1116)	(0.0629)
WMT	0.0804	0.0802	-0.0412	0.0639	0.1493	-0.0879	-0.1002	-0.1839	0.1769
	(0.0785)	(0.0693)	(0.0397)	(0.0817)	(0.0948)	(0.0467)	(0.0542)	(0.1192)	(0.0679)
average	0.0613	0.0016	0.0301	-0.0401	0.0732	-0.0170	-0.0687	-0.0351	0.0588

Table 8: Estimates of the adjusted base specification for the period 4 January 1993 - 3 August 2022

	δ	μ_D	μ_N	π_{11}	π_{12}	π_{21}	π_{22}	ξ_D	ξ_N
AAPL	0.0367	0.0464	0.0589	-0.0293	0.0866	-0.0277	-0.0089	-0.0667	0.0324
	(0.0151)	(0.0350)	(0.0269)	(0.0172)	(0.0182)	(0.0132)	(0.0140)	(0.0250)	(0.0193)
AMGN	0.1171	-0.0059	0.0204	-0.0205	0.0408	-0.0743	-0.0569	-0.0045	0.0546
	(0.0182)	(0.0293)	(0.0186)	(0.0184)	(0.0235)	(0.0117)	(0.0150)	(0.0278)	(0.0177)
AXP	-0.0776	-0.0037	0.0234	-0.0657	-0.0053	-0.0128	-0.0508	0.0296	0.0021
	(0.0186)	(0.0283)	(0.0176)	(0.0173)	(0.0226)	(0.0108)	(0.0141)	(0.0255)	(0.0159)
CSCO	0.0241	-0.0073	0.0291	-0.0660	0.0062	-0.0020	-0.0504	-0.0044	0.0404
	(0.0175)	(0.0329)	(0.0217)	(0.0174)	(0.0217)	(0.0115)	(0.0143)	(0.0263)	(0.0174)
CVX	-0.1072	-0.0504	0.0317	-0.1171	-0.0674	-0.0102	-0.0368	0.0960	-0.0146
	(0.0182)	(0.0223)	(0.0142)	(0.0175)	(0.0218)	(0.0111)	(0.0139)	(0.0261)	(0.0166)
HD	0.0121	0.0080	0.0466	0.0011	-0.0843	0.0326	-0.0003	0.0190	-0.0297
	(0.0178)	(0.0261)	(0.0170)	(0.0180)	(0.0210)	(0.0117)	(0.0137)	(0.0269)	(0.0175)
HON	0.0503	-0.0341	0.0572	-0.0352	-0.0611	0.0316	0.0007	0.0554	-0.0312
	(0.0176)	(0.0254)	(0.0167)	(0.0176)	(0.0216)	(0.0116)	(0.0142)	(0.0266)	(0.0175)
IBM	-0.0246	0.0216	-0.0305	-0.0532	0.0407	-0.0274	-0.0865	0.0274	0.0450
	(0.0165)	(0.0226)	(0.0158)	(0.0177)	(0.0205)	(0.0124)	(0.0144)	(0.0257)	(0.0180)
INTC	-0.0053	0.0257	0.0184	-0.0531	0.0489	-0.0198	-0.0573	-0.0302	0.0176
	(0.0158)	(0.0310)	(0.0228)	(0.0177)	(0.0191)	(0.0130)	(0.0140)	(0.0261)	(0.0191)
JNJ	0.0635	-0.0084	0.0122	-0.0591	-0.0596	0.0093	-0.0010	0.0800	-0.0067
	(0.0187)	(0.0184)	(0.0114)	(0.0185)	(0.0228)	(0.0114)	(0.0141)	(0.0277)	(0.0172)
JPM	-0.0147	-0.0672	0.0360	-0.1204	-0.0472	0.0154	-0.0639	0.0882	-0.0058
	(0.0179)	(0.0295)	(0.0191)	(0.0177)	(0.0219)	(0.0114)	(0.0142)	(0.0254)	(0.0164)
MCD	0.0974	0.0121	0.0151	-0.0635	-0.0492	-0.0028	0.0229	0.0613	-0.0305
	(0.0182)	(0.0208)	(0.0133)	(0.0184)	(0.0227)	(0.0118)	(0.0145)	(0.0277)	(0.0177)
MMM	-0.0144	0.0081	0.0217	-0.0186	-0.0089	-0.0219	-0.0168	0.0125	-0.0232
	(0.0190)	(0.0204)	(0.0124)	(0.0178)	(0.0229)	(0.0109)	(0.0140)	(0.0273)	(0.0167)
MRK	0.0043	-0.0006	-0.0153	-0.0297	-0.0536	-0.0059	-0.0083	0.0491	0.0116
	(0.0172)	(0.0228)	(0.0153)	(0.0179)	(0.0201)	(0.0120)	(0.0135)	(0.0268)	(0.0180)
MSFT	-0.0369	0.0101	0.0318	-0.0802	0.0022	-0.0135	-0.0437	0.0236	0.0082
	(0.0172)	(0.0260)	(0.0175)	(0.0179)	(0.0214)	(0.0121)	(0.0144)	(0.0263)	(0.0177)
NKE	0.0291	0.0274	0.0254	-0.0028	-0.0471	0.0136	-0.0069	0.0307	-0.0335
	(0.0175)	(0.0266)	(0.0176)	(0.0181)	(0.0219)	(0.0120)	(0.0145)	(0.0266)	(0.0176)
PG	0.0853	0.0573	-0.0056	-0.0722	0.0154	0.0077	-0.0024	0.0486	-0.0849
	(0.0166)	(0.0186)	(0.0130)	(0.0177)	(0.0192)	(0.0124)	(0.0134)	(0.0267)	(0.0186)
TRV	0.0881	-0.0639	-0.0170	-0.1338	-0.1703	-0.0448	-0.0684	0.1495	0.0448
	(0.0203)	(0.0239)	(0.0137)	(0.0178)	(0.0242)	(0.0102)	(0.0138)	(0.0269)	(0.0154)
UNH	-0.0295	0.0277	-0.0059	0.0177	-0.0417	-0.0357	-0.0441	-0.0010	0.0644
	(0.0193)	(0.0292)	(0.0176)	(0.0174)	(0.0218)	(0.0104)	(0.0131)	(0.0263)	(0.0158)
VZ	0.0423	0.0060	0.0183	-0.0381	-0.0454	0.0008	0.0153	0.0032	-0.0303
	(0.0203)	(0.0220)	(0.0126)	(0.0189)	(0.0243)	(0.0108)	(0.0139)	(0.0286)	(0.0163)
WBA	0.0800	0.0256	-0.0003	-0.0385	-0.0206	-0.0078	-0.0105	0.0241	-0.0215
	(0.0191)	(0.0258)	(0.0157)	(0.0185)	(0.0231)	(0.0112)	(0.0140)	(0.0284)	(0.0172)
WMT	0.0693	0.0168	0.0045	-0.0231	0.0179	-0.0302	-0.0170	-0.0225	0.0389
	(0.0189)	(0.0225)	(0.0138)	(0.0186)	(0.0233)	(0.0114)	(0.0143)	(0.0278)	(0.0170)
average	0.0009	0.0064	0.0157	-0.0426	-0.0138	-0.0088	-0.0264	0.0208	0.0038

Table 9: Estimates of the intraday dynamic (short run) parameters in the coupled component model

	ω_D	β_D	γ_D	γ_D^*	ρ_D	ρ_D^*	ν_D
AAPL	0.5120	0.9224	0.0445	-0.0090	0.0379	-0.0095	8.9697
	(0.0178)	(0.0098)	(0.0040)	(0.0023)	(0.0049)	(0.0027)	(0.7261)
AMGN	0.3015	0.9401	0.0433	-0.0062	0.0413	-0.0006	7.9214
	(0.0201)	(0.0073)	(0.0037)	(0.0022)	(0.0047)	(0.0025)	(0.5848)
AXP	0.2427	0.9505	0.0453	-0.0117	0.0393	-0.0161	9.6933
	(0.0225)	(0.005)	(0.0035)	(0.0021)	(0.0039)	(0.0025)	(0.8454)
CSCO	0.3771	0.9476	0.0398	-0.0098	0.0388	-0.0177	10.9149
	(0.0202)	(0.0054)	(0.0033)	(0.0021)	(0.0040)	(0.0024)	(0.9721)
CVX	0.1010	0.9566	0.0393	-0.0087	0.0319	-0.0143	12.2095
	(0.0222)	(0.0047)	(0.0032)	(0.0020)	(0.0036)	(0.0023)	(1.3019)
HD	0.2088	0.9405	0.0424	-0.0104	0.0442	-0.0165	8.9748
	(0.0200)	(0.0066)	(0.0037)	(0.0023)	(0.0045)	(0.0027)	(0.7057)
HON	0.1458	0.9316	0.0457	-0.0140	0.0504	-0.0149	8.2666
	(0.0196)	(0.0071)	(0.0041)	(0.0024)	(0.0045)	(0.0028)	(0.6201)
IBM	0.0407	0.9438	0.0420	-0.0058	0.0454	-0.0084	7.3982
	(0.0204)	(0.0067)	(0.0039)	(0.0022)	(0.0047)	(0.0026)	(0.4915)
INTC	0.4081	0.9601	0.0312	-0.0044	0.0325	-0.0100	12.1822
	(0.0210)	(0.0044)	(0.0028)	(0.0017)	(0.0038)	(0.0022)	(1.2472)
JNJ	-0.1855	0.9431	0.0462	-0.0037	0.0447	-0.0114	7.1226
	(0.0213)	(0.0059)	(0.0037)	(0.0023)	(0.0043)	(0.0026)	(0.4638)
JPM	0.2474	0.9610	0.0440	-0.0068	0.0413	-0.0106	7.9424
	(0.0258)	(0.0038)	(0.0035)	(0.0021)	(0.0039)	(0.0023)	(0.5833)
MCD	-0.0319	0.9259	0.0390	-0.0059	0.0504	-0.0099	7.9088
	(0.0180)	(0.0101)	(0.0044)	(0.0023)	(0.0052)	(0.0028)	(0.5602)
MMM	-0.0632	0.9509	0.0365	-0.0092	0.0432	-0.0108	6.8735
	(0.0207)	(0.0056)	(0.0036)	(0.0022)	(0.0045)	(0.0026)	(0.4265)
MRK	0.0681	0.9253	0.0457	-0.0032	0.0453	-0.0108	6.8977
	(0.0183)	(0.0107)	(0.0045)	(0.0026)	(0.0053)	(0.0028)	(0.4164)
MSFT	0.2224	0.9417	0.0435	-0.0041	0.0541	-0.0095	10.5668
	(0.0211)	(0.0062)	(0.0036)	(0.0021)	(0.0047)	(0.0025)	(0.9601)
NKE	0.2109	0.9490	0.0388	-0.0057	0.0373	-0.0080	7.1371
	(0.0203)	(0.0066)	(0.0038)	(0.0023)	(0.0047)	(0.0025)	(0.4686)
PG	-0.1294	0.9369	0.0431	-0.0044	0.0421	-0.0141	7.9902
	(0.0194)	(0.0074)	(0.0038)	(0.0023)	(0.0044)	(0.0027)	(0.5637)
TRV	0.0780	0.9375	0.0514	-0.0068	0.0509	-0.0135	8.0345
	(0.0215)	(0.0070)	(0.0042)	(0.0025)	(0.0049)	(0.0027)	(0.5940)
UNH	0.3059	0.9455	0.0430	-0.0046	0.0405	-0.0121	6.9643
	(0.0207)	(0.0070)	(0.0038)	(0.0024)	(0.0048)	(0.0027)	(0.4471)
VZ	0.0316	0.9440	0.0338	-0.0056	0.0401	-0.0157	9.6899
	(0.0188)	(0.0068)	(0.0035)	(0.0021)	(0.0042)	(0.0025)	(0.8191)
WBA	0.2059	0.9296	0.0370	-0.0059	0.0527	-0.0092	7.1348
	(0.0183)	(0.0109)	(0.0043)	(0.0025)	(0.0055)	(0.0028)	(0.4771)
WMT	0.0037	0.9448	0.0387	-0.0022	0.0381	-0.0129	7.5265
	(0.0197)	(0.0072)	(0.0036)	(0.0021)	(0.0044)	(0.0026)	(0.5068)
average	0.1458	0.9457	0.0413	-0.0066	0.0424	-0.0118	8.4471

Table 10: Estimates of the overnight dynamic (short run) parameters in the coupled component model

	ω_N	β_N	γ_N	γ_N^*	ρ_N	ρ_N^*	ν_N
AAPL	-0.3529	0.9130	0.0668	-0.0163	0.0722	-0.0147	2.7968
	(0.0215)	(0.0088)	(0.0067)	(0.0037)	(0.0052)	(0.0032)	(0.0824)
AMGN	-0.6651	0.9442	0.0464	-0.0085	0.0492	-0.0114	2.9895
	(0.0224)	(0.0061)	(0.0050)	(0.0028)	(0.0043)	(0.0025)	(0.0941)
AXP	-0.5432	0.9604	0.0453	-0.0227	0.0419	-0.0171	3.8124
	(0.0263)	(0.0036)	(0.0042)	(0.0027)	(0.0036)	(0.0023)	(0.1517)
CSCO	-0.4062	0.9515	0.0429	-0.0177	0.0420	-0.0156	3.2009
	(0.0226)	(0.0051)	(0.0046)	(0.0026)	(0.0038)	(0.0025)	(0.1036)
CVX	-0.6673	0.9704	0.0332	-0.0141	0.0293	-0.0085	4.2939
	(0.0257)	(0.0029)	(0.0034)	(0.0021)	(0.0029)	(0.0018)	(0.1947)
HD	-0.6194	0.9471	0.0563	-0.0228	0.0407	-0.0135	3.2386
	(0.0239)	(0.0054)	(0.0049)	(0.0031)	(0.0040)	(0.0028)	(0.1158)
HON	-0.6042	0.9535	0.0511	-0.0221	0.0402	-0.0169	3.4149
	(0.0246)	(0.0046)	(0.0045)	(0.0028)	(0.0040)	(0.0026)	(0.1251)
IBM	-0.7911	0.9561	0.0529	-0.0149	0.0391	-0.0152	2.7288
	(0.0254)	(0.0046)	(0.0050)	(0.0028)	(0.0040)	(0.0025)	(0.0825)
INTC	-0.4058	0.9522	0.0426	-0.0154	0.0366	-0.0091	2.9076
	(0.0222)	(0.0070)	(0.0056)	(0.0030)	(0.0041)	(0.0023)	(0.0886)
JNJ	-0.8996	0.9553	0.0411	-0.0169	0.0404	-0.0141	3.8619
	(0.0231)	(0.0047)	(0.0042)	(0.0026)	(0.0038)	(0.0024)	(0.1558)
JPM	-0.4007	0.9645	0.0431	-0.0230	0.0382	-0.0120	4.0353
	(0.0266)	(0.0032)	(0.0040)	(0.0023)	(0.0036)	(0.0021)	(0.1655)
MCD	-0.7882	0.9450	0.0458	-0.0182	0.0428	-0.0146	3.3642
	(0.0218)	(0.0057)	(0.0047)	(0.0029)	(0.0042)	(0.0025)	(0.1198)
MMM	-0.8937	0.9618	0.0432	-0.0122	0.0377	-0.0131	3.0316
	(0.0255)	(0.0040)	(0.0043)	(0.0028)	(0.0040)	(0.0024)	(0.1051)
MRK	-0.7276	0.9410	0.0492	-0.0147	0.0484	-0.0127	3.0998
	(0.0221)	(0.0072)	(0.0052)	(0.0030)	(0.0047)	(0.0027)	(0.1055)
MSFT	-0.6351	0.9395	0.0615	-0.0127	0.0497	-0.0059	3.0077
	(0.0235)	(0.0066)	(0.0057)	(0.0031)	(0.0043)	(0.0026)	(0.0933)
NKE	-0.7892	0.9421	0.0482	-0.0215	0.0500	-0.0130	2.3774
	(0.0225)	(0.0068)	(0.0055)	(0.0032)	(0.0048)	(0.0030)	(0.0675)
PG	-0.9665	0.9423	0.0389	-0.0218	0.0431	-0.0133	3.3955
	(0.0204)	(0.0059)	(0.0045)	(0.0028)	(0.0041)	(0.0026)	(0.1217)
TRV	-0.8770	0.9595	0.0532	-0.0176	0.0423	-0.0110	3.0239
	(0.0273)	(0.0043)	(0.0050)	(0.0028)	(0.0040)	(0.0024)	(0.1012)
UNH	-0.7343	0.9411	0.0583	-0.0152	0.0540	-0.0108	2.4406
	(0.0244)	(0.0066)	(0.0059)	(0.0034)	(0.0049)	(0.0031)	(0.0734)
VZ	-0.8247	0.9546	0.0460	-0.0207	0.0378	-0.0067	3.3764
	(0.0237)	(0.0049)	(0.0048)	(0.0028)	(0.0037)	(0.0024)	(0.1237)
WBA	-0.7554	0.9444	0.0524	-0.0191	0.0347	-0.0132	2.9146
	(0.0221)	(0.0064)	(0.0052)	(0.0031)	(0.0042)	(0.0026)	(0.0933)
WMT	-0.8219	0.9548	0.0359	-0.0140	0.0386	-0.0078	3.1159
	(0.0218)	(0.0053)	(0.0046)	(0.0026)	(0.0037)	(0.0023)	(0.1040)
average	-2.3158	0.9534	0.0538	-0.0172	0.0431	-0.0111	2.9224

Table 11: *P*-values of several Wald tests for equivalence of intraday and overnight parameters

|	$\omega_D = \omega_N$	$\beta_D = \beta_N$	$\gamma_D = \gamma_N$	$\gamma_D^* = \gamma_N^*$	$\rho_D = \rho_N$	$\rho_D^* = \rho_N^*$	$\nu_D = \nu_N$	$(\beta_D, \gamma_D, \gamma_D^*, \rho_D, \rho_D^*)$ $= (\beta_N, \gamma_N, \gamma_N^*, \rho_N, \rho_N^*)$
AAPL	0.0000	0.0383	0.0002	0.0602	0.6333	0.4958	0.0000	0.0004
AMGN	0.0000	0.0135	0.0847	0.4483	0.5638	0.9770	0.0000	0.0712
AXP	0.0000	0.0038	0.3198	0.4366	0.6111	0.7747	0.0000	0.0174
CSCO	0.0000	0.4678	0.0687	0.4818	0.7708	0.9134	0.0000	0.5013
CVX	0.0000	0.0005	0.8338	0.8613	0.3071	0.5348	0.0000	0.0000
HD	0.0000	0.0214	0.0823	0.2431	0.4522	0.8383	0.0000	0.0388
HON	0.0000	0.0000	0.6198	0.5625	0.4696	0.8084	0.0000	0.0000
IBM	0.0000	0.0000	0.1462	0.4487	0.3018	0.9004	0.0000	0.0000
INTC	0.0011	0.0000	0.0001	0.0782	0.6772	0.9067	0.0000	0.0000
JNJ	0.0000	0.0104	0.5033	0.6873	0.4442	0.7145	0.0000	0.0195
JPM	0.0178	0.1913	0.4605	0.7202	0.6614	0.8045	0.0000	0.6930
MCD	0.0000	0.0000	0.6827	0.4688	0.1335	0.7570	0.0000	0.0000
MMM	0.0000	0.0014	0.3625	0.4237	0.4467	0.7678	0.0000	0.0005
MRK	0.0000	0.0000	0.3137	0.5681	0.3690	0.9049	0.0000	0.0000
MSFT	0.0000	0.3791	0.0031	0.1797	0.5895	0.9612	0.0000	0.0004
NKE	0.0000	0.6250	0.0138	0.1773	0.8798	0.4279	0.0000	0.0055
PG	0.0158	0.0021	0.2876	0.4449	0.5844	0.8589	0.0000	0.0037
TRV	0.0000	0.0000	0.2641	0.6783	0.1740	0.6906	0.0000	0.0000
UNH	0.0000	0.3858	0.0032	0.1498	0.8052	0.5753	0.0000	0.0186
VZ	0.0000	0.0002	0.0662	0.3118	0.4195	0.9303	0.0000	0.0002
WBA	0.0000	0.0000	0.2483	0.3740	0.0446	0.8408	0.0000	0.0000
WMT	0.0000	0.0002	0.1928	0.4695	0.3049	0.6820	0.0000	0.0000
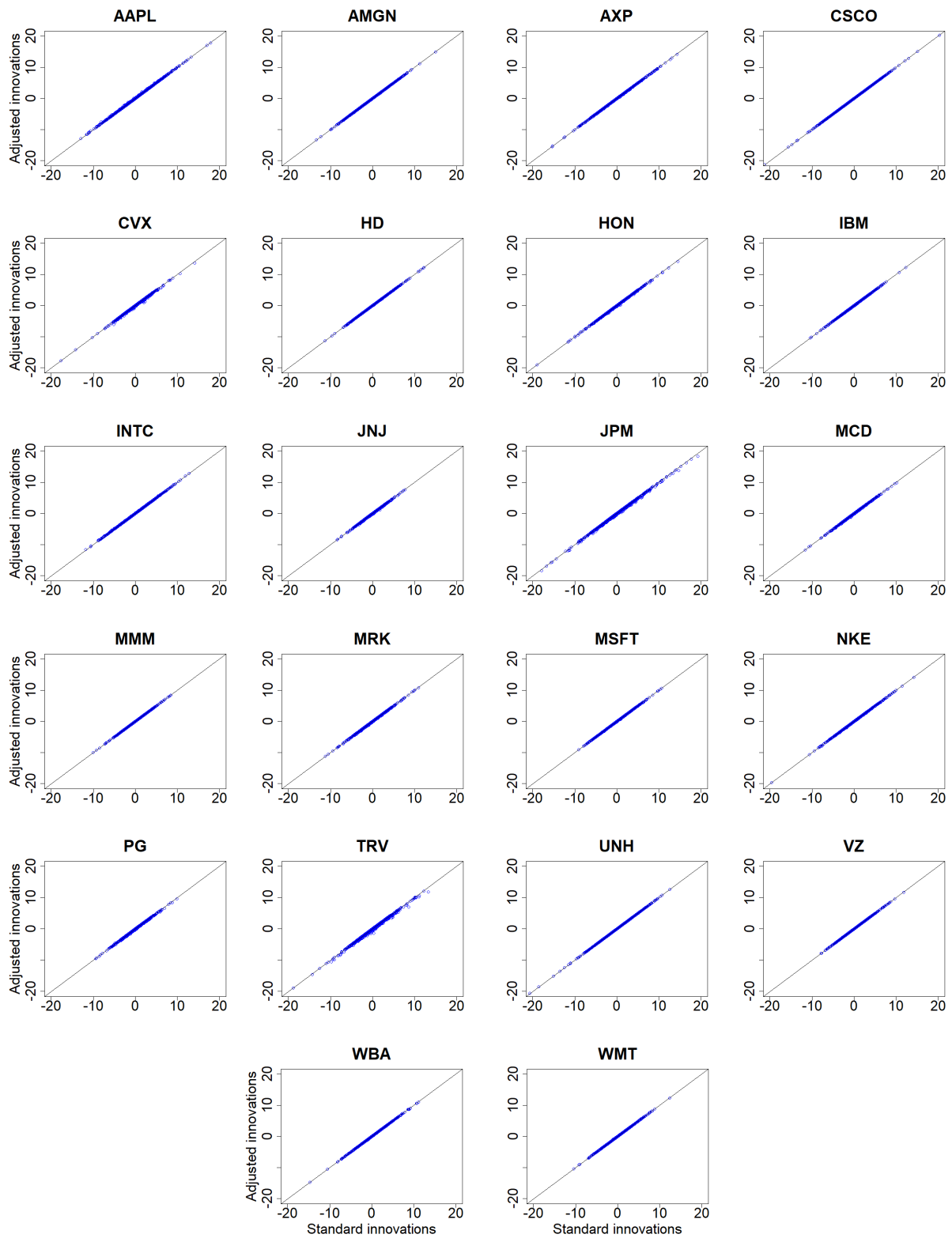
Figure 29: Intraday innovations from the standard base specification plotted against intraday innovations from the adjusted base specification.
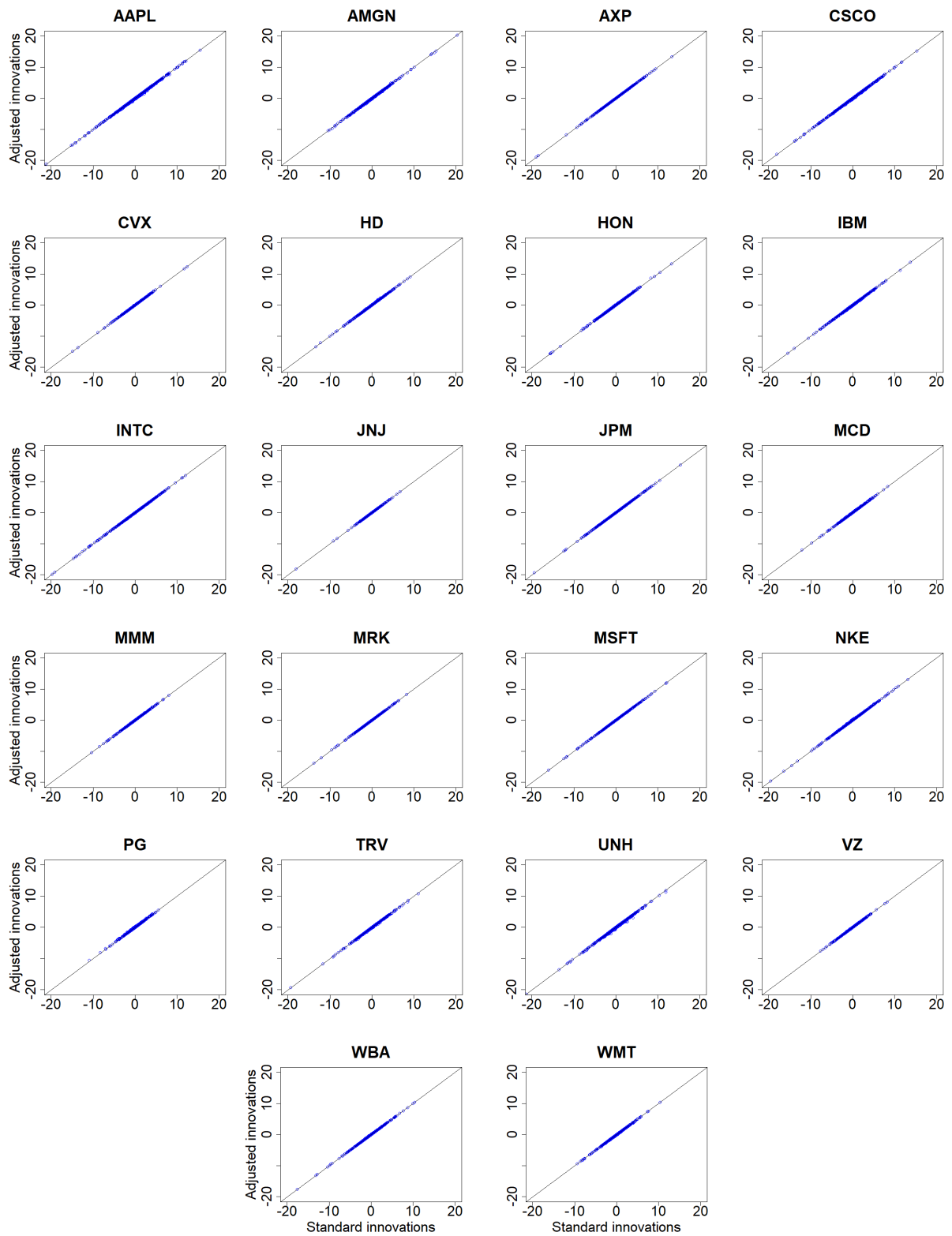
Figure 30: Overnight innovations from the standard base specification plotted against overnight innovations from the adjusted base specification.
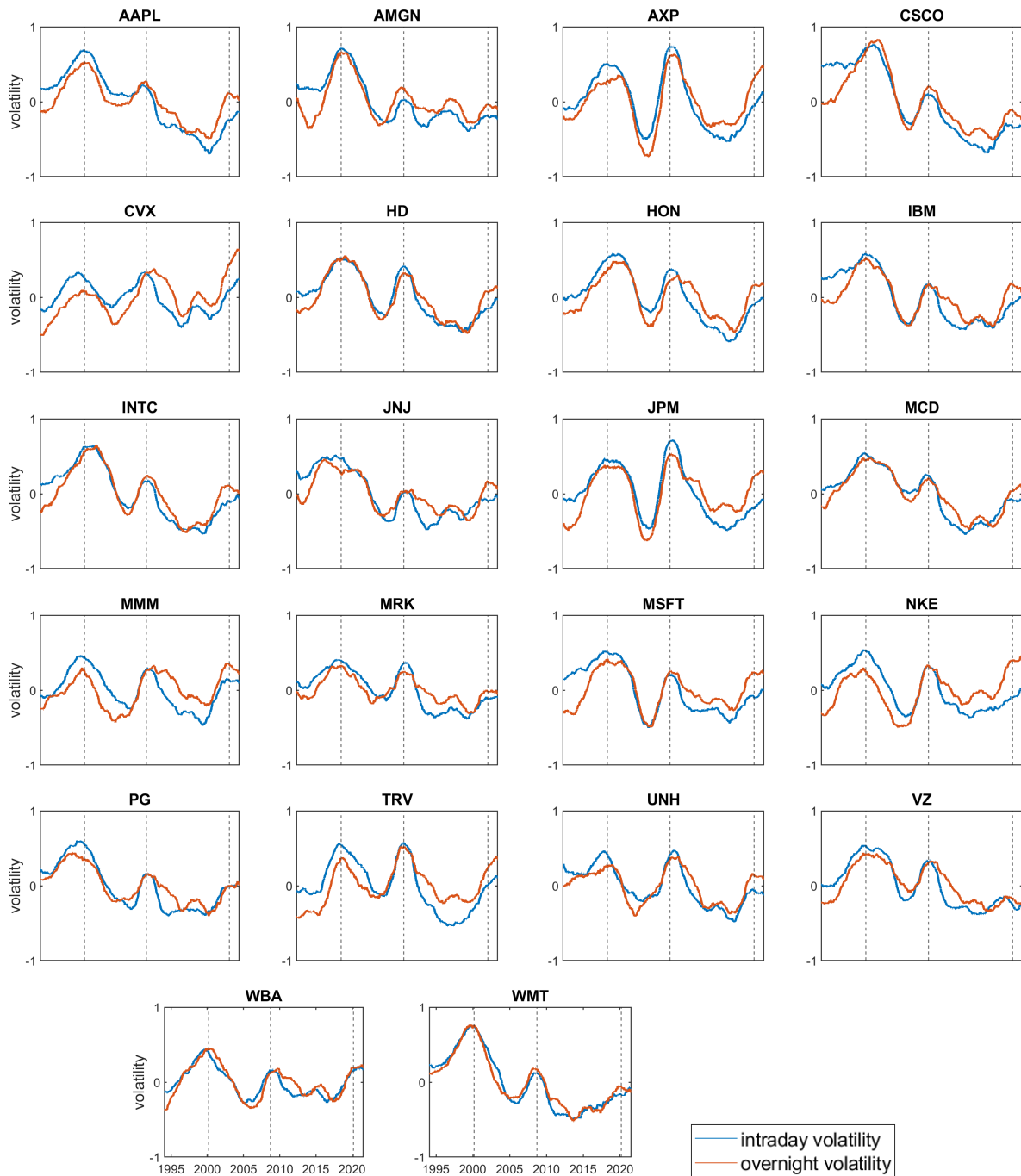
Figure 31: The long run component $\sigma^k(\cdot)$, for $k \in \{D, N\}$, of the coupled component model. The three vertical lines represent the following crises: dot-com bubble (10 March 2000), financial crisis (16 September 2008) and the corona crisis (9 March 2020).
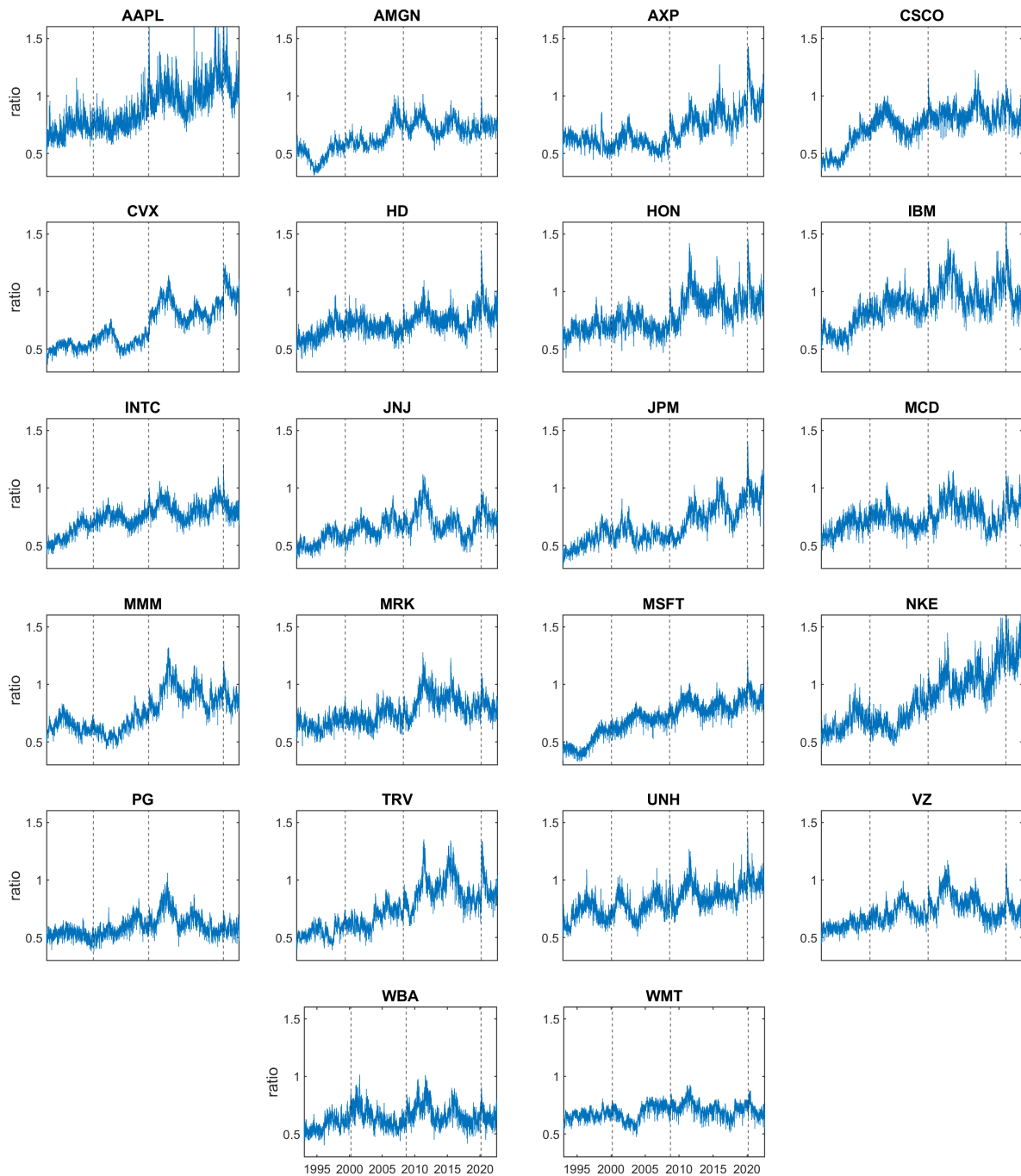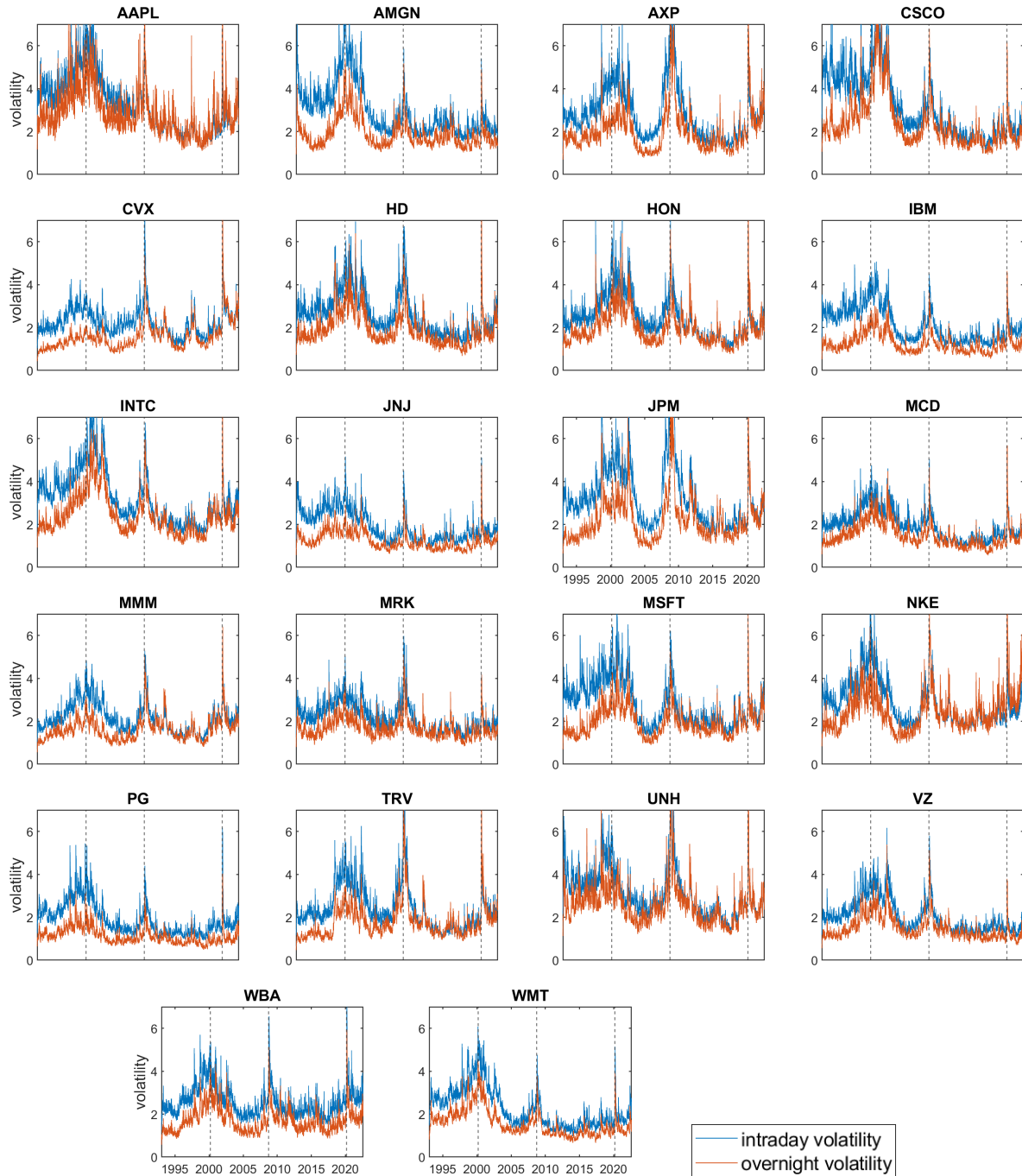
Figure 32: The ratio of overnight to intraday volatility, where volatility is measured as $\sqrt{\frac{\nu_k}{\nu_k - 2}} \exp\left[2\lambda_t^k + 2\sigma_t^k\left(\frac{t}{T}\right)\right]$, of the coupled component model. The three vertical lines represent the following crises: dot-com bubble (10 March 2000), financial crisis (16 September 2008) and the corona crisis (9 March 2020).
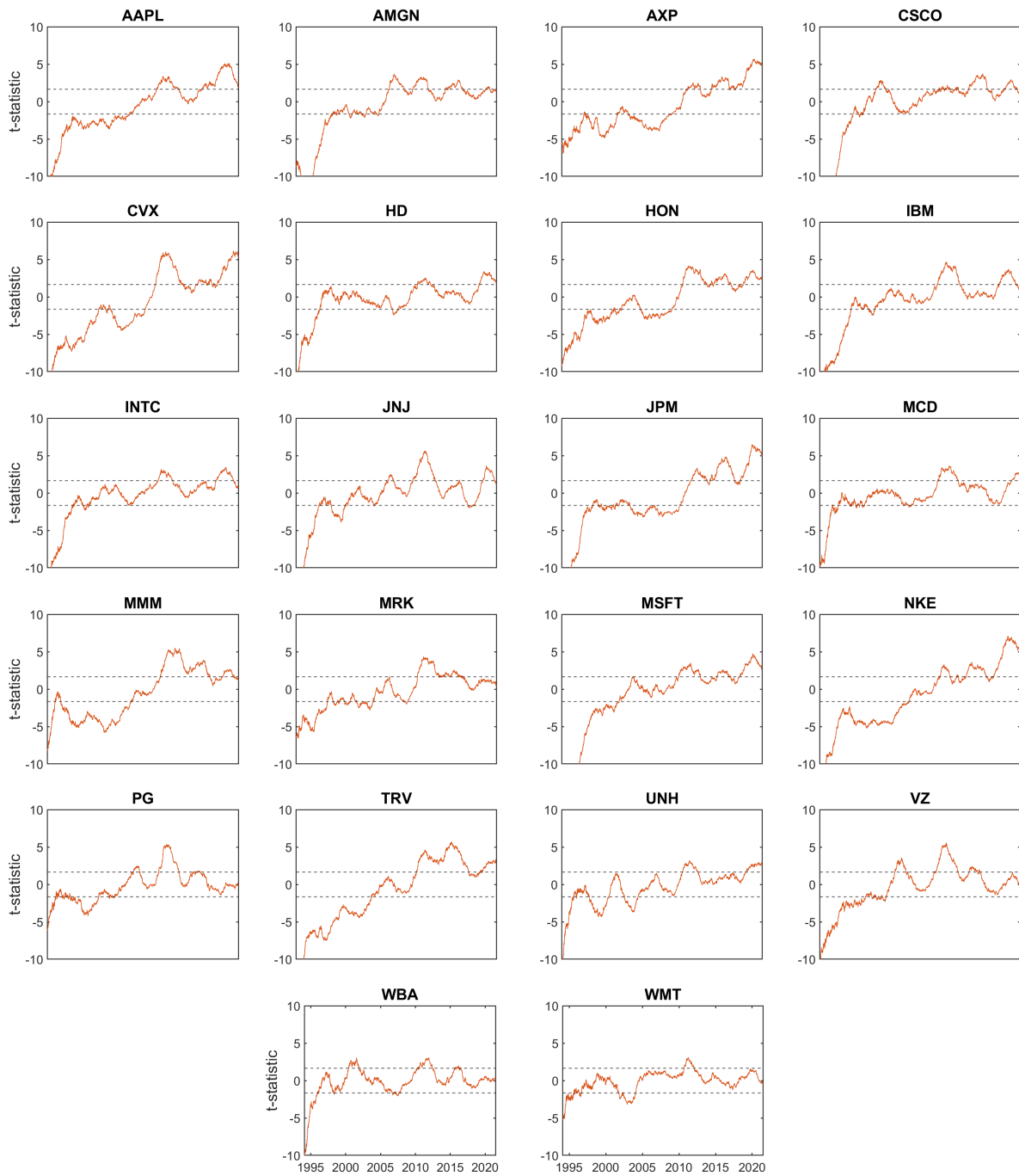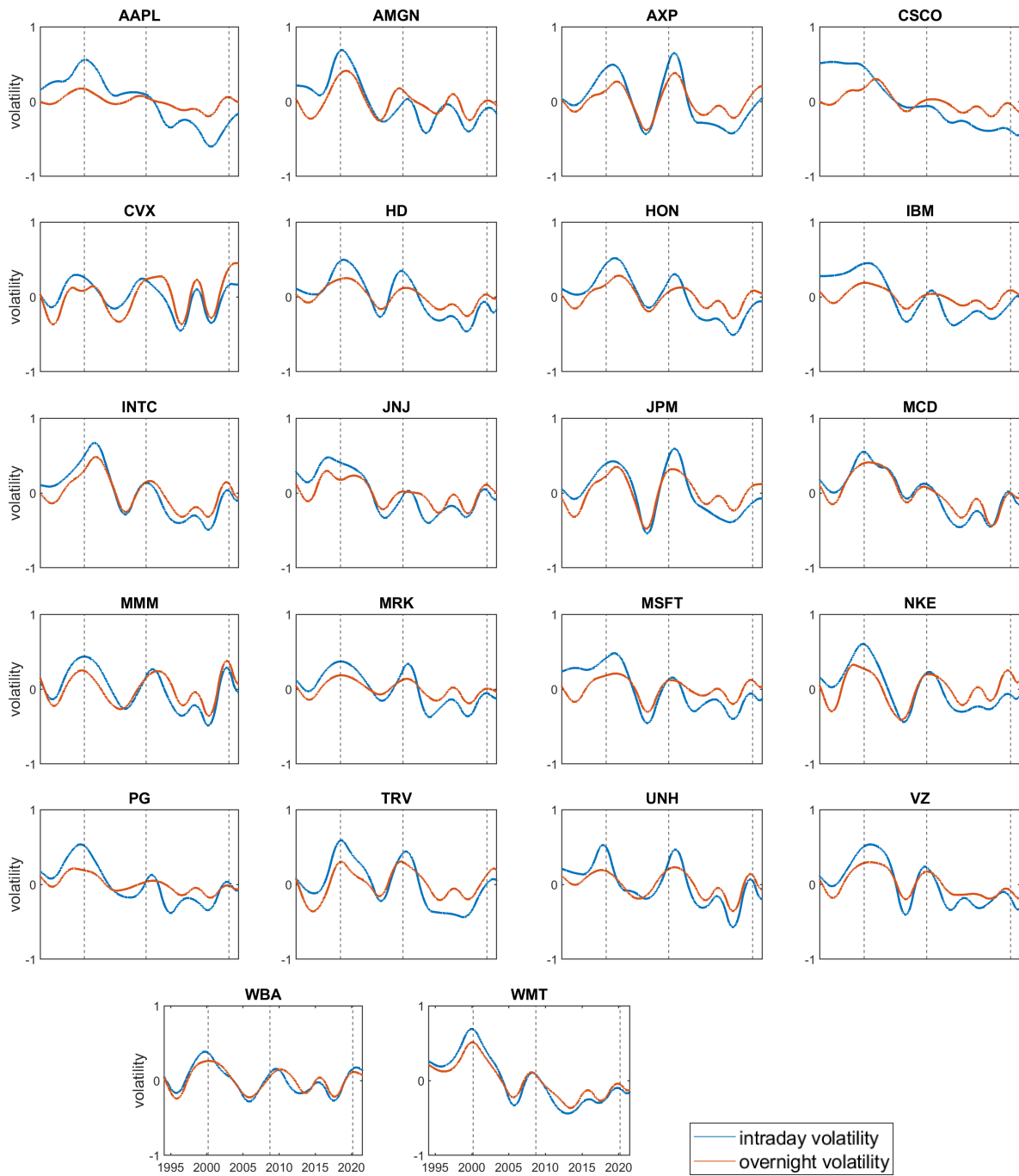
Figure 33: Total intraday and overnight volatility, measured as $\sqrt{\frac{\nu_k}{\nu_k-2}\exp\left[2\lambda_t^k + 2\sigma_t^k\left(\frac{t}{T}\right)\right]}$, of the coupled component model. The three vertical lines represent the following crises: dot-com bubble (10 March 2000), financial crisis (16 September 2008) and the corona crisis (9 March 2020).

Figure 34: T-statistics of the constancy of ratio test of the coupled component model. The horizontal lines represent the 95% confidence intervals.

Figure 35: The long run component $\lambda_{1,t}^k$, for $k \in \{D, N\}$, of the two component model. The three vertical lines represent the following crises: dot-com bubble (10 March 2000), financial crisis (16 September 2008) and the corona crisis (9 March 2020).
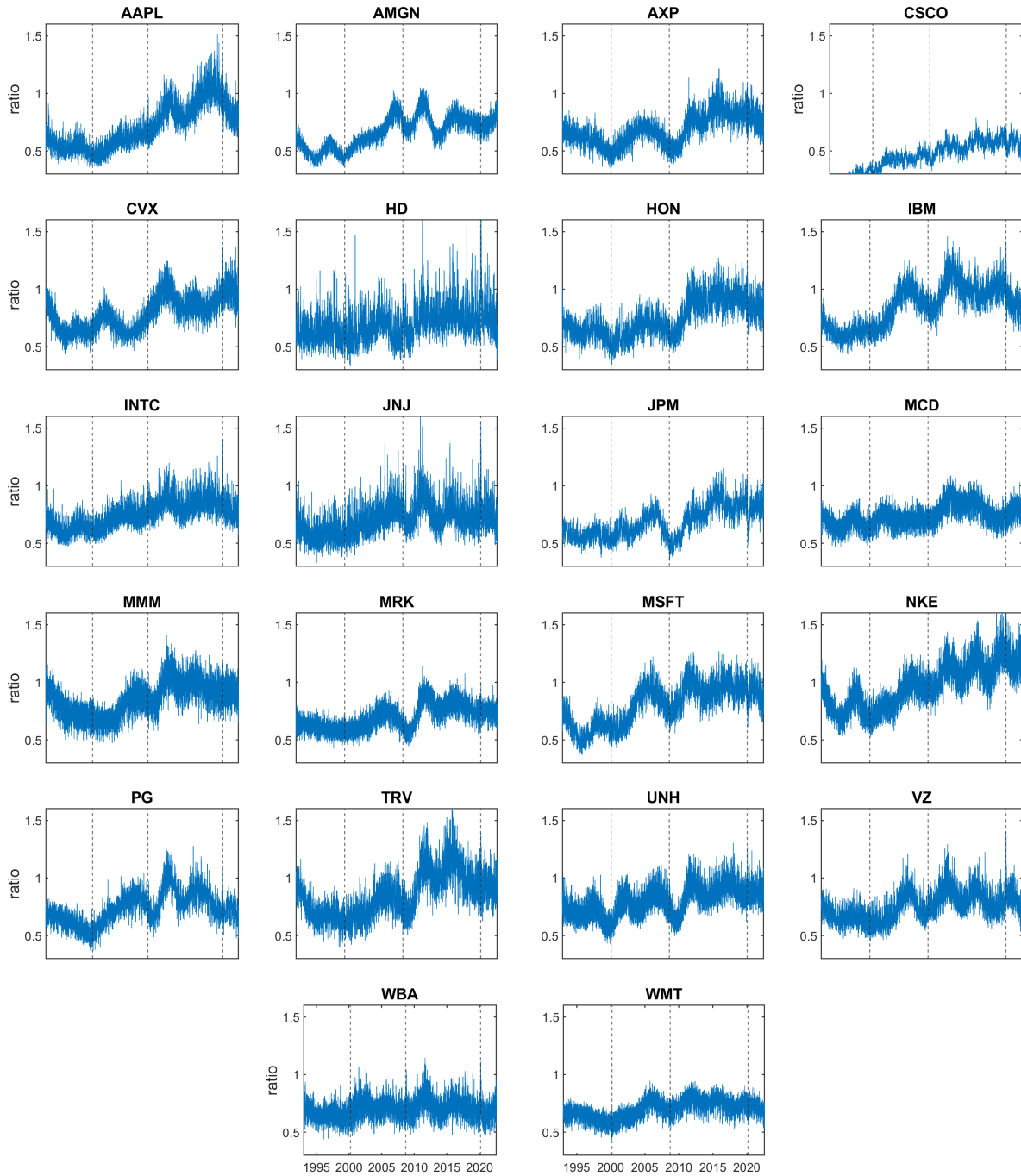
Figure 36: The ratio of overnight to intraday volatility, where volatility is measured as $\sqrt{\frac{\nu_k}{\nu_k-2}\exp\left[2\omega_k + 2\lambda_{1,t}^k + 2\lambda_{2,t}^k\right]}$, of the two component model. The three vertical lines represent the following crises: dot-com bubble (10 March 2000), financial crisis (16 September 2008) and the corona crisis (9 March 2020).
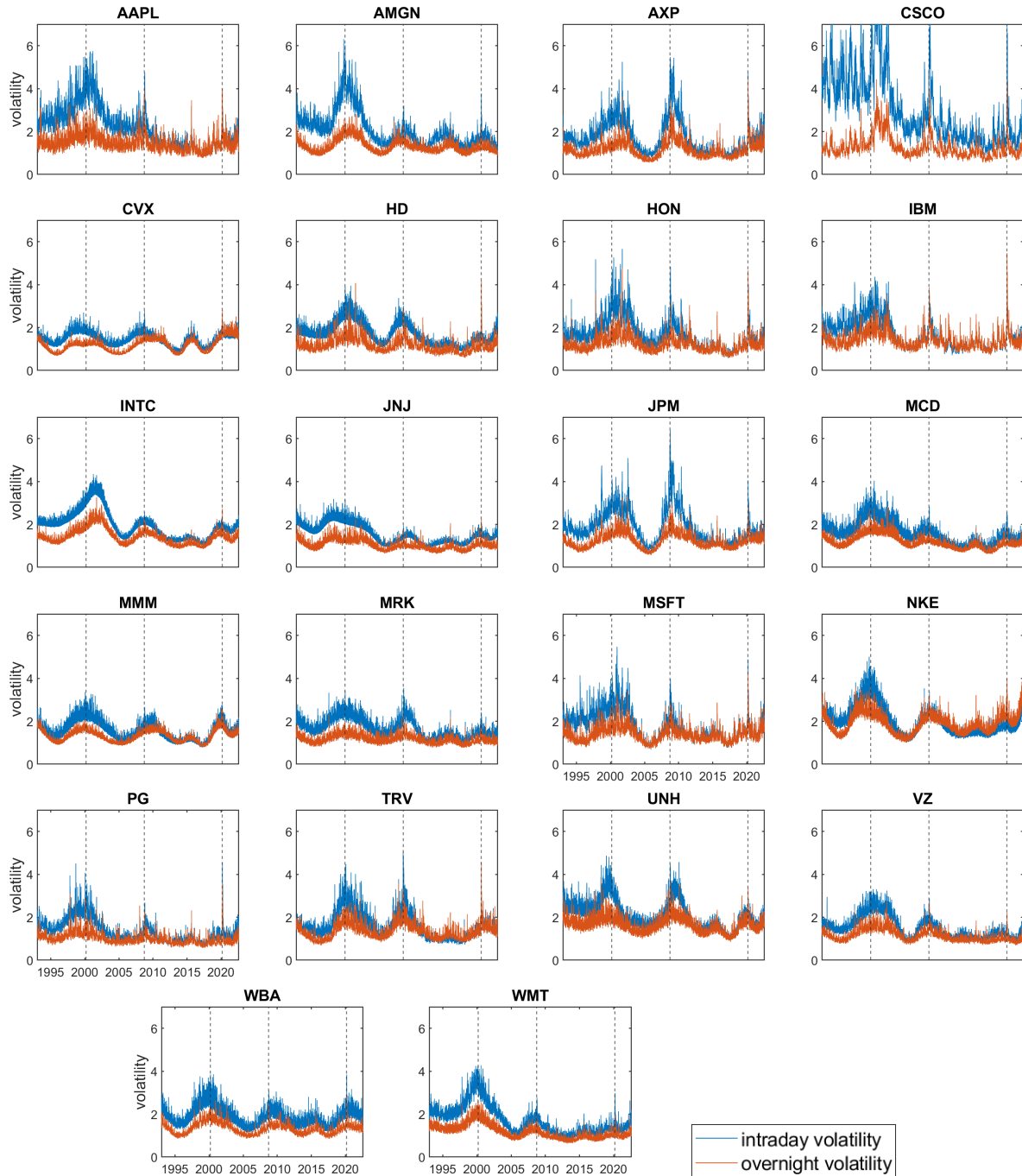
Figure 37: Total intraday and overnight volatility, measured as $\sqrt{\frac{\nu_k}{\nu_k-2}\exp\left[2\omega_k + 2\lambda_{1,t}^k + 2\lambda_{2,t}^k\right]}$, of the two component model. The three vertical lines represent the following crises: dot-com bubble (10 March 2000), financial crisis (16 September 2008) and the corona crisis (9 March 2020).

Appendix D Proofs

To find $\int K(s)^2$ I use:

$$K(s) = \frac{3}{4}\left(1 - s^2\right),$$

with $s \in \{0, 1\}$. Now compute the integral:

$$
\begin{aligned}
\int K(s)^2 &= \int \left[\frac{3}{4}\left(1 - s^2\right)\right]^2 ds, \\
&= \int \frac{9}{16}\left(1 - s^2\right)^2 ds, \\
&= \int \frac{9}{16}\left(1 - 2s^2 + s^4\right) ds, \\
&= \frac{9}{16}\int \left(1 - 2s^2 + s^4\right) ds, \\
&= \frac{9}{16}\left(s - \frac{2}{3}s^3 + \frac{1}{5}s^5\right).
\end{aligned}
$$